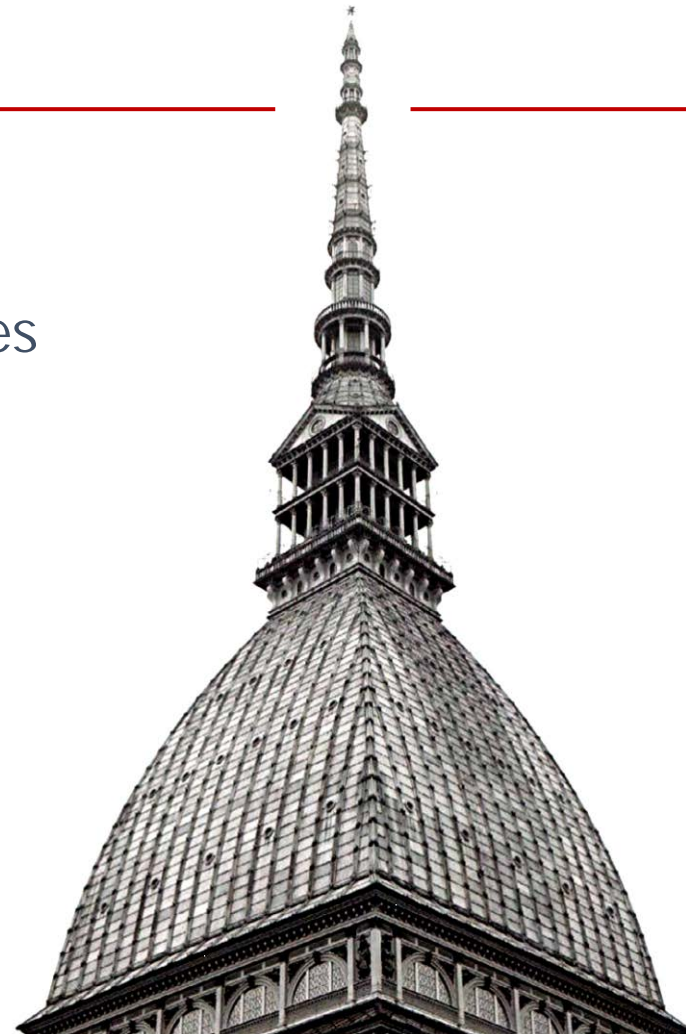


© Prof. M.M. Gola

Chapters

- 1 Plane elastic fields
- 2 Elastic stresses in discs and thick-walled tubes
- 3 Plastic stresses in thick-walled tubes
- 4 Rotating discs**
- 5 Shaft-hub system
- 5 Shaft-hub system
- 6 Engine Failures



Index of contents

1. Constant thickness
 2. Variable thickness disc
 3. Uniform strength disc
 4. Stepwise profile approximation
 5. Temperature and its gradient
 6. Case study of stresses in a turbine disc
 7. Comparison between Grammel and FEM
 8. The shape of a turbine disc - elastic stresses
 9. Burst design of a turbine disc
 10. Summary of disc life and failure criteria
- Appendices:** increasing disc speed up to burst
11. **Appendix 1 (movie frames)**
Disc only, without slots and blades
 12. **Appendix 2 (movie frames)**
Rotating disc with slots and blades
 13. **Appendix 3: the Hallinan burst criterion**

How would you feel if this happened to you?

American Airlines
Boeing 767-200
uncontained CF6-80A
engine failure that led
to aircraft fire.

On 12.30 PM, Friday,
June 2, 2006 at LAX.

The aircraft was undergoing a ground run-up of the (left) No.1 engine when the problem occurred. The CF6-80A was being tested after the crew bringing the aircraft in from New York City reported abnormal power response from the engine during the flight. The turbine disk exited the engine and sliced through the aircraft belly and lodged in the outboard side of the #2 engine.

<http://www.skybrary.aero/bookshelf/books/1374.pdf>



1. Constant thickness (1/6)

The force per unit volume due to rotation is:

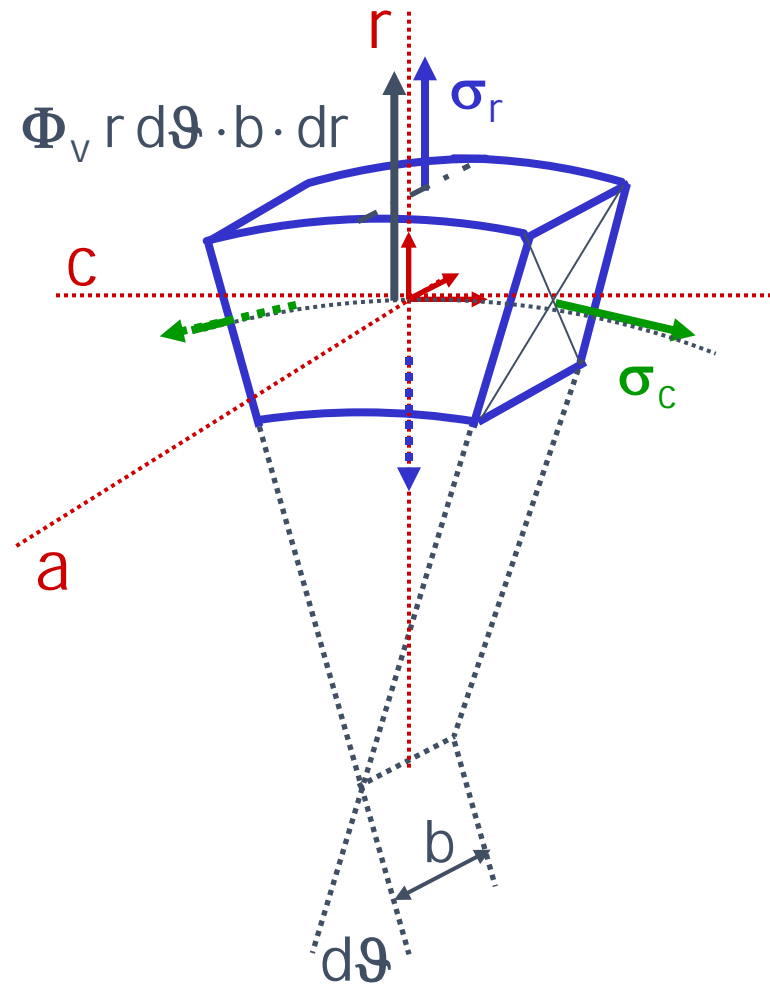
$$\Phi_v = \rho \omega^2 r$$

→ radius
→ angular speed
→ density

which for a constant thickness disc produces the equilibrium equation:

$$r \cdot \frac{d\sigma_r}{dr} + (\sigma_r - \sigma_c) + \rho \omega^2 r^2 = 0$$

Now the same scheme will be applied as in Ch. 2 / Sect. 5



1. Constant thickness (2/6)

$$r \cdot \frac{d\epsilon_c}{dr} + (\epsilon_c - \epsilon_r) = 0$$

$$\frac{d\epsilon_c}{dr} = \frac{1}{E} \frac{d}{dr} (\sigma_c - v \sigma_r)$$

$$(\epsilon_c - \epsilon_r) = \frac{1}{E} (1 + v) (\sigma_c - \sigma_r)$$

$$r \cdot \frac{d\sigma_r}{dr} + (\sigma_r - \sigma_c) + \rho \omega^2 r^2 = 0$$

$$r \left(\frac{d\sigma_c}{dr} - v \frac{d\sigma_r}{dr} \right) + (1 + v) r \frac{d\sigma_r}{dr} + (1 + v) \rho \omega^2 r^2 = 0$$

$$r \left(\frac{d\sigma_c}{dr} + \frac{d\sigma_r}{dr} \right) = -(1 + v) \rho \omega^2 r^2$$

$$\sigma_r + \sigma_c = -(1 + v) \rho \omega^2 \frac{r^2}{2} + A'$$

1. Constant thickness (3/6)

$$\frac{1}{r} \frac{d}{dr} [(r\sigma_r)r] = A - \frac{(3+\nu)}{2} \rho \omega^2 r^2$$

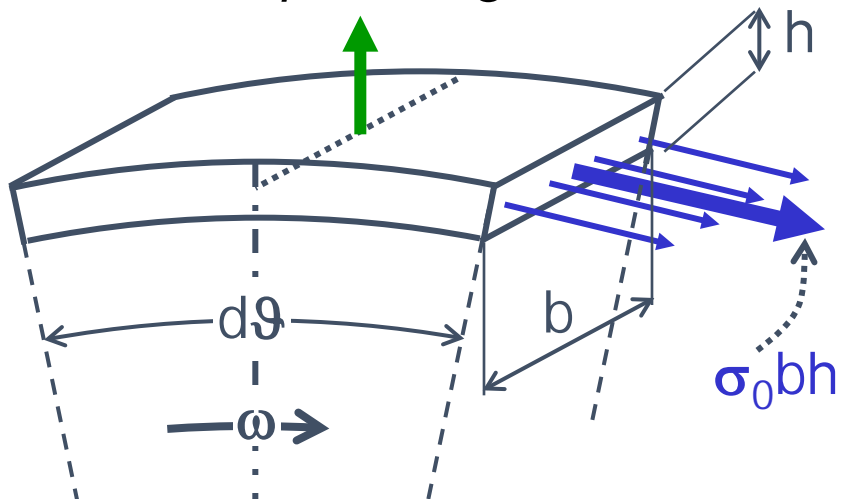
and by integration

$$\sigma_r = A + \frac{B}{r^2} - \frac{3+\nu}{8} \rho \omega^2 r^2$$

$$r \cdot \frac{d\sigma_r}{dr} + (\sigma_r - \sigma_c) + \rho \omega^2 r^2 = 0$$

$$\sigma_c = A - \frac{B}{r^2} - \frac{1+3\nu}{8} \rho \omega^2 r^2$$

Had we a (very) thin shell rotating at outer, or external, radius r_e , the circumferential stress σ_0 , calculated through the radial equilibrium equation:



$$(\sigma_0 b h) d\theta = (\omega^2 r_e) \rho (b h r_e d\theta)$$

$$\sigma_0 = \rho \omega^2 r_e^2$$

1. Constant thickness (4/6)

$$\sigma_r = A + \frac{B}{r^2} - \sigma_0 \frac{3 + \nu D^2}{8} \frac{D_e^2}{D_e^2}$$

$$\sigma_c = A - \frac{B}{r^2} - \sigma_0 \frac{1 + 3\nu D^2}{8} \frac{D_e^2}{D_e^2}$$

The integration constants are found through the boundary conditions:

$$r = \frac{D_i}{2} \rightarrow \sigma_r^\omega = 0$$

$$r = \frac{D_e}{2} \rightarrow \sigma_r^\omega = 0$$

σ_0 plays the role of a reference stress, incorporating the disc dimension and its rotational speed

$$A = \sigma_0 \frac{3 + \nu}{8} \left(1 + \frac{r_i^2}{r_e^2} \right)$$

$$B = -\sigma_0 \frac{3 + \nu}{8} r_i^2$$

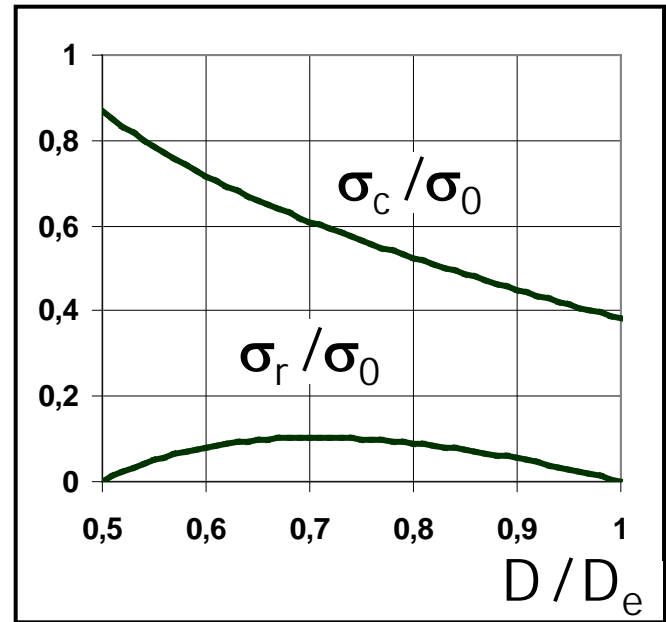
Which substituted in the formulas at the upper-left corner, give expressions for stresses due to the centrifugal effect alone: 

1. Constant thickness (5/6)

$$\sigma_r^\omega = \sigma_0 \frac{3 + \nu}{8} \left[1 + \frac{D_i^2}{D_e^2} - \frac{D_i^2}{D^2} - \frac{D^2}{D_e^2} \right]$$

$$\sigma_c^\omega = \sigma_0 \frac{3 + \nu}{8} \left[1 + \frac{D_i^2}{D_e^2} + \frac{D_i^2}{D^2} - \frac{(1 + 3\nu)}{(3 + \nu)} \frac{D^2}{D_e^2} \right]$$

$\sigma_{r,\max}^\omega$ at $D = \sqrt{D_i D_e}$ or: $\frac{D}{D_e} = \sqrt{\frac{D_i}{D_e}}$



Finally, radial displacement is:

$$\begin{aligned} u^\omega &= \frac{D}{2} \frac{1}{E} (\sigma_c - \nu \sigma_r) = \\ &= \sigma_0 D \frac{3 + \nu}{16E} \left[(1 - \nu) \left(1 + \frac{D_i^2}{D_e^2} \right) + (1 + \nu) \frac{D_i^2}{D^2} - \frac{1 - \nu^2}{3 + \nu} \frac{D^2}{D_e^2} \right] \end{aligned}$$

1. Constant thickness (6/6)

In the special case of a solid disc:

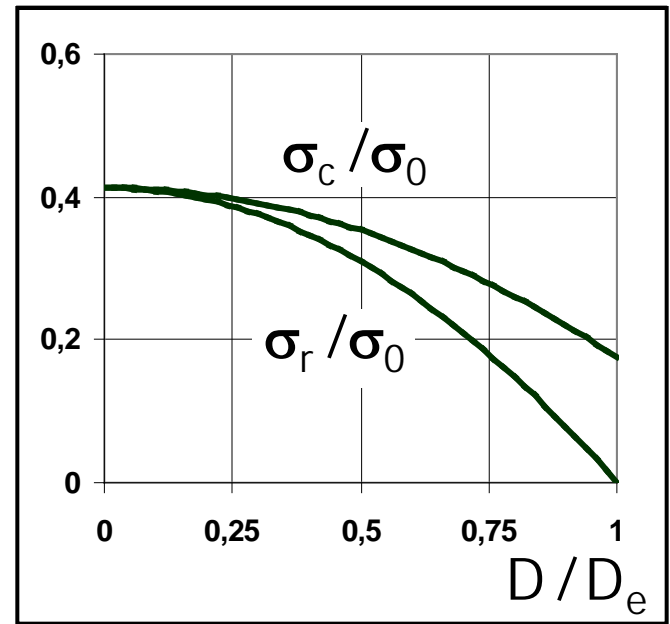
$$A = \sigma_0 \frac{(3 + \nu)}{8} ; \quad B = 0$$

Then:

$$\sigma_r^\omega = \sigma_0 \frac{(3 + \nu)}{8} \left[1 - \frac{D^2}{D_e^2} \right]$$

$$\sigma_c^\omega = \sigma_0 \frac{(3 + \nu)}{8} \left[1 - \frac{(1 + 3\nu)}{(3 + \nu)} \frac{D^2}{D_e^2} \right]$$

$$u^\omega = \frac{1}{2} \frac{D}{E} (\sigma_c^\omega - \nu \sigma_r^\omega) = \sigma_0 D \frac{(3 + \nu)}{16E} \left[(1 - \nu) - \frac{(1 - \nu^2)}{(3 + \nu)} \frac{D^2}{D_e^2} \right]$$



2. Variable thickness disc (1/2)

Turbine discs seldom are made flat. They are made thicker towards the centre, and are tapered to a smaller thickness toward the periphery. This is to avoid the pronounced stress concentrations in the central part.

When a disc has a variable thickness $b=b(r)$, the radial equilibrium equation is:

$$\frac{d}{dr}(\sigma_r r b) - \sigma_c b = -\rho \omega^2 r^2 b$$

This is exactly integrable, together with compatibility and material equations, in very few cases: the hyperbolic disc, the constant stress disc. The hyperbolic disc solution is due to **A. Stodola** Dampf- und Gas-Turbinen, Springer, Berlin 1924, several editions in english as "Steam and gas turbines", Mc Graw-Hill, NY



2. Variable thickness disc (2/2)

For all these early (pre-numerical) solutions, a large amount of sources is available; however, the reader is urged to refer to some of the main classical textbooks such as, for instance, the one from Stodola or the one from J. P. den Hartog, Advanced Strength of Materials, Mc Graw-Hill, 1952

For the case called “constant stress” or “uniform strength” solution, let us quote from J.P. den Hartog, page 65:

In view of the considerable complications in the design of flat or hyperbolic rotating disks, it is remarkable that a simple solution has been found to the question of designing the thickness variation $t(r)$ of a disk so as to make its stresses equal over the entire area. The solution was found, about 1900, by engineers of the De Laval Company in Sweden and was first published in Stodola famous book “Steam and Gas Turbines”.

3. Uniform strength disc (1/9)

So, let us now start from the equilibrium equation:

$$\frac{d}{dr}(\sigma_r r b) - \sigma_c b = -\rho \omega^2 r^2 b$$

The desired stress field will have

- 1) $\sigma_a=0$ and
- 2) $\sigma_r=\text{constant}$
- 3) $\sigma_c=\text{constant}$.

Condition 2) implies that the disc is solid: otherwise, stress σ_r would be zero at the inner rim of a hole and should be zero over the whole disc.

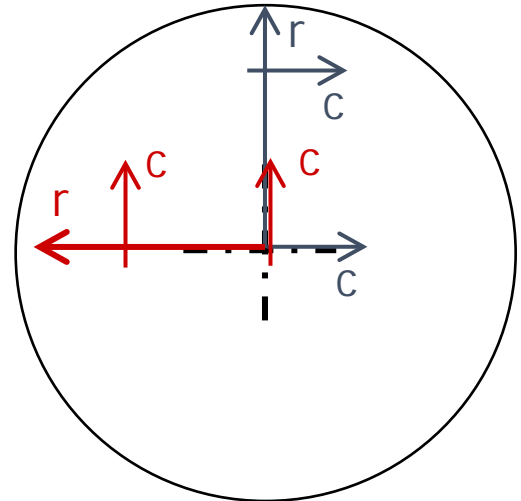
Which proves contradictory, as shown by the equilibrium equation: a zero σ_r would imply a non-constant σ_c .

3. Uniform strength disc (2/9)

Conditions 2) 3) imply that at the centre, i.e., $r=0$,

4) $\sigma_r = \sigma_c$

due to the fact that radial and circumferential directions at the centre are not distinguishable.



3. Uniform strength disc (3/9)

Equilibrium equation, with $\sigma_r = \sigma_c = \sigma$ (constant), produces now:

$$\sigma_r b + r b \cancel{\frac{d\sigma_r}{dr}} + r \sigma_r \frac{db}{dr} - \sigma_c b = -\rho \omega^2 r^2 b$$

because $\sigma_r = \sigma_c$

$=0$ because σ_r constant

$$r \sigma \frac{db}{dr} = -\rho \omega^2 r^2 b \Rightarrow \frac{1}{b} \frac{db}{dr} = -\frac{\rho \omega^2}{\sigma} r$$

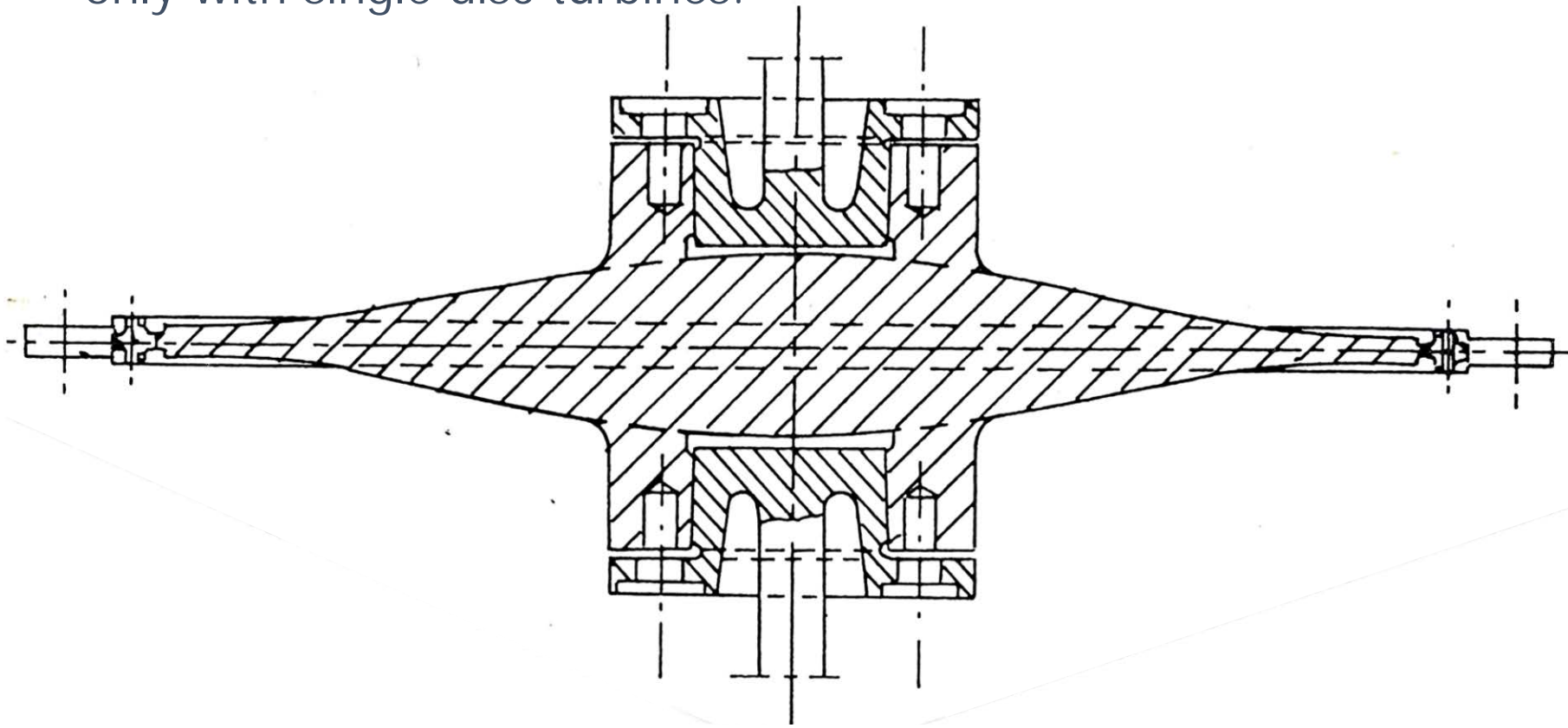
$$\frac{d}{dr}(\ln b) = -\frac{\rho \omega^2}{\sigma} r \Rightarrow \ln b = -\frac{\rho \omega^2}{2\sigma} r^2 + A$$

for $r=0 \quad b=b_0$, then $b = b_0 e^{-\frac{\rho \omega^2}{2\sigma} r^2}$

3. Uniform strength disc (4/9)

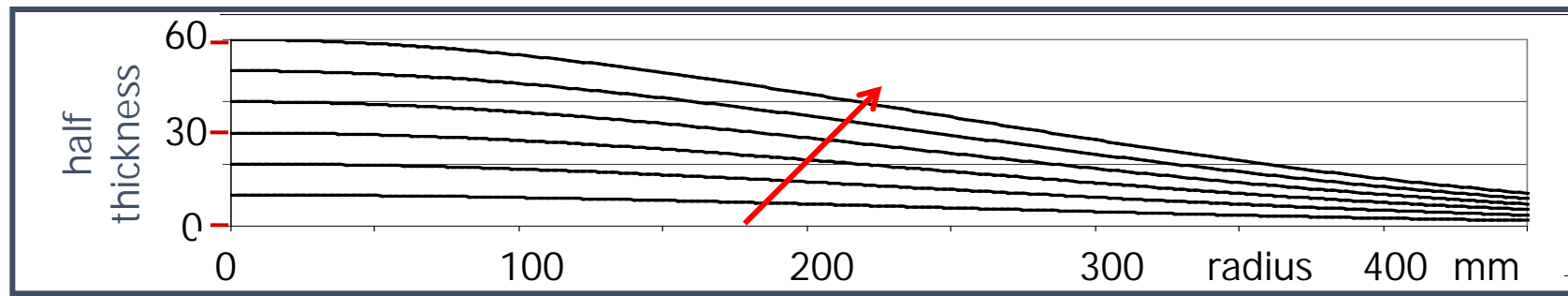
A disc of this type has a number of drawbacks:

- 1) it extends to infinity (but there is a remedy to this)
- 2) it does not have a central bore, and requires a special coupling to the shaft, as shown on below; this is possible only with single disc turbines.



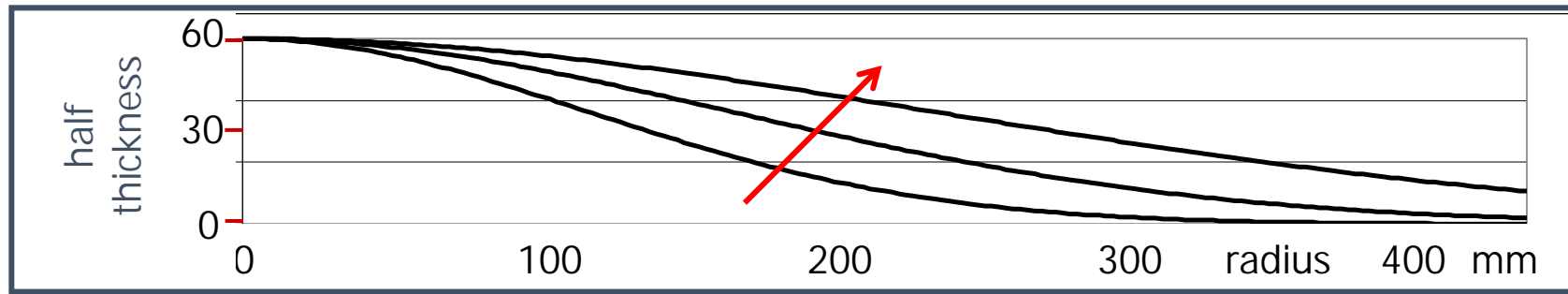
3. Uniform strength disc (5/9)

3) for the same stress there is an infinity of solutions



disc profiles with different central thickness, fixed stress:

$b_0 = 20, 40, 60, 80, 100, 120 \text{ mm}$, $n = 10^4 \text{ rpm}$, $r = 7800 \text{ kg/m}^3$
 $\sigma = 500 \text{ MPa}$



disc profiles with different stress, fixed central thickness:

$b_0 = 120 \text{ mm}$, $n = 10^4 \text{ rpm}$, $r = 7800 \text{ kg/m}^3$, $\sigma = 500, 250, 125 \text{ MPa}$

3. Uniform strength disc (6/9)

The presence of blades produces a certain stress for a certain thickness.

The solution for thickness then becomes unique.

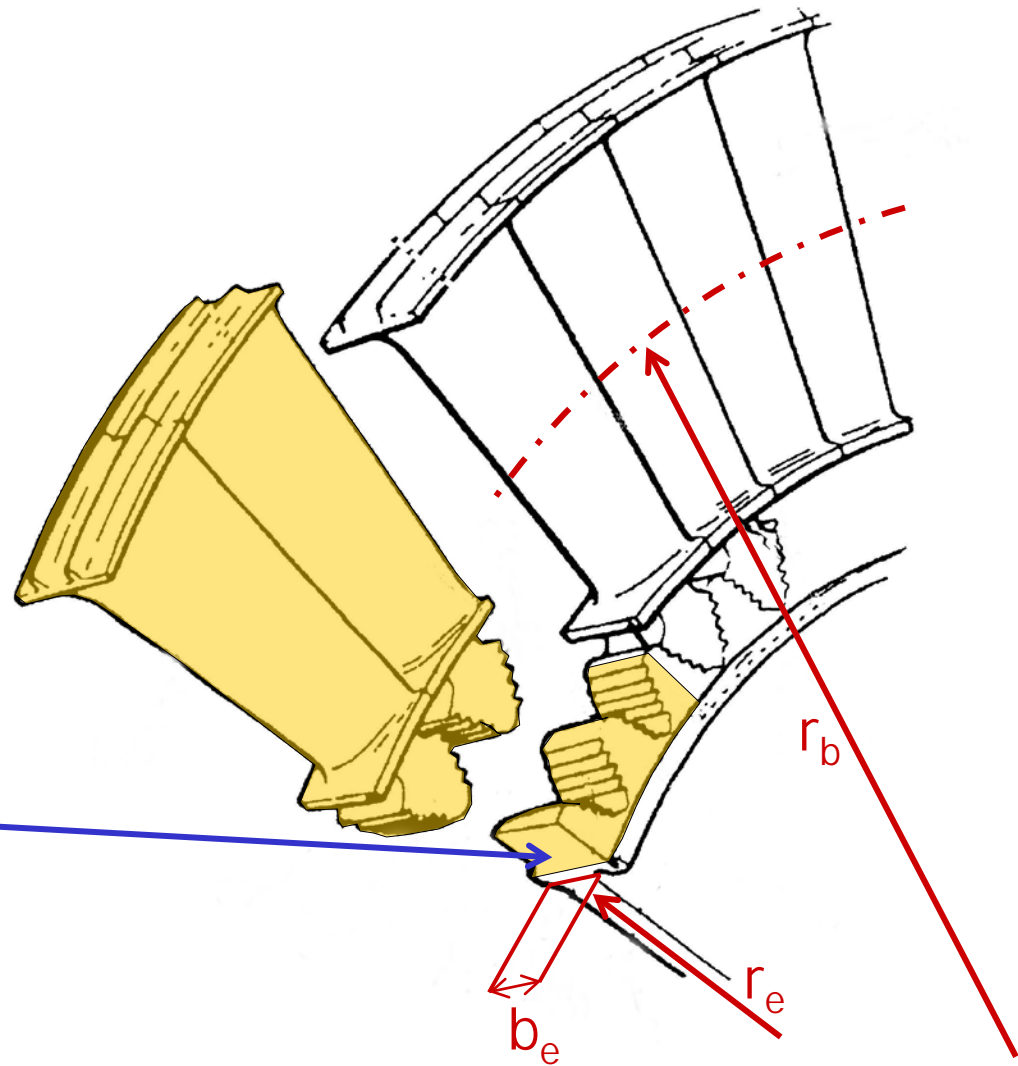
M_b : mass of all blades*

r_e : outer rim radius

r_b : blade mass centroid radius

b_e : outer rim thickness

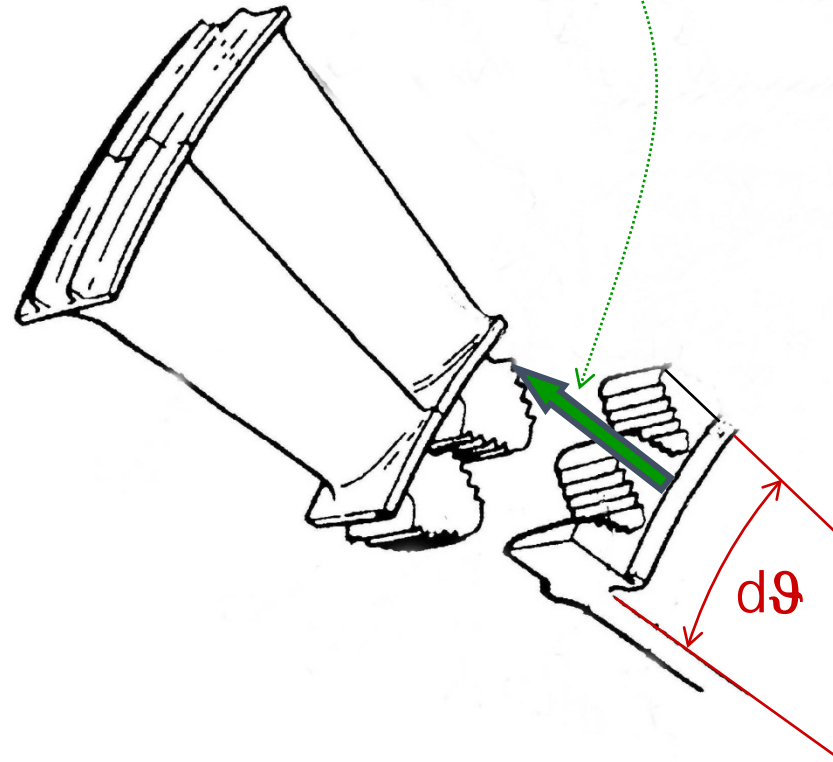
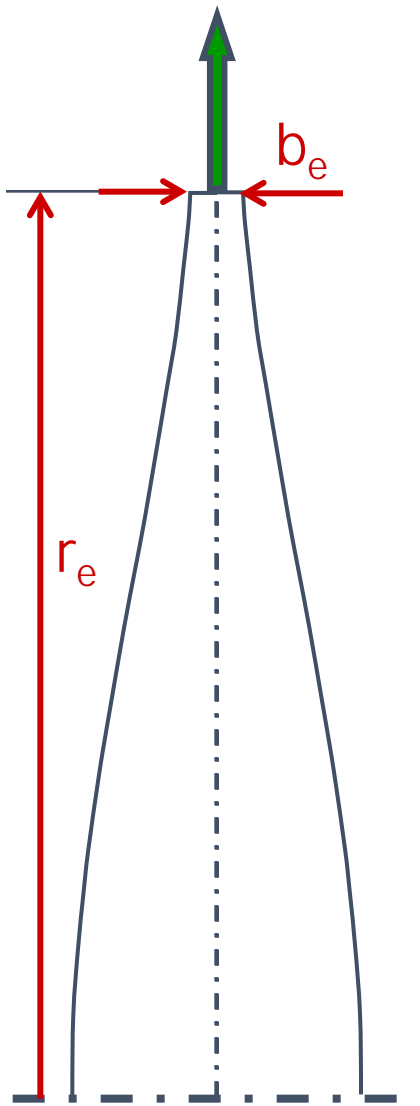
*included "slot" attachment
on disc without circumferential continuity



3. Uniform strength disc (7/9)

The centrifugal force of the blade mass contained within angle $d\theta$ is:

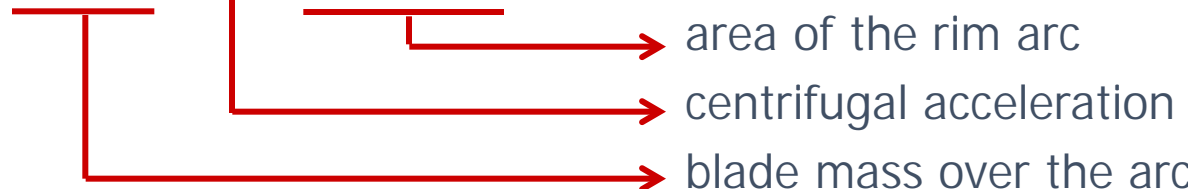
$$\left(M_b \frac{d\theta}{2\pi} \right) \omega^2 r_b$$



3. Uniform strength disc (8/9)

... then radial stress at the outer rim is:

$$\sigma_{re}^b = M_b \frac{d\theta}{2\pi} \omega^2 r_b \frac{1}{b_e r_e d\theta}$$



$$\sigma_{re}^b = \frac{M_b \omega^2 r_b}{2\pi b_e r_e} \equiv \sigma \text{ i.e. the constant stress}$$

which into: $b = b_0 e^{-\frac{\rho \omega^2}{2\sigma} r^2}$

finally gives: $b = b_0 e^{-\frac{\pi \rho b_e r_e}{M_b r_b} r^2}$

However, b_0 must be such that:

$$r = r_e \Rightarrow b_e = b_0 e^{-\frac{\pi \rho b_e r_e^3}{M_b r_b}}$$

$$\frac{\pi \rho b_e r_e (r_e^2 - r^2)}{M_b r_b}$$

then: $b = b_e e^{-\frac{\pi \rho b_e r_e (r_e^2 - r^2)}{M_b r_b}}$

3. Uniform strength disc (9/9)

Let us quote again from den Hartog.

The constant stress disc is the best design, if it can be applied.

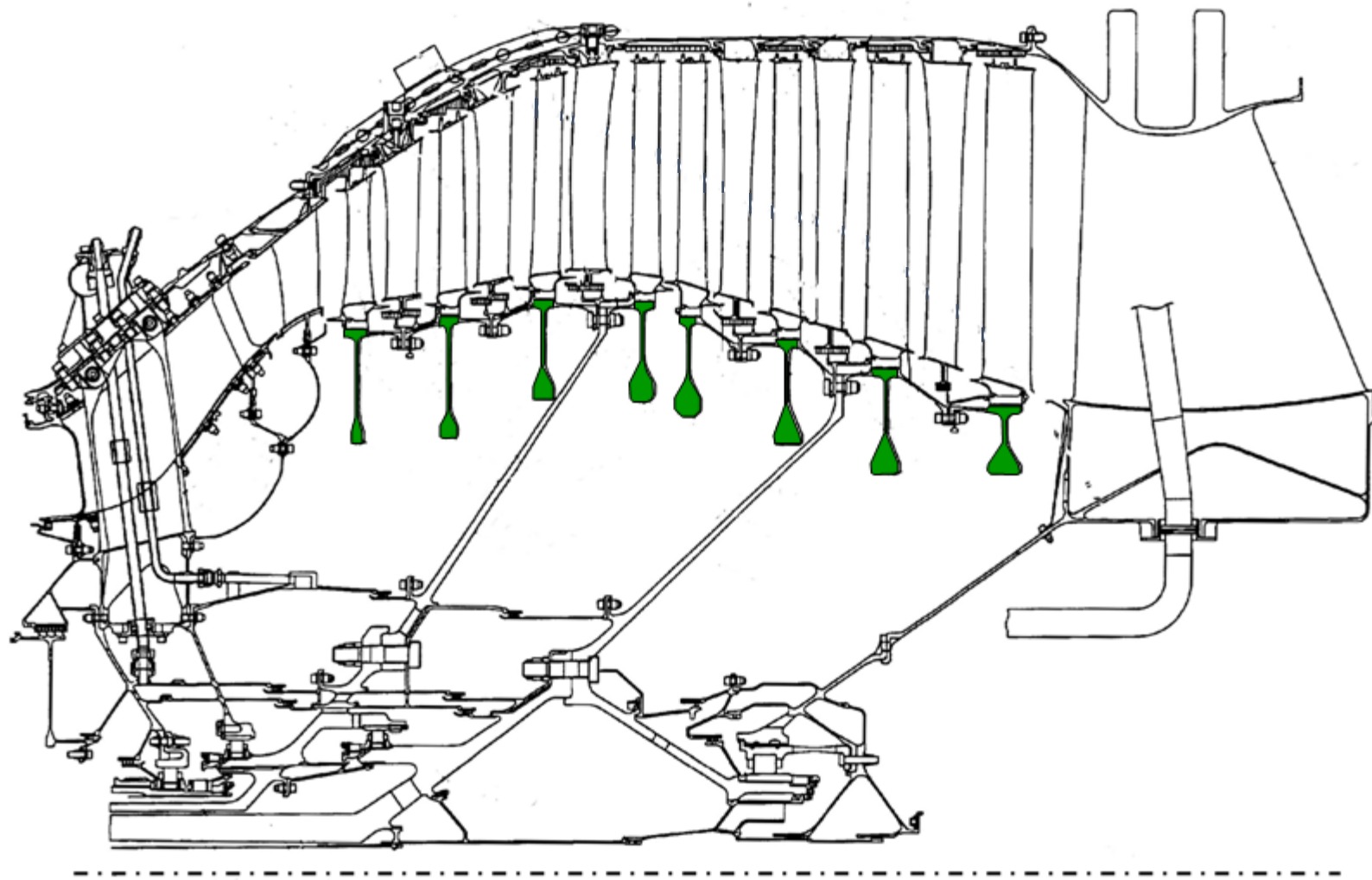
(it is clear from the following that he means: it can be applied only in “single disc cases”, and is subject to severe practical restrictions)

For multidisk designs the constructional complications are so severe that disks with a central hole are usually applied. Then a hyperbolic disk is better than a flat one. Flat discs are used for simplicity only in cases of low rpm or low stress.

With these three general types almost all design problems can be answered.

... the shape can be broken up by intermediate radii into two or more annular disks. Each of these is approximated as well as possible by a hyperbola or by a flat disk, and all these disks then are joined together by a proper boundary condition.

4. Stepwise profile approximation (1/11)



4. Stepwise profile approximation (2/11)

In the detail design of high speed rotating disks, such as those found in the compressor and turbine sections of gas turbine engines for aircraft, today finite element models are employed to analyze the complex shape of the disks.

However, simplified calculation of mechanical stresses in the elastic field is important for preliminary sizing and for cross-checking the validity of a finite element model.

To this purpose, two main methods are available, both of them easy to implement with self-made software:

- the stepwise method due to Grammel*, which will be explored in detail in this section
- the finite-difference method proposed by Manson** in 1947

* GRAMMEL R., En neues Verfahren zur Berechnung rotierender Scheiben. Dinglers J., 1923

** Manson, S. S., Determination of elastic stresses in gas-turbine disks, NACA-report-871, 1947

4. Stepwise profile approximation (3/11)

We shall here explore only the case of disc with a central bore.

The purpose is to describe a simple numerical method, attributed to the german scholar Grammel, which can be easily implemented on an electronic sheet, and which was originally devised for manual calculations. We start with the displacements due to inner and outer **pressures**, to **rotation**, to temperature.

$$u = \frac{1}{2} \frac{D}{E} \left\{ -\frac{\frac{D_i^2}{D^2}(1+\nu) + \frac{D_i^2}{D_e^2}(1-\nu)}{1 - \frac{D_i^2}{D_e^2}} \sigma_{ri} + \frac{(1-\nu) + \frac{D_i^2}{D^2}(1+\nu)}{1 - \frac{D_i^2}{D_e^2}} \sigma_{re} \right\}$$

$$u^\omega = \sigma_0 D \frac{(3+\nu)}{16E} \left[(1-\nu) \left(1 + \frac{D_i^2}{D_e^2} \right) + (1+\nu) \frac{D_i^2}{D^2} - \frac{(1-\nu^2)}{(3+\nu)} \frac{D^2}{D_e^2} \right]$$

4. Stepwise profile approximation (3/11)

We shall here explore only the case of disc with a central bore.

The purpose is to describe a simple numerical method, attributed to the german scholar Grammel, which can be easily implemented on an electronic sheet, and which was originally devised for manual calculations. We start with the displacements due to inner and outer pressures, to rotation, to **temperature**.

$$u^T = \frac{D}{2} \frac{\alpha^* T_e - T_i}{3} \frac{1 - \frac{D_i}{D_e}}{\left(1 + \frac{D_i}{D_e}\right)} \left[(1 - \nu) \frac{1 + \frac{D_i^2}{D_e^2} + \frac{D_i}{D_e}}{1 + \frac{D_i}{D_e}} - (2 - \nu) \frac{D}{D_e} + (1 + \nu) \frac{\frac{D_i^2}{D_e^2} \frac{D_e^2}{D^2}}{1 + \frac{D_i}{D_e} \frac{D^2}{D_e^2}} \right] + \frac{D}{2} \alpha^* (T - T_0)$$

4. Stepwise profile approximation (4/11)

These are calculated at $r=r_i$ and $r=r_e$; a matrix notation is convenient:

→ this term will be described later

$$\begin{Bmatrix} u_e \\ u_i \end{Bmatrix} = \begin{bmatrix} S & P \\ Q & R \end{bmatrix} \begin{Bmatrix} \sigma_{re} \\ \sigma_{ri} \end{Bmatrix} + \begin{Bmatrix} u_e^\omega \\ u_i^\omega \end{Bmatrix} + \begin{Bmatrix} u_e^T \\ u_i^T \end{Bmatrix}$$

→ calculate it with the formula of previous slide

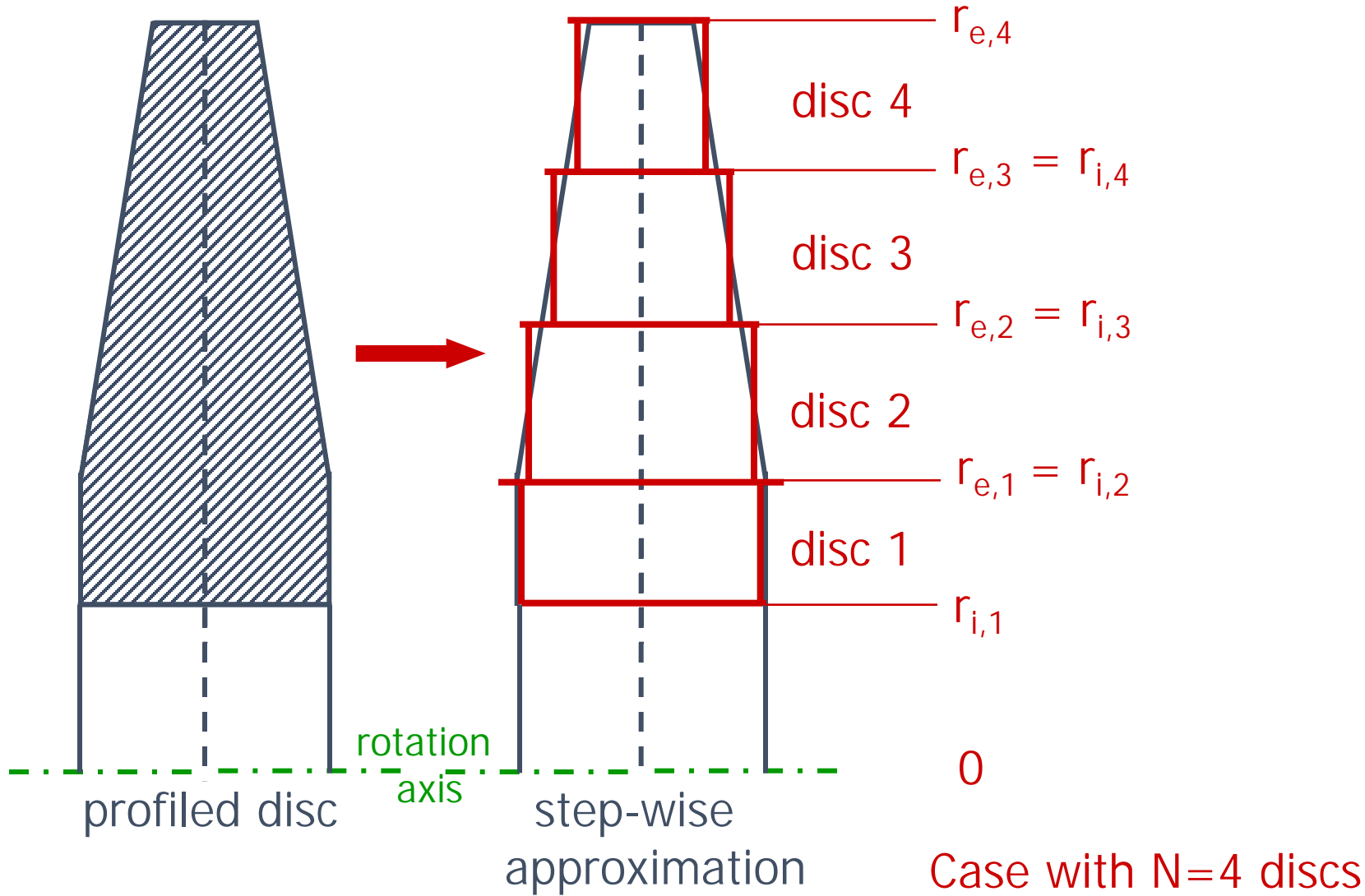
$$S = \frac{1}{2} \frac{D_e}{E} \frac{(1 - v) + \frac{D_i^2}{D_e^2} (1 + v)}{1 - \frac{D_i^2}{D_e^2}}$$

$$P = -\frac{1}{2} \frac{D_e}{E} \frac{2 \frac{D_i^2}{D_e^2}}{1 - \frac{D_i^2}{D_e^2}}$$

$$Q = \frac{1}{2} \frac{D_i}{E} \frac{2}{1 - \frac{D_i^2}{D_e^2}}$$

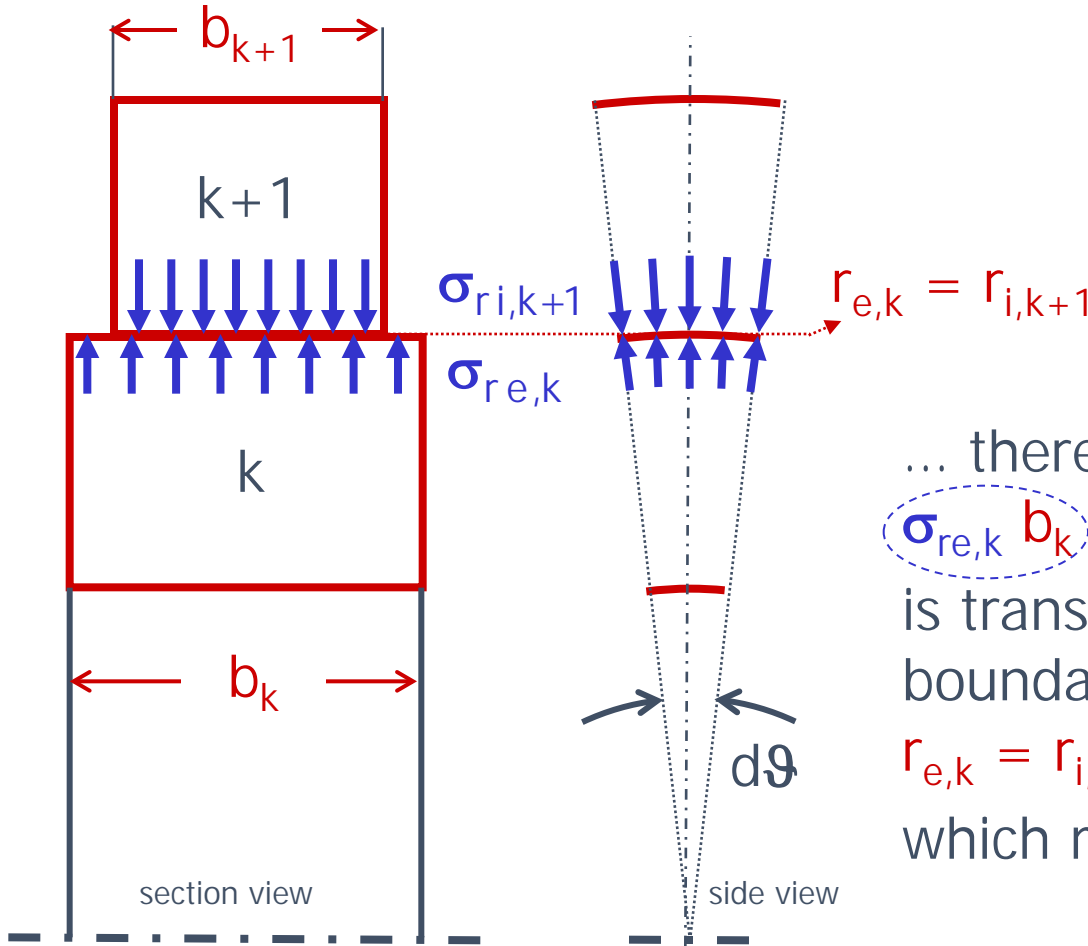
$$R = -\frac{1}{2} \frac{D_i}{E} \frac{(1 + v) + \frac{D_i^2}{D_e^2} (1 - v)}{1 - \frac{D_i^2}{D_e^2}}$$

4. Stepwise profile approximation (5/11)



4. Stepwise profile approximation (6/11)

The analytical model we use for the flat disc section considers radial stress σ_r distributed uniformly over the width b ...



... therefore the force:

$$\sigma_{re,k} b_k r_{e,k} d\vartheta = \sigma_{ri,k+1} b_{k+1} r_{i,k+1} d\vartheta$$

is transmitted through the boundary surface at radius:

$$r_{e,k} = r_{i,k+1}$$

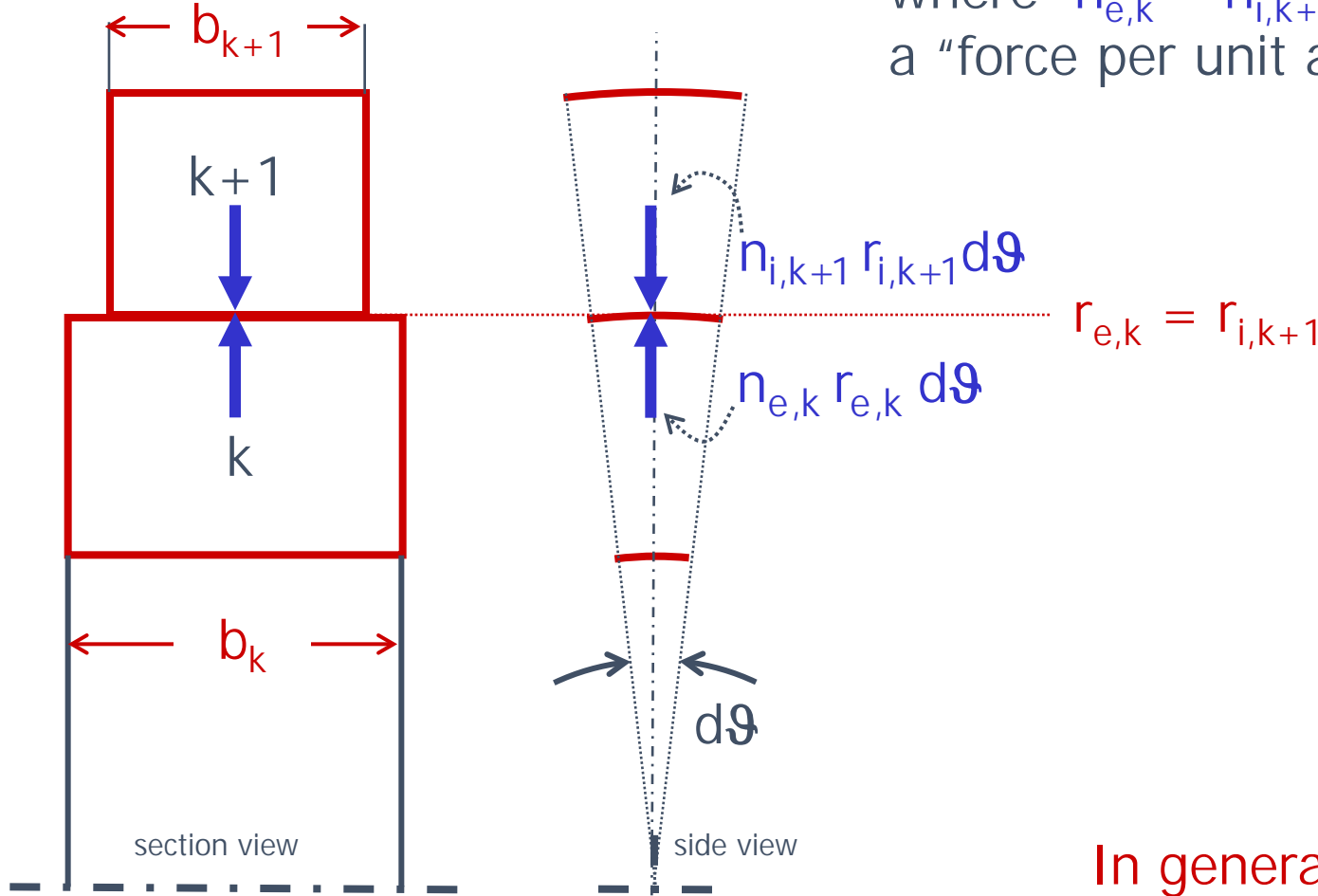
which means

$$n_{e,k} d\vartheta = n_{i,k+1} d\vartheta$$

4. Stepwise profile approximation (7/11)

Two disc elements k and $k+1$ will then exchange, through their contact surfaces, a total force: $n_{i,k+1} r_{i,k+1} d\theta = n_{e,k} r_{e,k} d\theta$

where $n_{e,k} = n_{i,k+1}$ is a “force per unit arc length”.



In general $k=1,2,\dots,N$

4. Stepwise profile approximation (8/11)

It is then convenient to rewrite the matrix form of displacement equations for each disc element k so that the boundary "unit arc-length" forces appear, remember that $n_{i,e} = \sigma_{i,e} b$:

$$\begin{Bmatrix} u_e \\ u_i \end{Bmatrix}_k = \begin{bmatrix} S/b_k & P/b_k \\ Q/b_k & R/b_k \end{bmatrix}_k \begin{Bmatrix} n_e \\ n_i \end{Bmatrix}_k + \begin{Bmatrix} u_e^\omega \\ u_i^\omega \end{Bmatrix}_k + \begin{Bmatrix} u_e^T \\ u_i^T \end{Bmatrix}_k$$

which in condensed form:

$$\begin{Bmatrix} u_e \\ u_i \end{Bmatrix}_k = \begin{bmatrix} S' & P' \\ Q' & R' \end{bmatrix}_k \begin{Bmatrix} n_e \\ n_i \end{Bmatrix}_k + \begin{Bmatrix} \tilde{u}_e \\ \tilde{u}_i \end{Bmatrix}_k$$

This will now be transformed into the so called "transfer form":

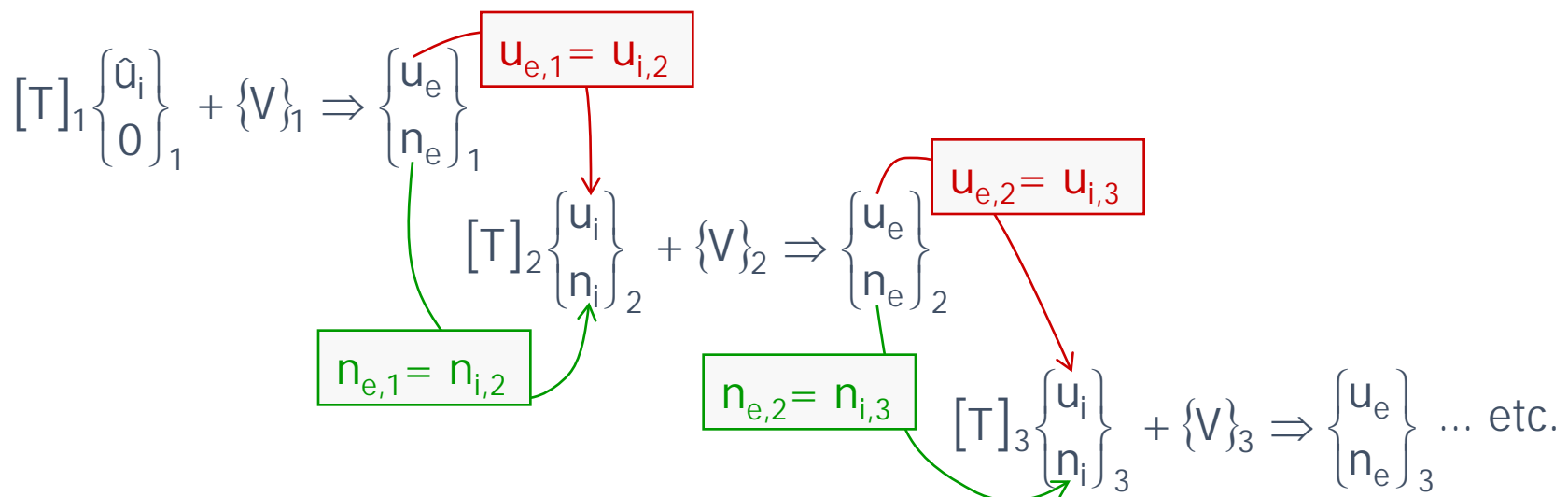
$$\begin{Bmatrix} u_e \\ n_e \end{Bmatrix}_k = \begin{bmatrix} \alpha & \beta \\ \gamma & \delta \end{bmatrix}_k \begin{Bmatrix} u_i \\ n_i \end{Bmatrix}_k + \begin{Bmatrix} \varsigma \\ \xi \end{Bmatrix}_k \equiv [T]_k \begin{Bmatrix} u_i \\ n_i \end{Bmatrix}_k + \{V\}_k$$

where:

4. Stepwise profile approximation (9/11)

$$\alpha = \frac{R'}{R'} \quad \beta = \left(S' - \frac{R'}{R'} Q' \right) \quad \varsigma = \tilde{u}_e - \frac{R'}{R'} \tilde{u}_i$$
$$\gamma = \frac{1}{R'} \quad \delta = -\frac{Q'}{R'} \quad \xi = -\frac{1}{R'} \tilde{u}_i$$

At this point calculations are easily implemented on an electronic sheet. Starting from the innermost disc, $k=1$, where $n_{i,1}=0$ and $u_{i,1}=\hat{u}_{i,1}$ unknown, we can implement a numerical feed-forward scheme:

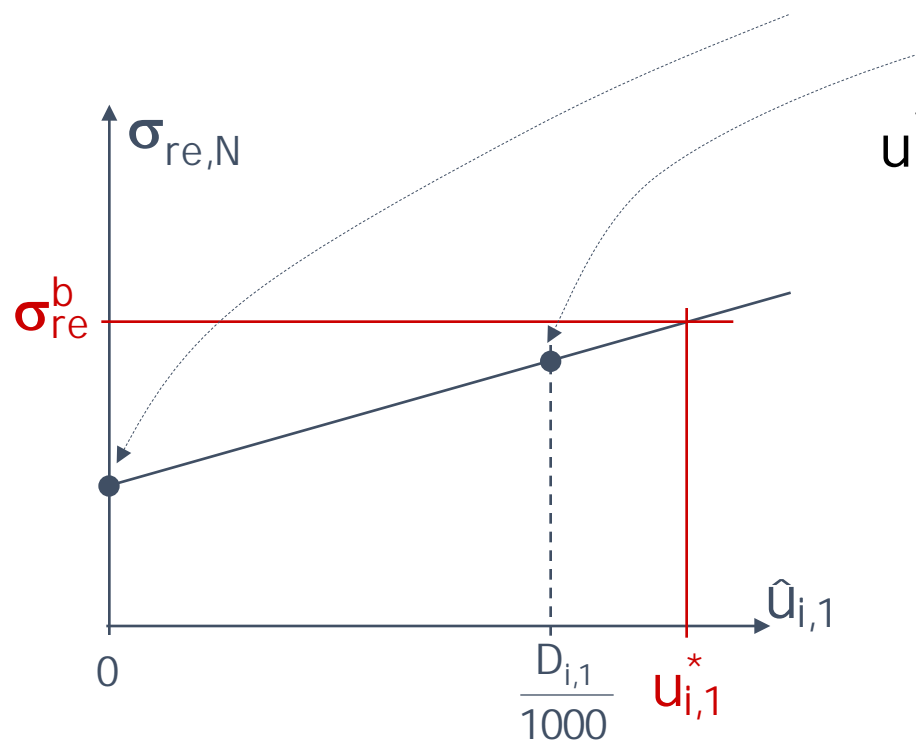


4. Stepwise profile approximation (10/11)

At the end, when $k=N$:

$$[T]_N \begin{Bmatrix} u_i \\ n_i \end{Bmatrix}_N + \{V\}_N \Rightarrow \begin{Bmatrix} u_e \\ n_e \end{Bmatrix}_N \quad \sigma_{re,N} = \frac{n_{e,N}}{b_N}$$

It is understood that $\sigma_{re,N}$ is a linear function of $\hat{u}_{i,1}$; one possibility, calculate it for $\hat{u}_{i,1} = 0$ and for $\hat{u}_{i,1} = D_{i,1} / 1000$.



However we know that that the blade system produces a radial stress:

$$\sigma_{re}^b = \frac{M_b \omega^2 r_b}{2\pi b_e^N r_e}$$

hence the displacement $u_{i,1}^*$ at the inner radius.

4. Stepwise profile approximation (11/11)

Once the displacement $u_{i,1} = u_{i,1}^*$ at the inner radius is known, all:

$\left\{ \begin{matrix} u_i \\ n_i \end{matrix} \right\}_k$ and $\left\{ \begin{matrix} u_e \\ n_e \end{matrix} \right\}_k$ can be calculated - for $k=1, \dots, N$ - as in slide 9 .

Then :

$$\sigma_{ri,k} = \frac{n_{i,k}}{b_k} \quad \sigma_{re,k} = \frac{n_{e,k}}{b_k}$$

and, from material constitutive equation for plane stress plus circumferential strain definition, σ_c is calculated at any radius:

$$\varepsilon_c = \frac{1}{E} (\sigma_c - \nu \sigma_r) + \alpha^* \Delta T \Rightarrow \sigma_c = E \varepsilon_c + \nu \sigma_r - E \alpha^* \Delta T$$

$$\sigma_c = E \frac{u}{r} + \nu \sigma_r - E \alpha^* \Delta T$$

5. Temperature and its gradient (1/7)

See Ch. 2, Sect. 5, Sl. 3. Thermal expansion adds to linear strain (in the case of isotropic material) an equal term in all directions $i=1,2,3$:

$$\varepsilon_i^T = \alpha^* \cdot \Delta T$$

linear thermal
expansion coefficient

temperature
increase from initial
or reference T_0

Then the plane stress Hooke law:

$$\varepsilon_r = \frac{1}{E} (\sigma_r - \nu \sigma_c) + \alpha^* \Delta T$$

$$\varepsilon_c = \frac{1}{E} (\sigma_c - \nu \sigma_r) + \alpha^* \Delta T$$

5. Temperature and its gradient (2/7)

$$r \cdot \frac{d\epsilon_c}{dr} + (\epsilon_c - \epsilon_r) = 0$$

$$\frac{d\epsilon_c}{dr} = \frac{1}{E} \frac{d}{dr} (\sigma_c - v \sigma_r) + \alpha^* \frac{d(\Delta T)}{dr}$$

$$(\epsilon_c - \epsilon_r) = \frac{1}{E} (1 + v) (\sigma_c - \sigma_r) \quad r \cdot \frac{d\sigma_r}{dr} + (\sigma_r - \sigma_c) = 0$$

$$r \left(\frac{d\sigma_c}{dr} - v \frac{d\sigma_r}{dr} \right) + (1 + v) r \frac{d\sigma_r}{dr} + r E \alpha^* \frac{d(\Delta T)}{dr} = 0$$

$$\frac{d}{dr} (\sigma_c + \sigma_r) = -E \alpha^* \frac{d(\Delta T)}{dr}$$

$$\frac{d}{dr} \left[\frac{1}{r} \frac{d}{dr} (r^2 \sigma_r) \right] = -E \alpha^* \frac{d(\Delta T)}{dr}$$

(Develop as in
Ch. 2 Sect. 5)

5. Temperature and its gradient (3/7)

This can be integrated only if the function $\Delta T(r)$ is known.

A simple approach interpolates temperature with a polynomial:

$$\Delta T = \sum_{k=0}^n a_k \left(\frac{r}{r_e} \right)^k$$

In the case of tubes, where heat is transmitted by conduction through the wall, the well known solution is:

$$\Delta T = \frac{\Delta T_e \ln\left(\frac{r}{r_i}\right) + \Delta T_i \ln\left(\frac{r_e}{r}\right)}{\ln\left(\frac{r_e}{r_i}\right)} = a \ln r + b \quad \frac{d(\Delta T)}{dr} = \frac{a}{r}$$

$$a = \frac{\Delta T_e - \Delta T_i}{\ln\left(\frac{r_e}{r_i}\right)} \quad b = \frac{-\Delta T_e \ln r_i + \Delta T_i \ln r_e}{\ln\left(\frac{r_e}{r_i}\right)}$$

5. Temperature and its gradient (4/7)

In a numerical approach it is convenient to split the disc in smaller elements, and interpolate linearly the temperature inside each of them. The **linear temperature interpolation** produces:

$$T = T_i + \frac{T_e - T_i}{r_e - r_i} (r - r_i) ; \Delta T = T - T_0 \quad (T_0 \text{ reference temperature})$$

$$\frac{d}{dr}(\Delta T) = \frac{T_e - T_i}{r_e - r_i}$$

Then the final differential equation is:

$$\frac{d}{dr} \left[\frac{1}{r} \frac{d}{dr} (r^2 \sigma_r) \right] = -E\alpha^* \frac{d(\Delta T)}{dr} = -E\alpha^* \frac{T_e - T_i}{r_e - r_i}$$

... ...

$$r^2 \sigma_r = -E\alpha^* \frac{T_e - T_i}{r_e - r_i} \frac{r^3}{3} + Ar^2 + B$$

5. Temperature and its gradient (5/7)

... which gives the radial stress:

$$\sigma_r = -E\alpha^* \frac{T_e - T_i}{r_e - r_i} \frac{r}{3} + A + \frac{B}{r^2}$$

Applying the equilibrium equation, stress σ_c is obtained:

$$\frac{d}{dr}(r\sigma_r) - \sigma_c = 0$$

$$\sigma_c = \frac{d}{dr} \left(-E\alpha^* \frac{T_e - T_i}{r_e - r_i} \frac{r^2}{3} + Ar + \frac{B}{r} \right)$$

$$\sigma_c = -E\alpha^* \frac{T_e - T_i}{r_e - r_i} \frac{2r}{3} + A - \frac{B}{r^2}$$

Boundary conditions:

$$r=r_i \rightarrow \sigma_r = 0 \quad r=r_e \rightarrow \sigma_r = 0$$

then

5. Temperature and its gradient (6/7)

$$-E\alpha^* \frac{T_e - T_i}{r_e - r_i} \frac{r_i}{3} + A + \frac{B}{r_i^2} = 0$$

$$-E\alpha^* \frac{T_e - T_i}{r_e - r_i} \frac{r_e}{3} + A + \frac{B}{r_e^2} = 0$$

By subtraction:

$$B = -\frac{E\alpha^*}{3} (T_e - T_i) \frac{r_e^2 r_i^2}{r_e^2 - r_i^2}$$

Multiplying the first times r_i^2

and the second times r_e^2 :

By subtraction:

$$A = \frac{E\alpha^*}{3} (T_e - T_i) \frac{r_e^2 + r_e r_i + r_i^2}{r_e^2 - r_i^2}$$

$$\sigma_r = \left(\frac{E\alpha^*}{3} \frac{T_e - T_i}{r_e - r_i} \right) \left(\frac{r_e^2 + r_e r_i + r_i^2}{r_e + r_i} - r - \frac{r_e^2 r_i^2}{r_e + r_i} \frac{1}{r^2} \right)$$

$$\sigma_c = \left(\frac{E\alpha^*}{3} \frac{T_e - T_i}{r_e - r_i} \right) \left(\frac{r_e^2 + r_e r_i + r_i^2}{r_e + r_i} - 2r + \frac{r_e^2 r_i^2}{r_e + r_i} \frac{1}{r^2} \right)$$

5. Temperature and its gradient (7/7)

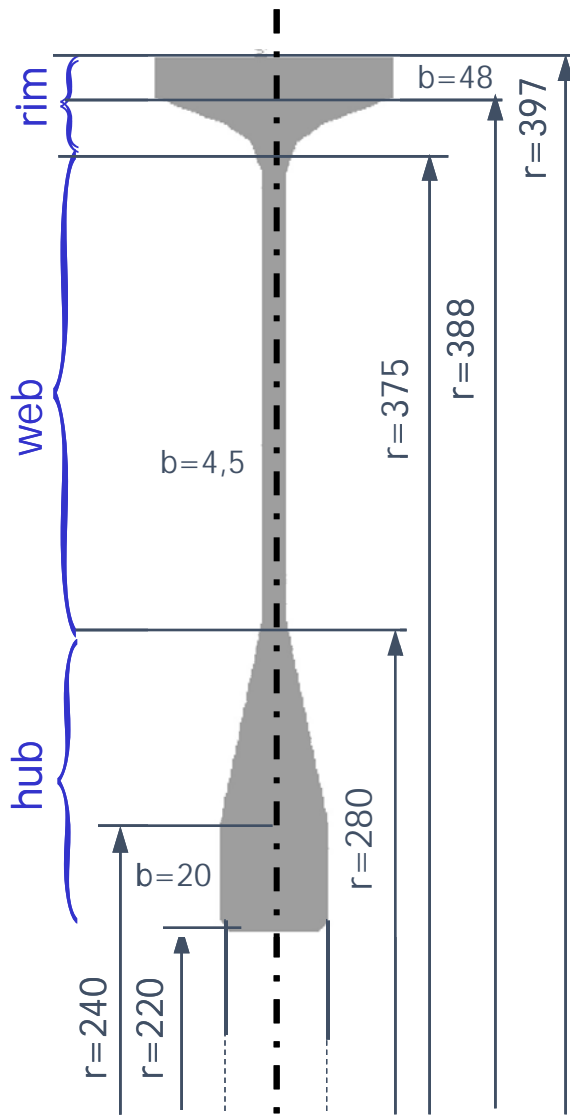
From:

$$u^T = r \varepsilon_c = r \frac{1}{E} (\sigma_c - v \sigma_r)$$

the displacement at diameter D, where the temperature is T :

$$u^T = \frac{D \alpha^*}{2} \frac{T_e - T_i}{3} \left[\frac{\left(1 - v\right) \frac{1 + \frac{D_i^2}{D_e^2} + \frac{D_i}{D_e}}{1 + \frac{D_i}{D_e}} - \left(2 - v\right) \frac{D}{D_e} + \dots}{\dots + \left(1 + v\right) \frac{\frac{D_i^2}{D_e^2} \frac{D_e^2}{D^2}}{1 + \frac{D_i}{D_e}}} + \frac{D}{2} \alpha^* (T - T_0) \right]$$

6. Case study of stresses in a turbine disc (1/10)



A rotating disc of a turbine disc is shown here (grey shape)

Bore radius: 220 mm

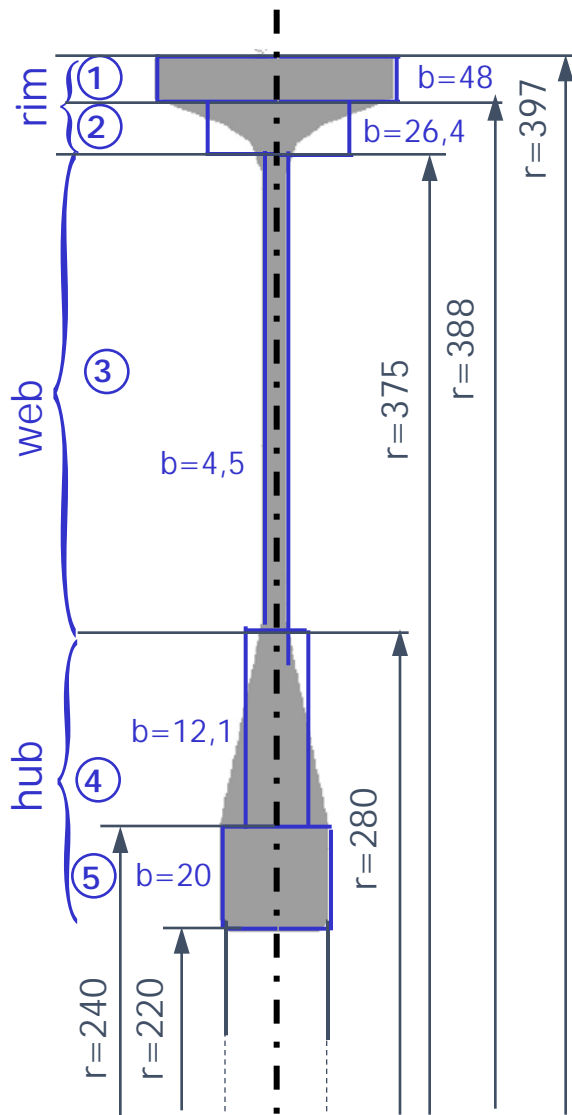
Outer radius at blade support: 397 mm

Hub: from bore dia. to 280 mm, tapered (linear approximation) from 240 mm

Web: from 280 mm to 375 mm

Rim: from 375 mm to outer dia, tapered (linear approximation) up to 397 mm

6. Case study of stresses in a turbine disc (2/10)



The disc cross-section is here shown (grey shape) together with its Grammel approximation (blue lines) in five constant thickness rings, or annular elements numbered 1 to 5.

Cylindrical sections are represented by cylindrical rings of the same thickness.

Tapered sections have a trapezoidal cross-section. They are approximated by a cylindrical ring whose thickness is calculated so that the total ring mass – i.e. volume too – is preserved.

The thickness formula to be employed is therefore:

$$b = \frac{b_i + b_e}{r_i + r_e} \left(r_i + \frac{r_e - r_i}{3} \cdot \frac{b_i + 2b_e}{b_i + b_e} \right)$$

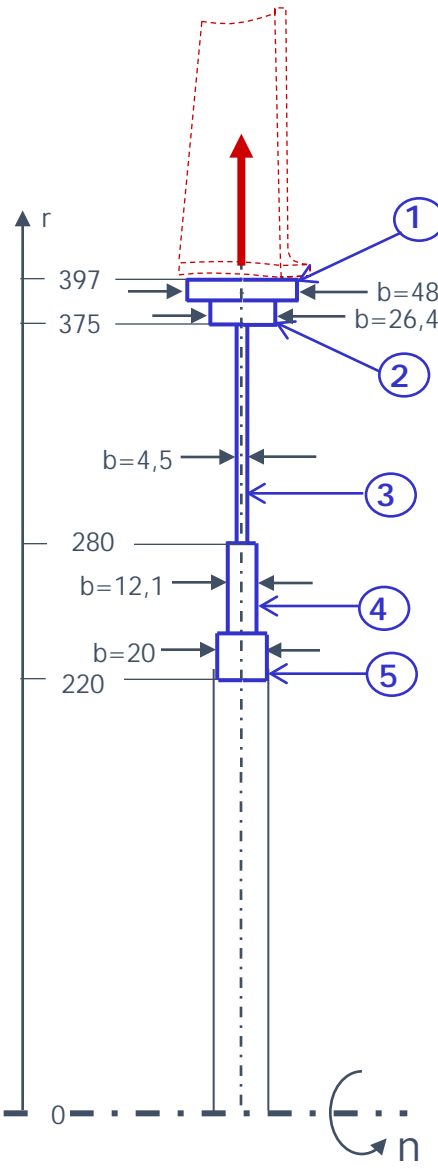
r_i = ring inner radius

r_e = ring outer radius

b_i = inner thickness

b_e = outer thickness

6. Case study of stresses in a turbine disc (3/10)



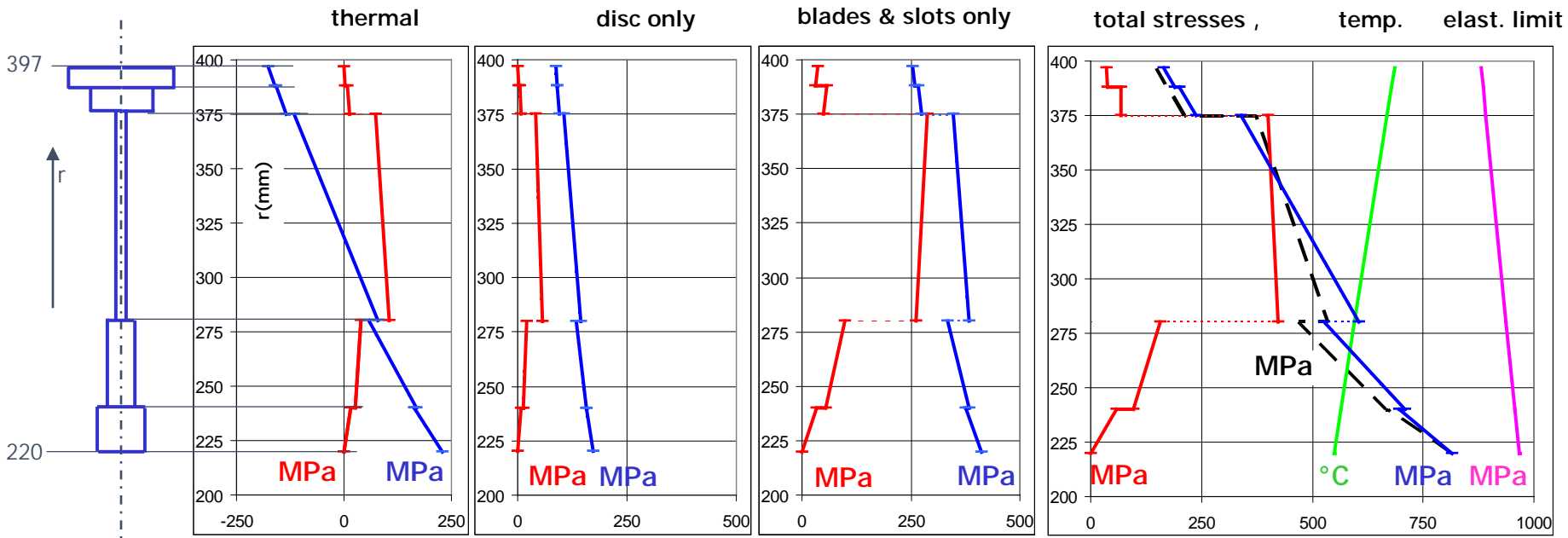
Some numerical examples will now be discussed in order to help grasp the essential in the shaping of a disc and related stresses towards its strength optimisation.

Data is:

$n = 3646$	rpm	rotation speed
$\rho = 8220$	kg/m^3	disc density
$E = 1,74 \cdot 10^5$	MPa	Young modulus (average)
$\alpha = 1,5 \cdot 10^5$	$^\circ\text{C}^{-1}$	thermal expansion coefficient
$M_b = 58,30$	kg	total mass of blades & slots
$M_d = 33,95$	kg	total disc mass
$\sigma_{r,e} = 36,1$	MPa	outer radius tensile stress (blade & slot pull)
$T = \text{profile}$	$^\circ\text{C}$	temperature: profile with radius (assumed linear: diagram in slide 9)
$R_{p0,2} = \text{profile}$	MPa	yield strength: profile with T and radius assumed linear (diag. in slide 9).

Disc cooling conditions are not discussed here (see Sect. 8, sl. 5, 6). Material properties are representative of those of INCONEL 718.

6. Case study of stresses in a turbine disc (4/10)



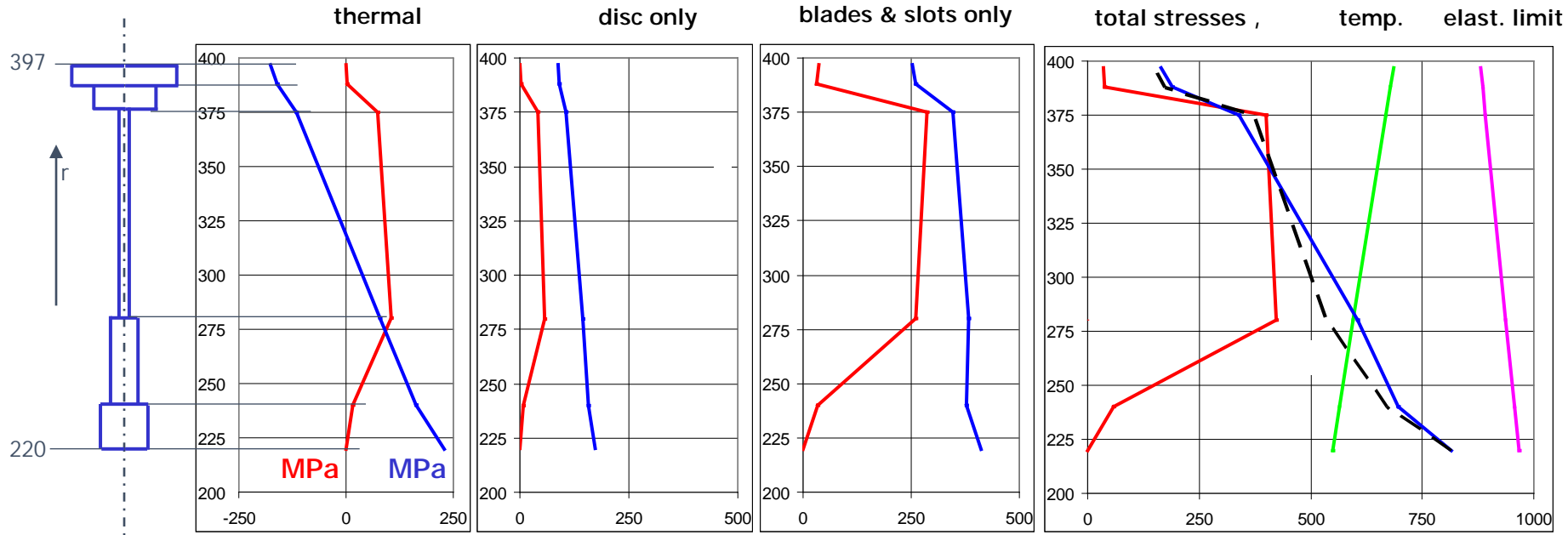
The diagrams above show stresses (horizontal axis) vs. radius r (vertical axis); the rightmost diagrams show also T , temperature, and $R_{p0,2}$, the elastic limit.

The jumps of stresses are here left in evidence.

The jump in this Sect. 6, are the discrete cylinder stepwise approximation of sl. 2. depends on the model discretisation, i.e., from the jump of thickness b when passing from b_k of element k to b_{k+1} of element $k+1$ (see Sect. 4 sl. 11 of this Chapter) which, in this Sect. 6, are the discrete cylinder stepwise approximation of sl. 2.

σ_r	(MPa)
σ_c	(MPa)
$\sigma_{eq(V. Mises)}$	(MPa)
$R_{p0,2}$	(MPa)
T	(°C)

6. Case study of stresses in a turbine disc (5/10)



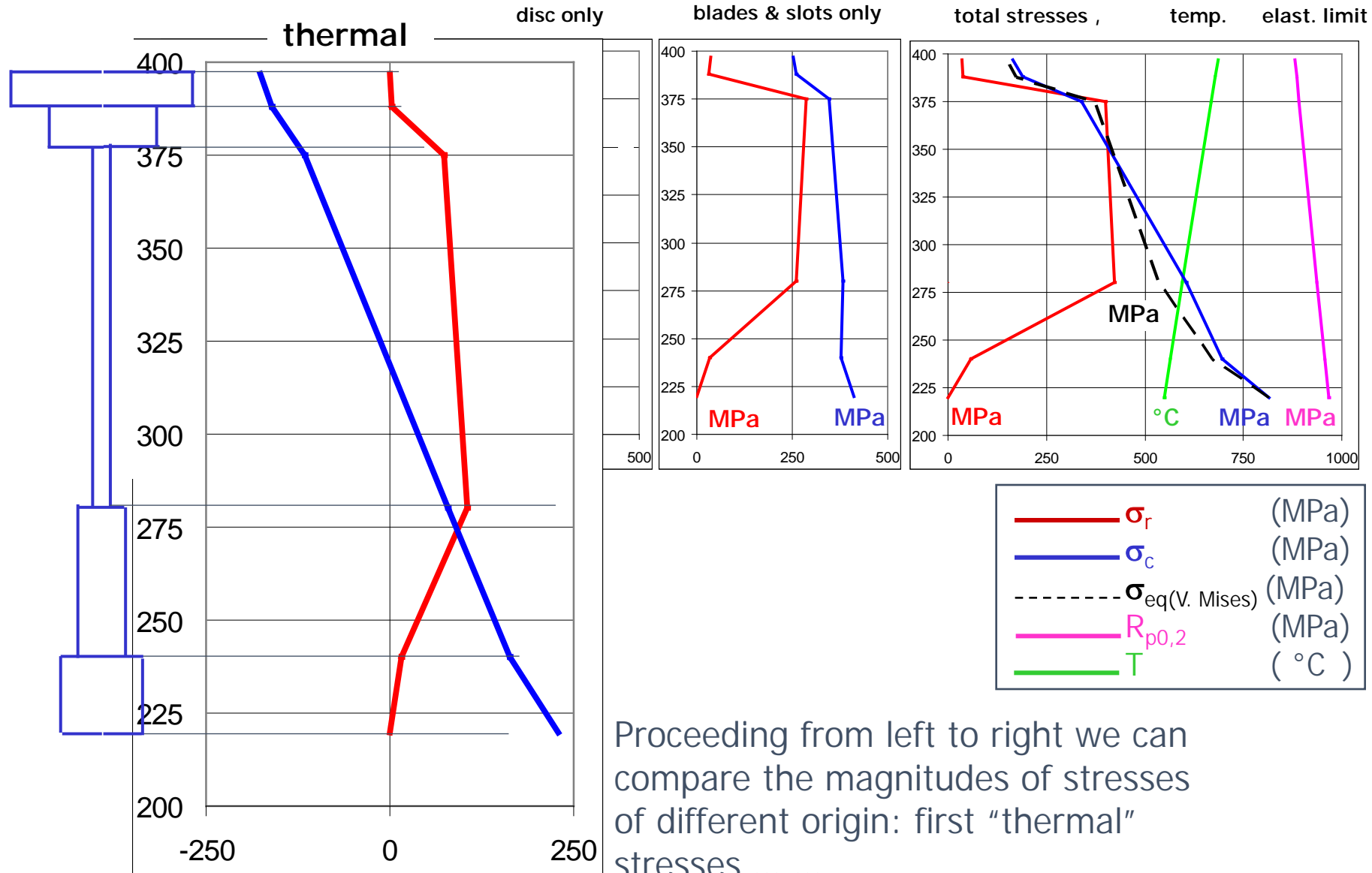
Of course, the real disc stresses will vary over the thickness in a continuous way, as in the version of the diagrams shown above.

They may be obtained for σ_r radial stresses by dividing the (radial) loads per unit length n by the real local disc thickness. In this example, real thicknesses are those shown in Sect. 6 sl. 1.

This being done, also σ_c (see Sect. 4 sl. 11) will vary without jumps. This representation is preferable to the previous one, and will be used throughout the next slides.

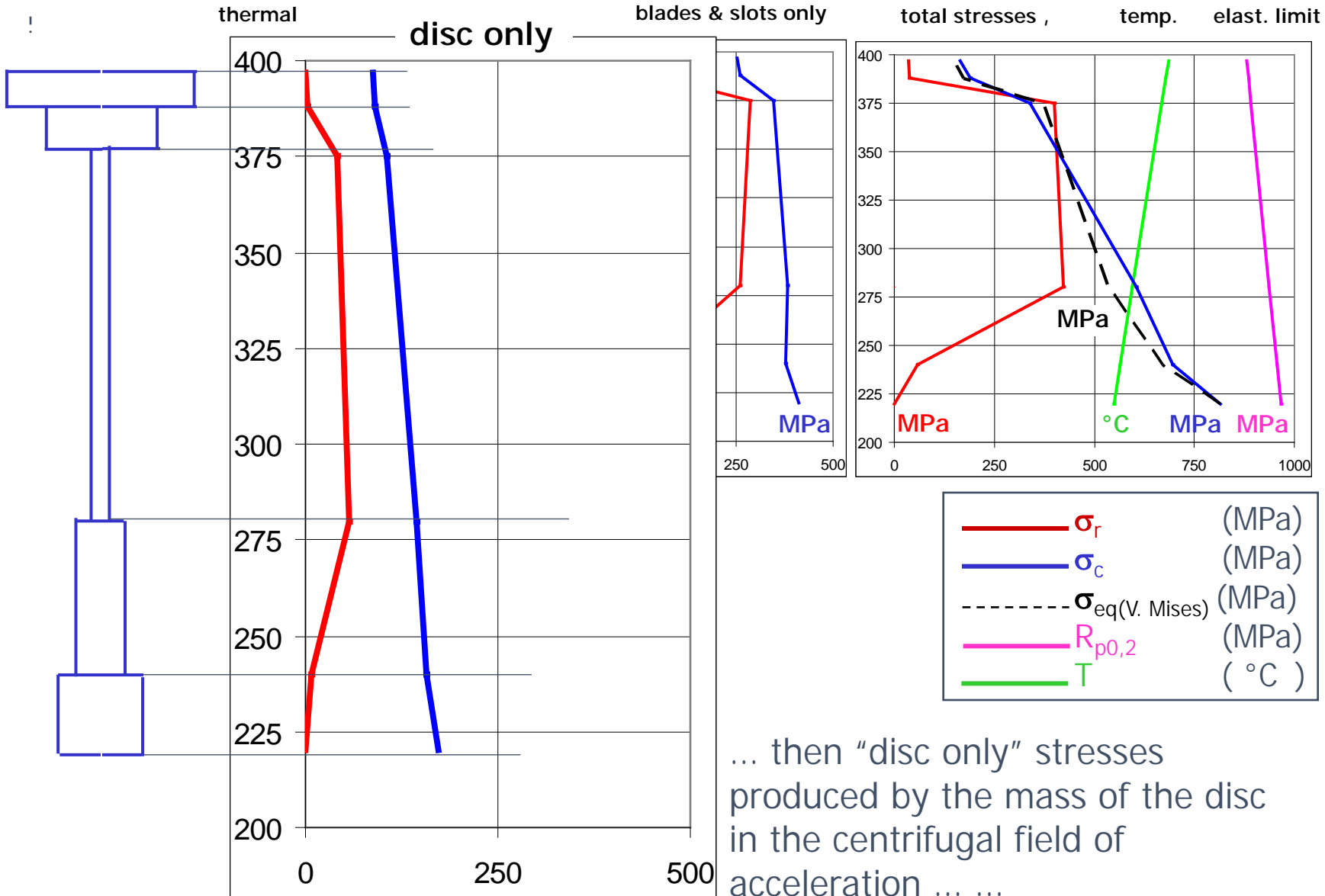
σ_r	(MPa)
σ_c	(MPa)
$\sigma_{eq(V. Mises)}$	(MPa)
$R_{p0,2}$	(MPa)
T	(°C)

6. Case study of stresses in a turbine disc (6/10)

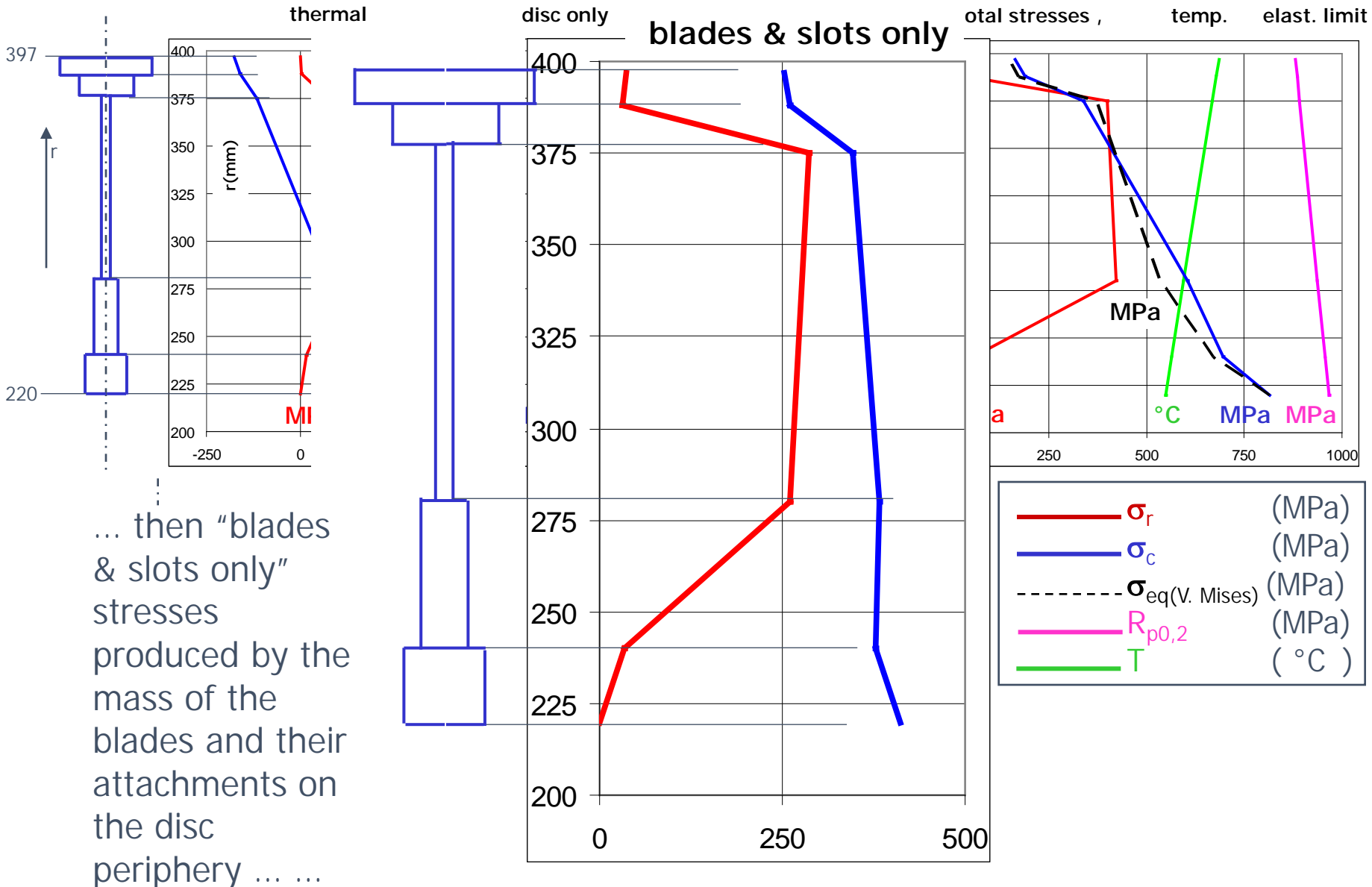


Proceeding from left to right we can compare the magnitudes of stresses of different origin: first "thermal" stresses

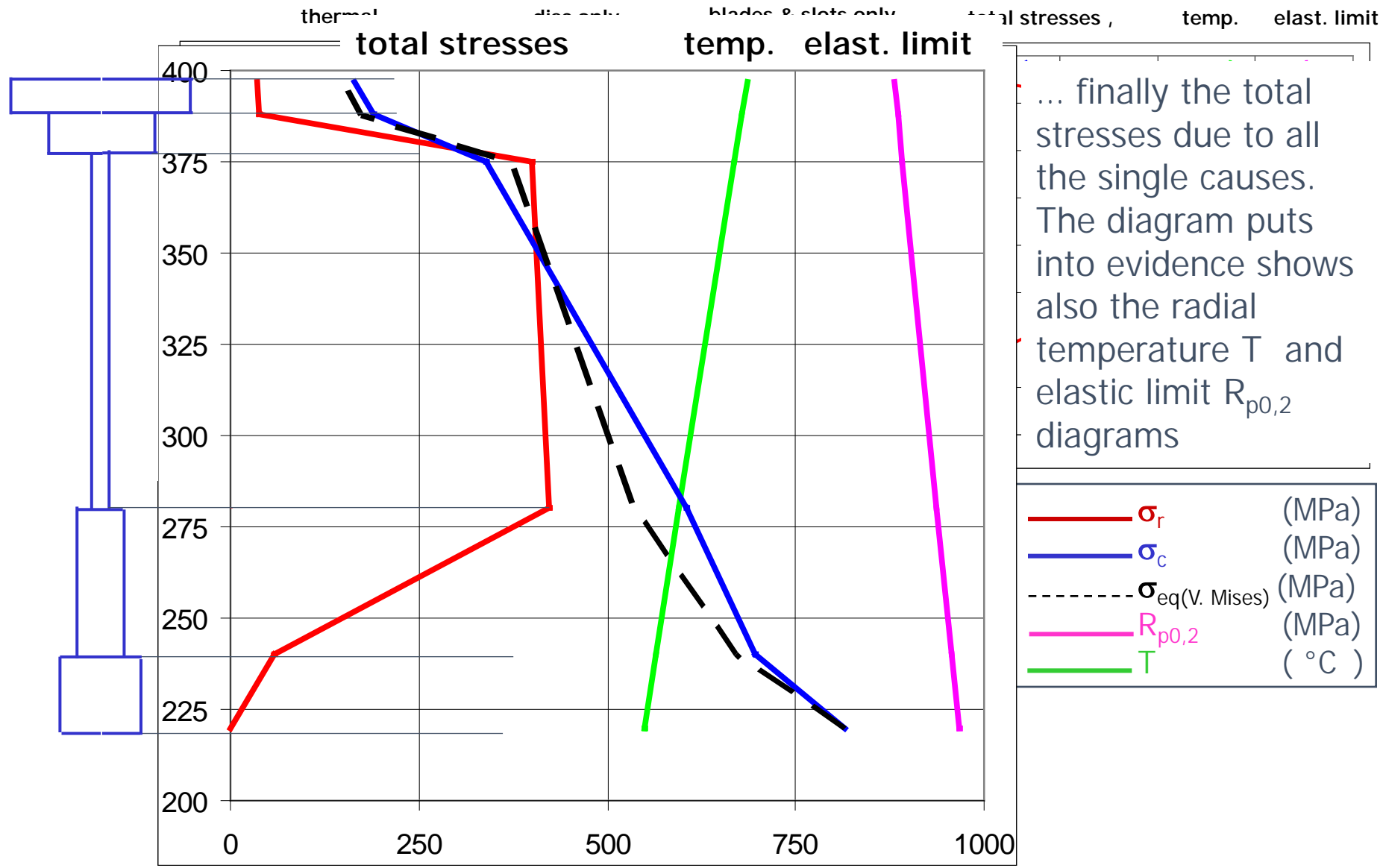
6. Case study of stresses in a turbine disc (7/10)



6. Case study of stresses in a turbine disc (8/10)



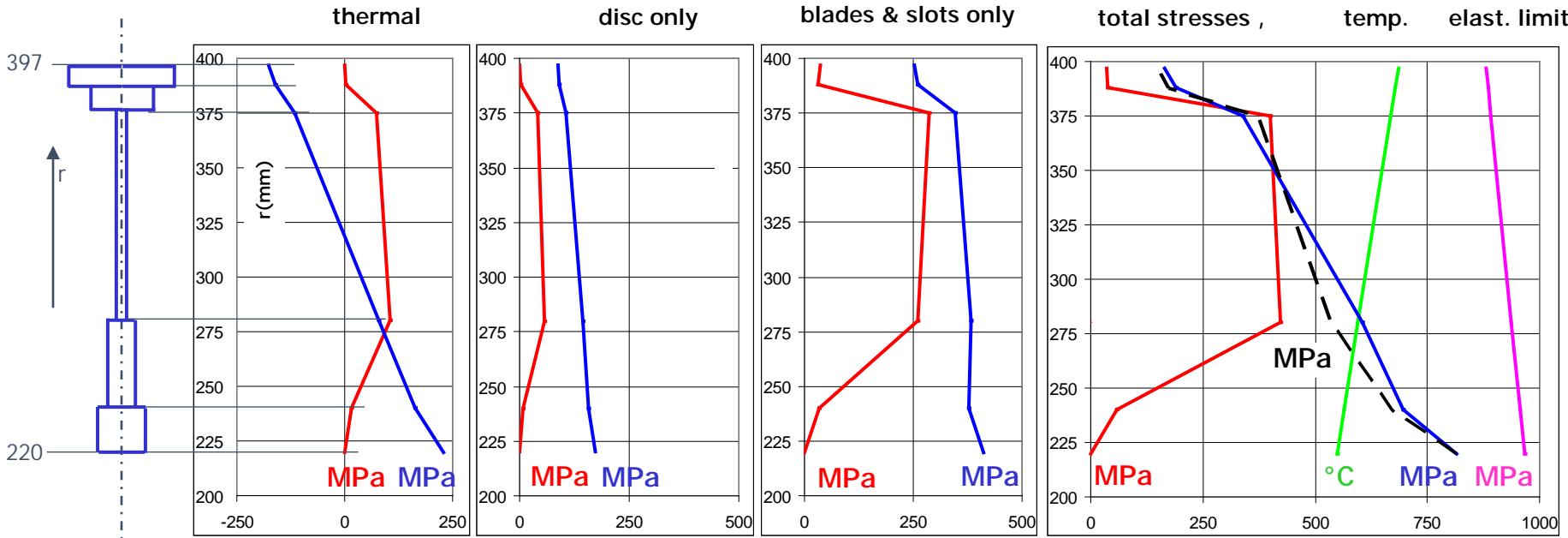
6. Case study of stresses in a turbine disc (9/10)



... finally the total stresses due to all the single causes. The diagram puts into evidence shows also the radial temperature T and elastic limit $R_{p0,2}$ diagrams

σ_r	(MPa)
σ_c	(MPa)
$\sigma_{eq(V. Mises)}$	(MPa)
$R_{p0,2}$	(MPa)
T	(°C)

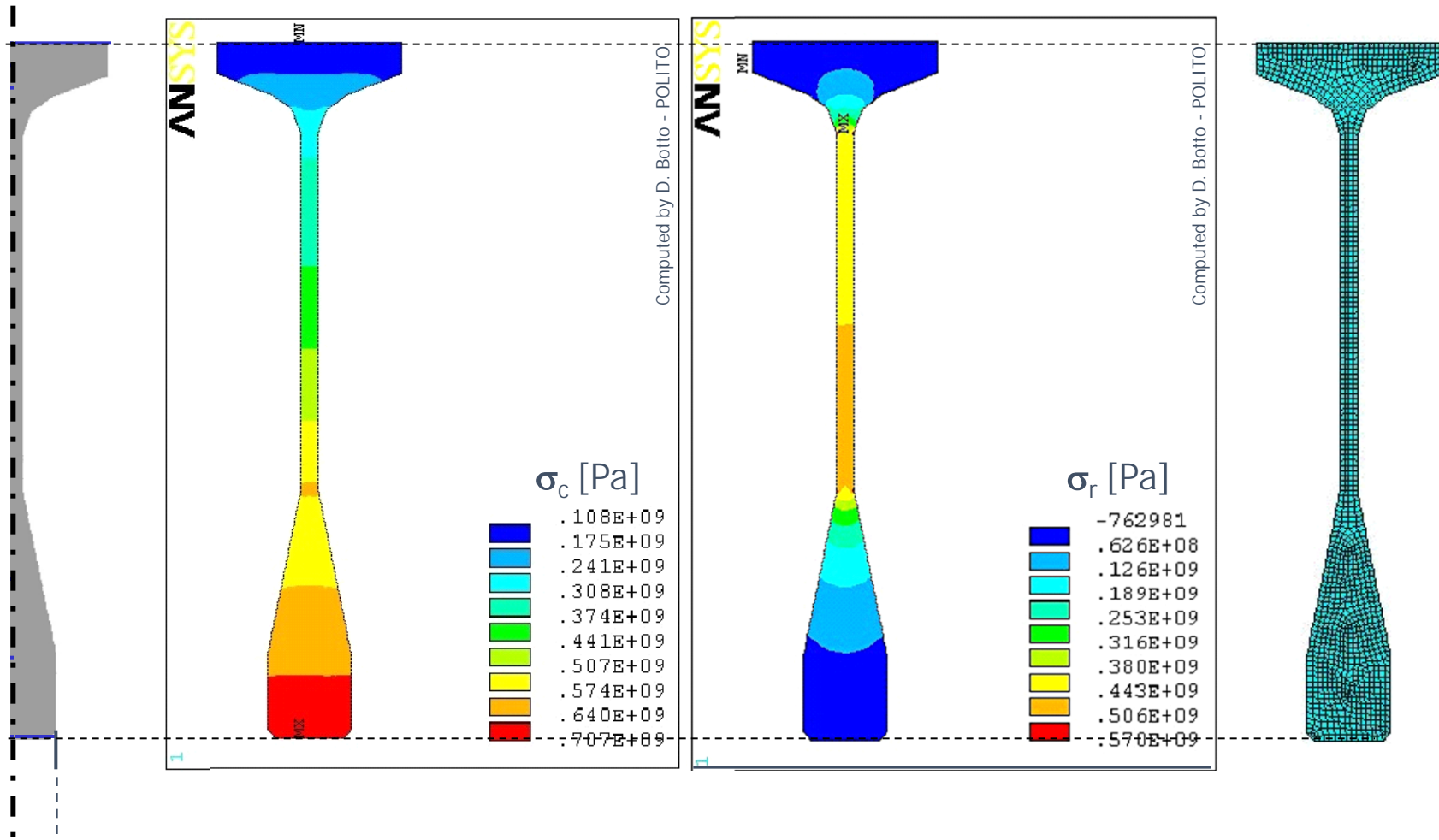
6. Case study of stresses in a turbine disc (10/10)



The stress diagrams should be analysed and commented. Some possible questions:

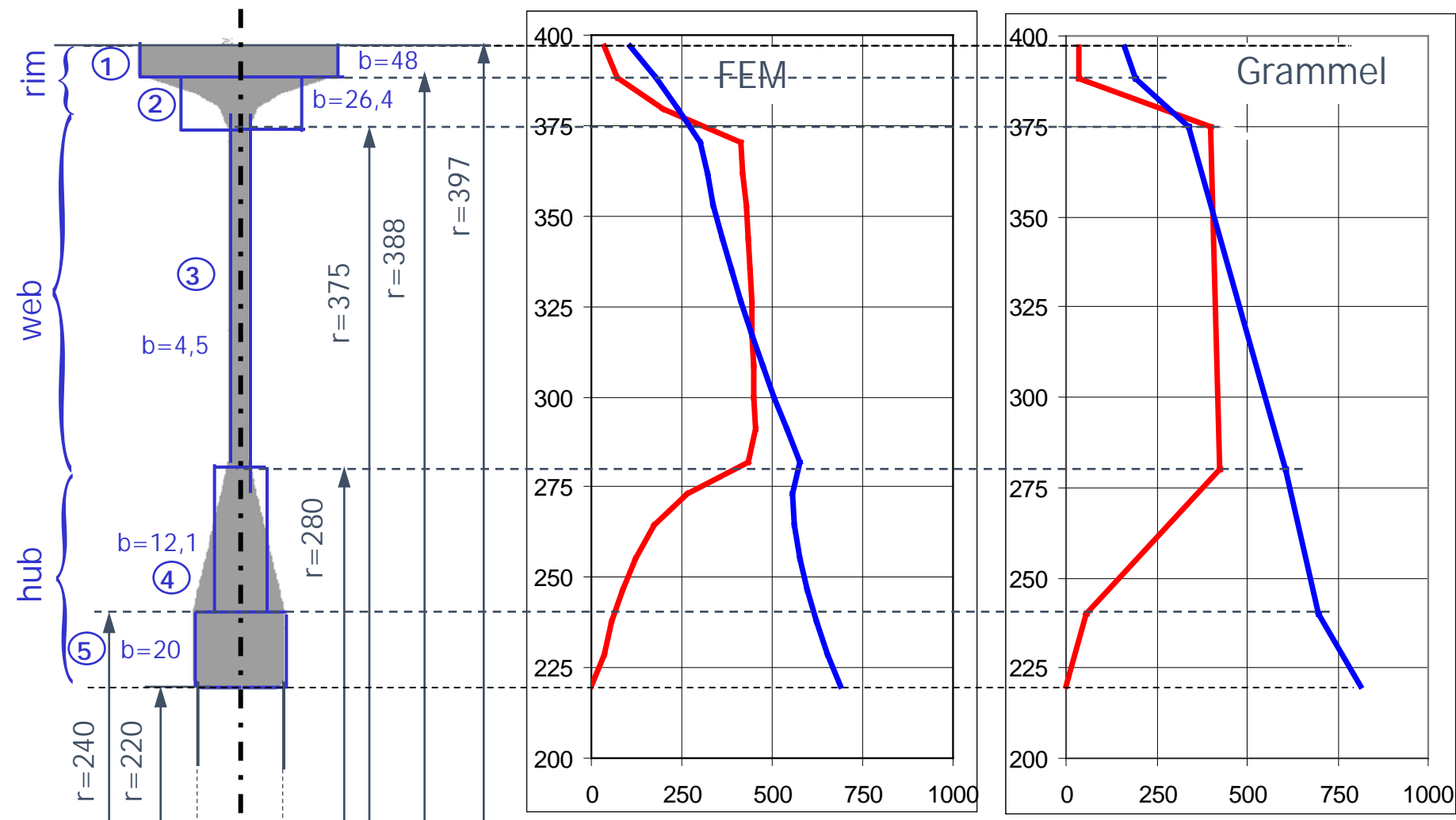
- why do the “thermal” σ_c change sign, and why are they negative at the outer radii?
- why does σ_r start and end zero in “thermal” and “disc only” diagrams?
- how does σ_c compare in the “thermal”, “disc only” and “blades & slots only” cases?

7. Comparison between Grammel and FEM (1/3)



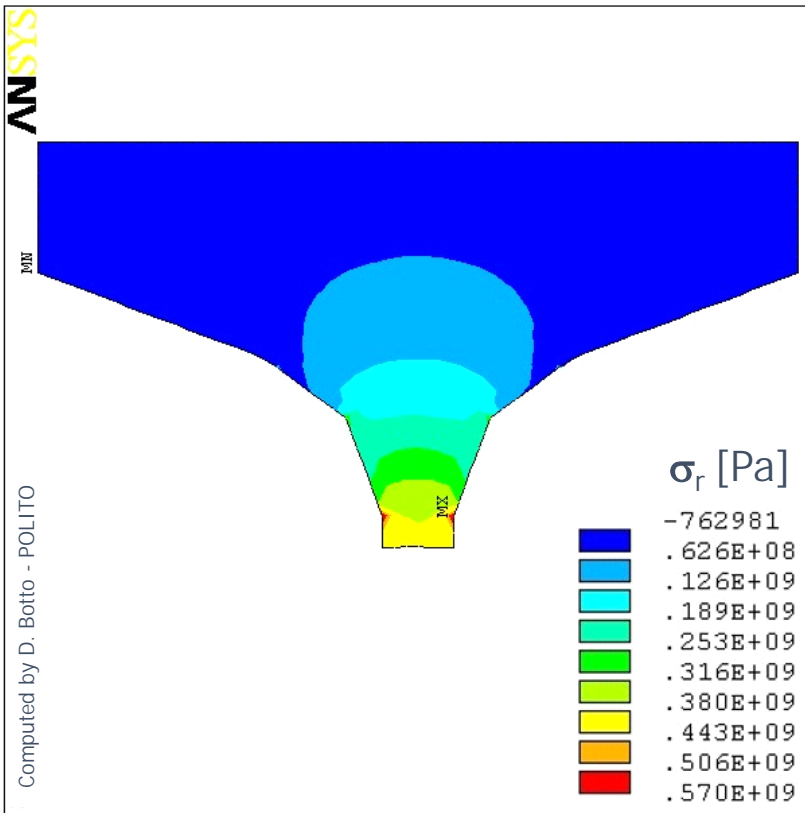
Colour maps of hoop and radial stress calculated with the finite element model shown on the right. Next slide will show diagrams of stress values along the disc central symmetry radius.

7. Comparison between Grammel and FEM (2/3)



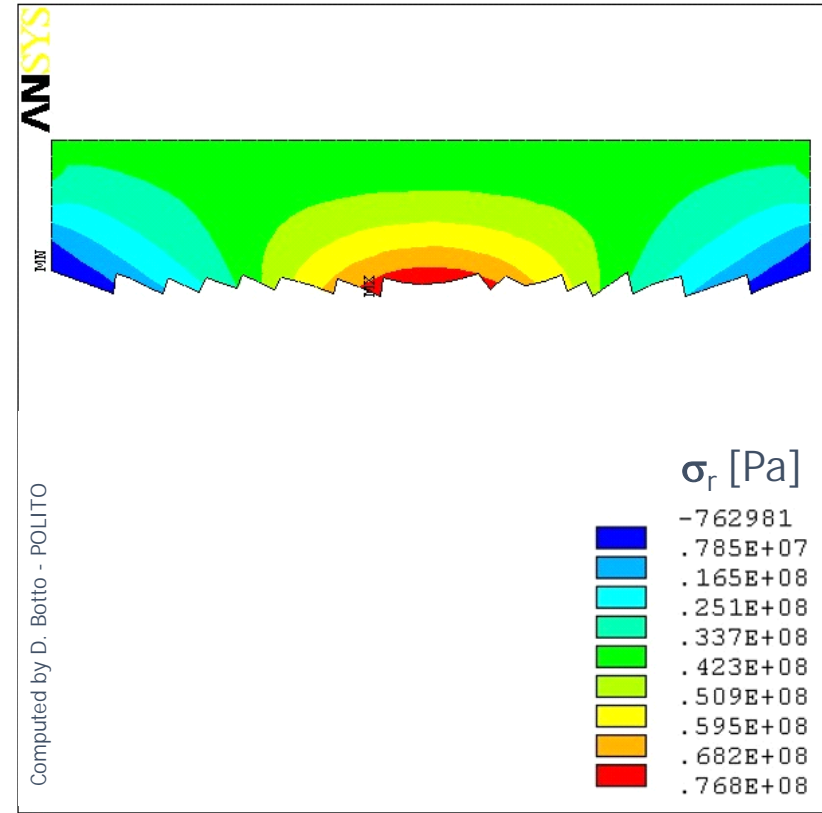
Comparison of Finite Elements results (on the centre symmetry axis) and Grammel results. Remark the differences due to modelling approximations.

7. Comparison between Grammel and FEM (3/3)



Details at the rim-web transition.
Colour map of radial stress on the rim area; stress gradients on the web-to-ring connection and local shape effects.

The limitation of Grammel is its being one-dimensional; FEM, on the contrary, gives stresses in two dimensions and therefore captures all local effects due to shape.



The rim is shown without web connection; the map is rescaled allowing to show gradients near the rim upper surface.

8. The shape of a turbine disc - elastic stresses (1/8)

This Section aims at exploring which is the best shape to be given to a certain rotating disc.

The next slide compares the disc examined so far with another one having the same bore (inner) and rim (outer) diameter, the same total disc mass ($\sim 33,95$ kg) but a different thickness distribution:

- the rim is kept at the same geometry in width (constrained by blade axial width) and in thickness
- the web and the hub are given the same thickness at 7,58 mm

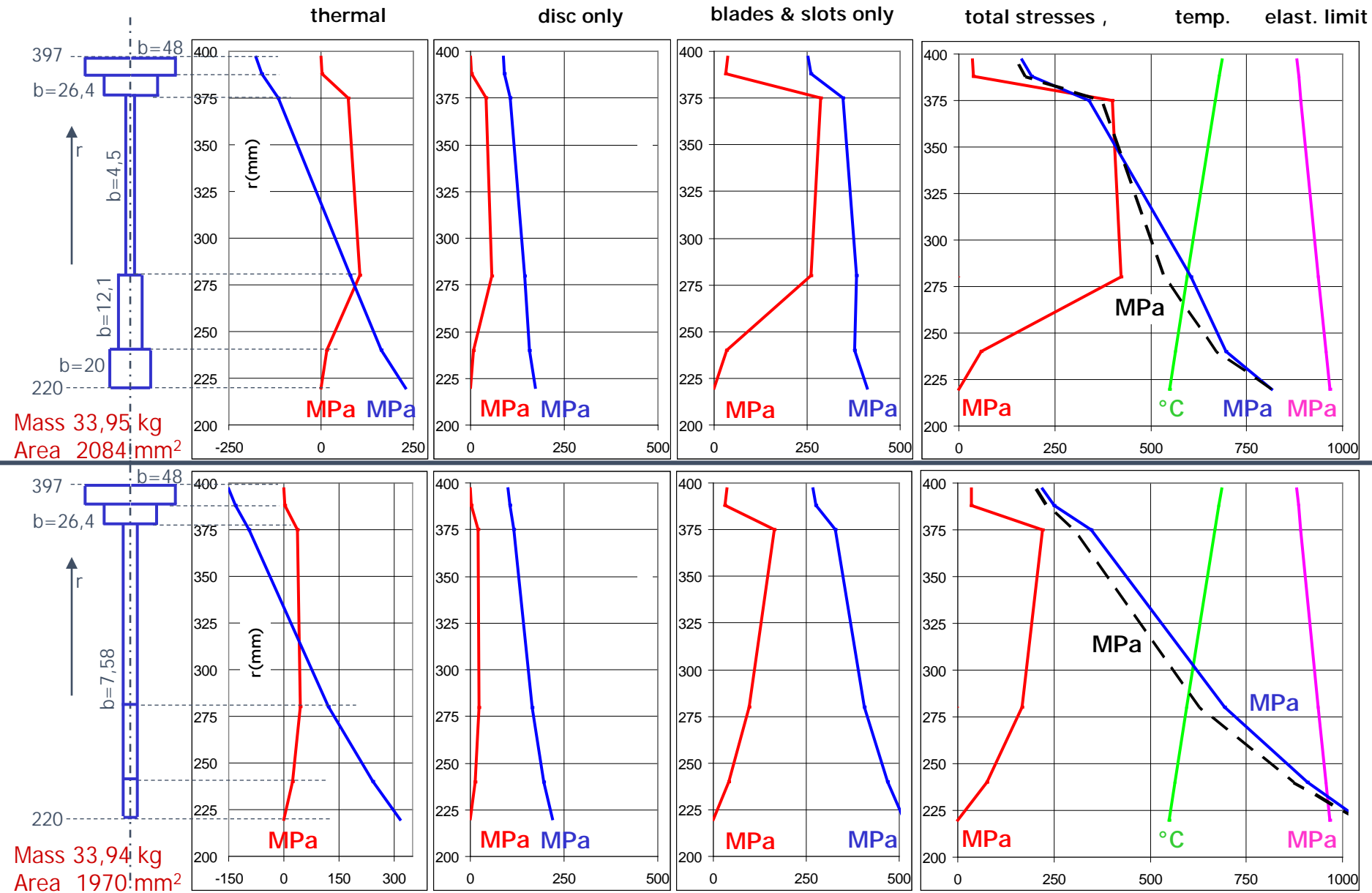
The stress diagrams show that **it is a better idea to have a thicker hub**, i.e. having more mass at a lower radius then subjected to lower centrifugal forces and to lower temperatures, reduces the maximum tensile stress, which is the circumferential (or "hoop") stress σ_c at the inner radius, by the following amounts:

- thermal (gradient) stresses: 230 vs. 316 MPa, i.e. -86 MPa
- disc only stresses: 173 vs. 218 MPa, i.e. -45 MPa
- blades & slots only stresses: 412 vs. 514 MPa, i.e. -102 MPa

Total: 815 MPa
vs. 1048 MPa, i.e.
-233 MPa

The rationale for a thick hub is then that if more mass, and the resulting cross-section area, is placed at lower radii, then it is less stressed by centrifugal forces; it has lower circumferential stress due to its own mass and can provide an amount of strength to take the radial pull of web, rim and blades (and connecting slots).

8. The shape of a turbine disc - elastic stresses (2/8)



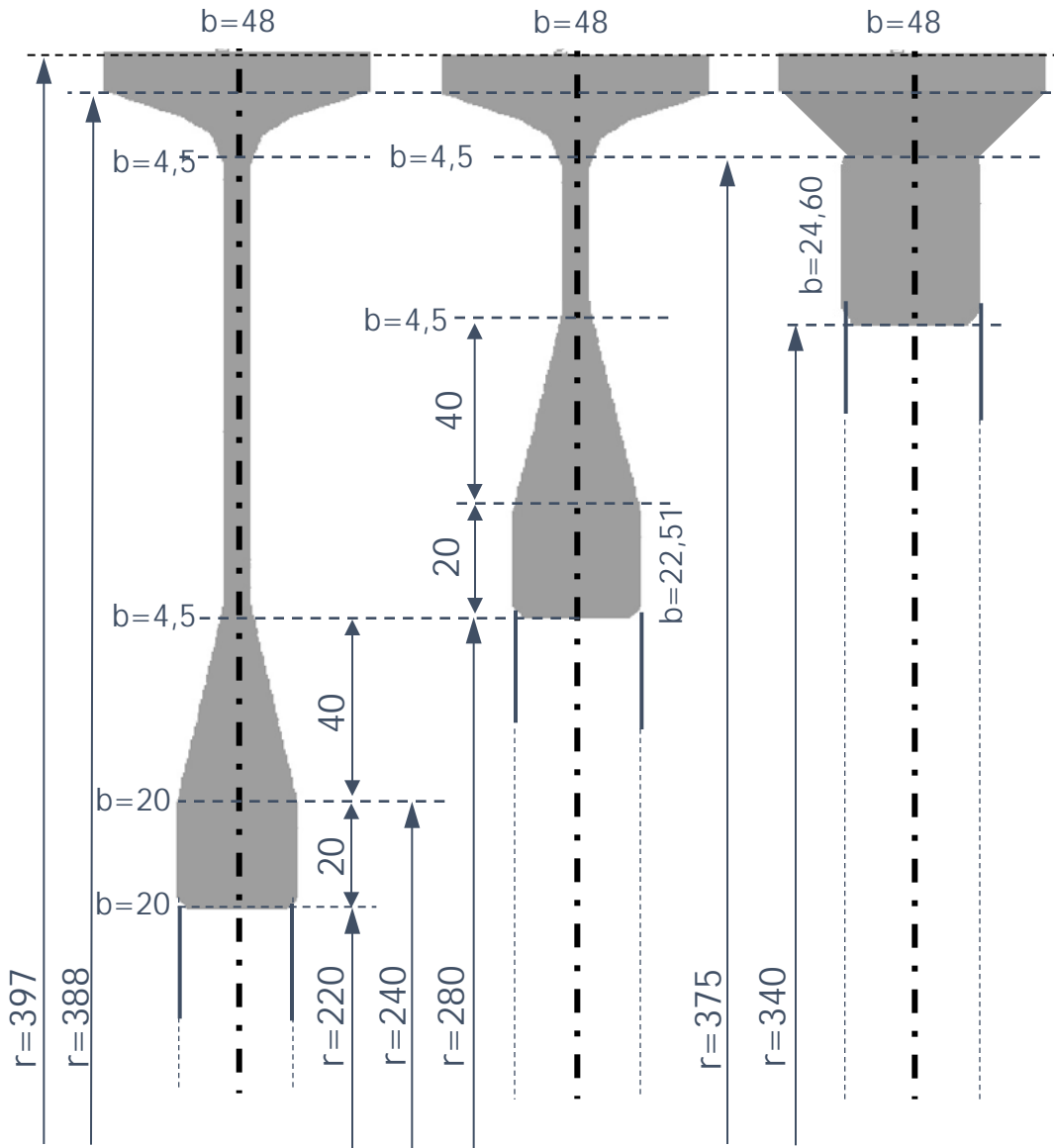
8. The shape of a turbine disc - elastic stresses (3/8)

In summary, keeping the same inner radius but moving some mass toward the centre reduces all stresses at the inner radius, "thermal", "disc mass" and "blades & slots mass" for three reasons:

- first - because it simply adds more area where stresses are highest, i.e. at the inner radius with an important effect on maximum thermal stress, reduced from $\sigma_c=316$ to $\sigma_c=230$ MPa, and on "blades & slots" stress, $\sigma_c=514$ to $\sigma_c=412$ MPa
- second - moving mass at lower radii implies less centrifugal force separating the "half disc" ($5,182 \cdot 10^5$ N in the $b=20$ mm hub case vs. $5,404 \cdot 10^5$ N with uniform thickness $b=7,58$ mm).
- third - at equal total volume and mass, the diametral cross-section area increases when we move the mass toward lower radii (here: 2084 mm^2 vs. 1970 mm^2), a further advantage for σ_c because the "half disc" sum of all centrifugal forces is spread on a larger area.

The combined effect of all these elements produces the noted σ_c reduction from 1048 to 815 MPa.

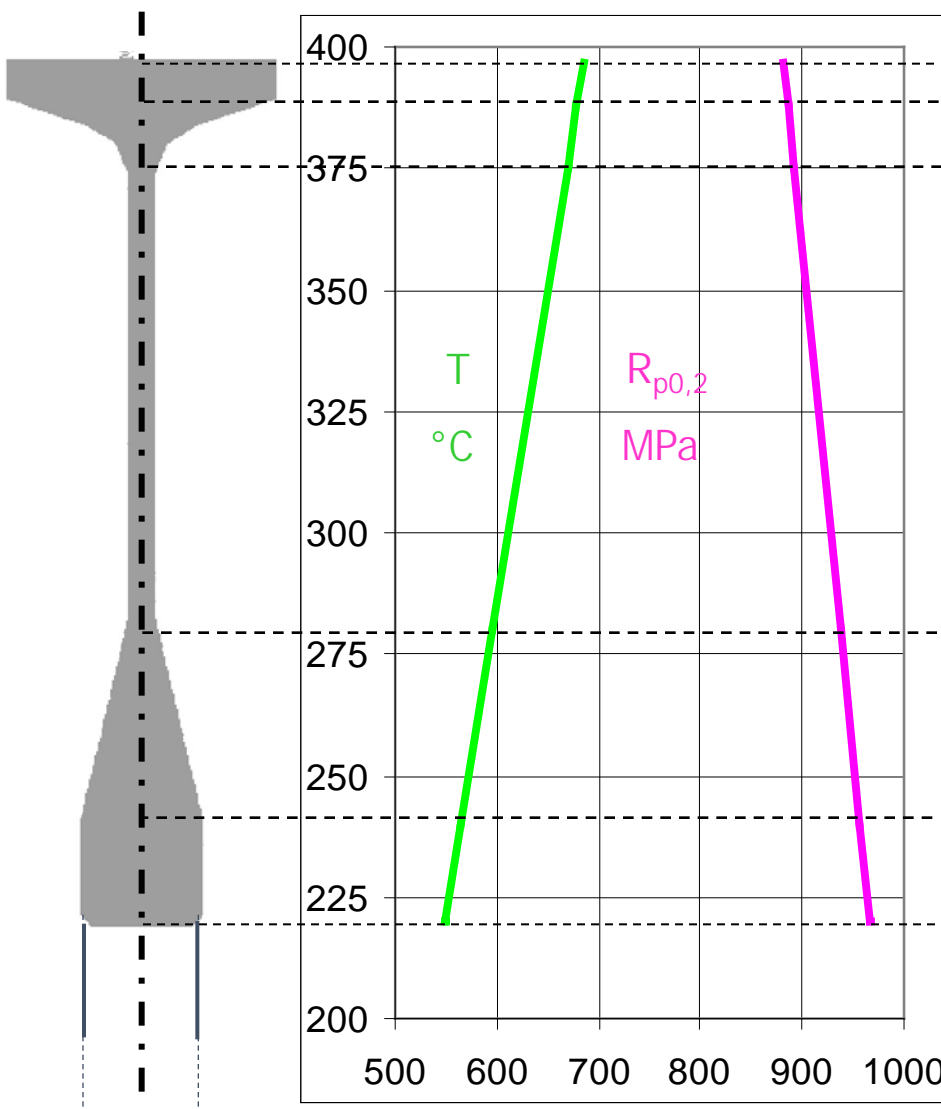
8. The shape of a turbine disc - elastic stresses (4/8)



The next slides explore the effect of placing the same mass (33,95 kg) at different radii.

Three geometries are explored with increasing bore diameter, according to the strategy shown on the left: the bore radius is increased by 60 mm steps, the web is then shortened, and the hub thickness must be (slightly) increased in order to obtain the equal total disc mass.

8. The shape of a turbine disc - elastic stresses (5/8)



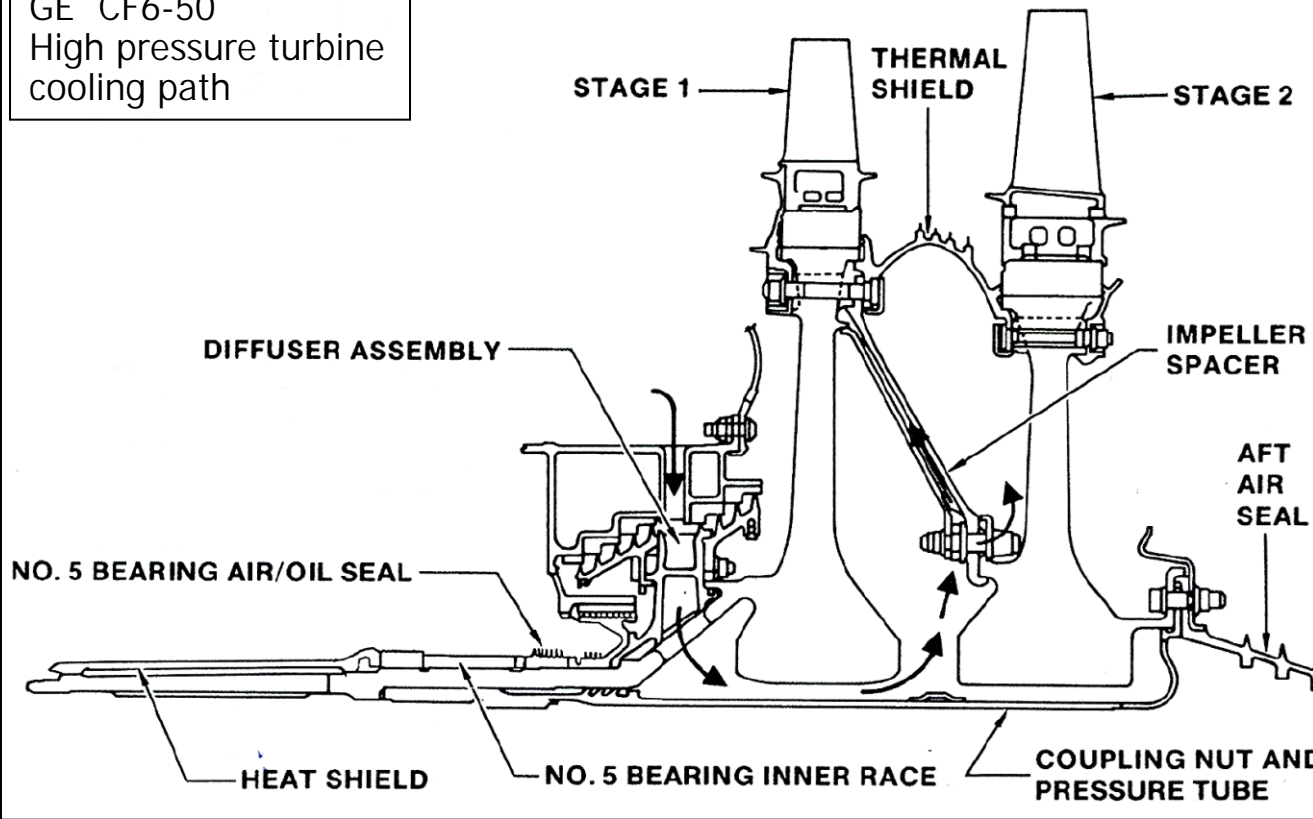
In all the diagrams that will follow, the assumption is made that the disc temperature follows the same profile (equal temperature at equal radius).

This may be a rough assumption since cooling conditions change markedly.

Here again both the real temperature profile and yield strength are approximated, for educational purposes, via a linear interpolation.

8. The shape of a turbine disc - elastic stresses (6/8)

GE CF6-50
High pressure turbine
cooling path



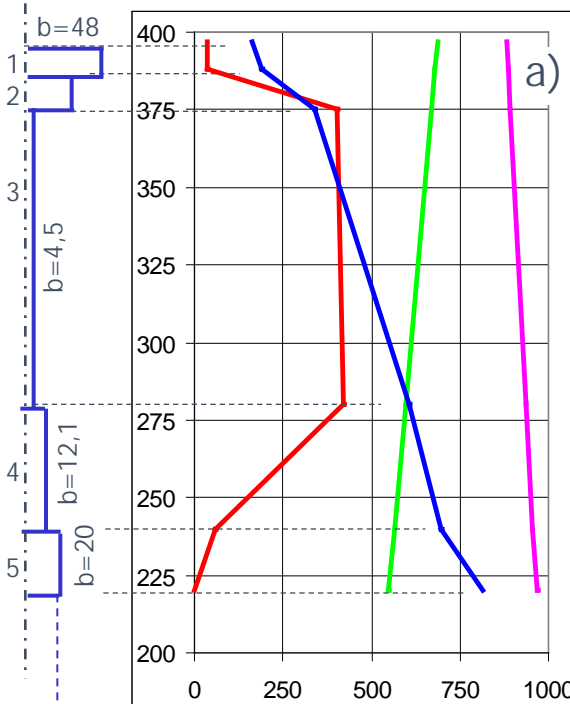
Of course this assumption of linearly varying temperature is too rough, and not realistic, because the intentional cooling obtained by bleeding air on the inner part of the disc cannot be effective if the disc does not extend sufficiently away from the hottest blade area.

So, in the real case, in shorter discs we should expect temperatures higher than the ones we assume here.

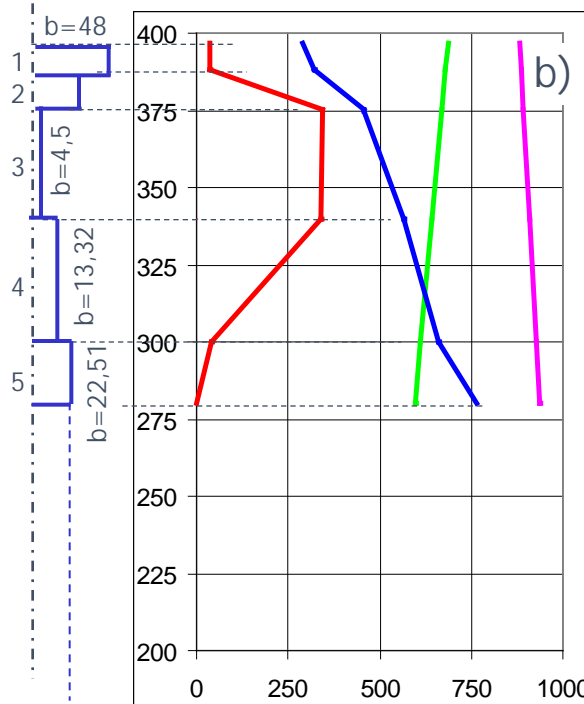
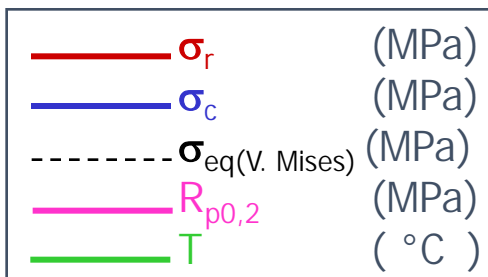
This would bring down the values of $R_{p0,2}$.

Please keep in mind that the subject of disc cooling needs a special expertise in thermal numerical analysis which is not explored in these notes.

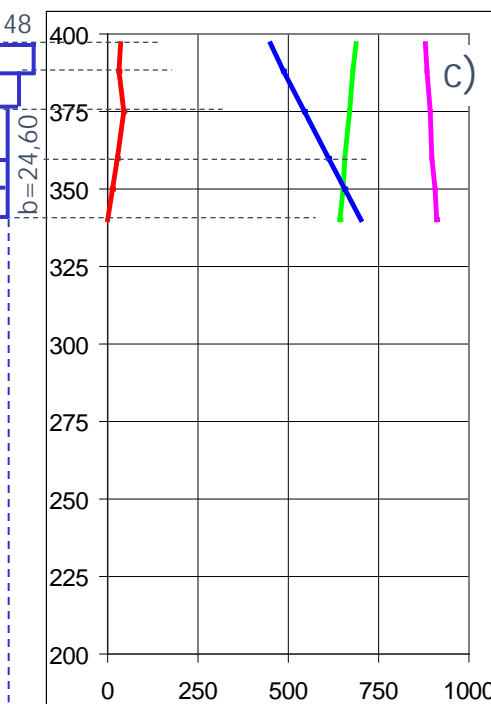
8. The shape of a turbine disc - elastic stresses (7/8)



- 1: $b = 48 \text{ mm}$
- 2: $b = 48 \text{ mm}$
- 3: $b = 4,5 \text{ mm}$
- 4: $b = 20 \text{ mm}$
- 5: $b = 20 \text{ mm}$



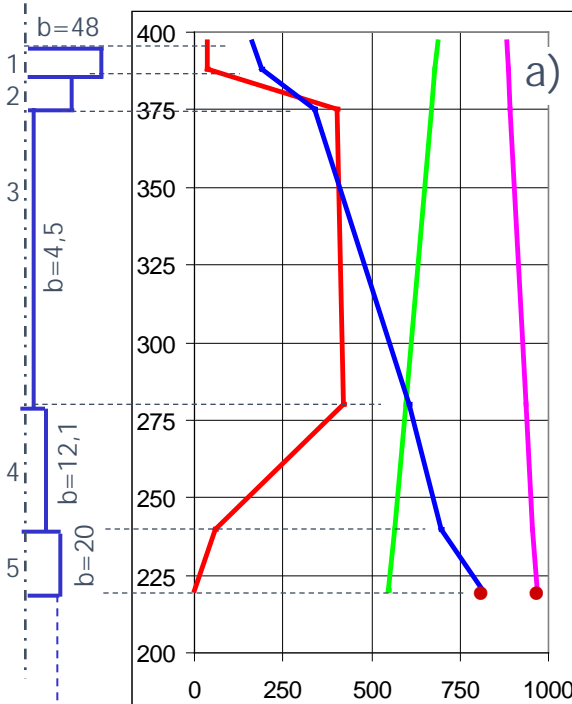
- 1: $b = 48 \text{ mm}$
- 2: $b = 26,37 \text{ mm}$
- 3: $b = 4,5 \text{ mm}$
- 4: $b = 13,32 \text{ mm}$
- 5: $b = 22,51 \text{ mm}$



- 1: $b = 48,00 \text{ mm}$
- 2: $b = 36,37 \text{ mm}$
- 3: $b = 24,60 \text{ mm}$
- 4: $b = 24,60 \text{ mm}$
- 5: $b = 24,60 \text{ mm}$

This slide shows the stepwise geometry of the three discs illustrated in sl. 4 of this Section.
 Disc mass for all cases is 33,95 kg
 The interplay of various thermal and centrifugal factors will become evident through careful inspection of data in next slide.

8. The shape of a turbine disc - elastic stresses (8/8)



max Tresca eq. stress ●: 815 MPa
 $R_{p0,2}$ at ● radius: 966 MPa
 eq. stress / $R_{p0,2}$ ratio: 0,84

At point ● σ_c , due to split causes:

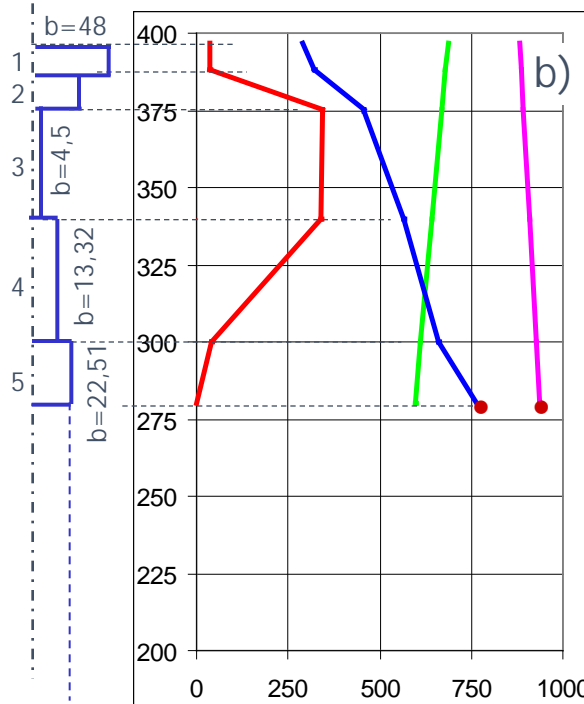
Thermal: 230 MPa

Disc own mass: 173 MPa

Blades & slots: 412 MPa

Total: 815 MPa

Half-disc centr. force: $5,18 \cdot 10^5$ N
 Half blades & slots force: $1,38 \cdot 10^6$ N
 Total diametral cross-section: 4169 mm²
 Total mean hoop stress σ_c : 455 MPa



max Tresca eq. stress ●: 766 MPa
 $R_{p0,2}$ at ● radius: 938 MPa
 eq. stress / $R_{p0,2}$ ratio: 0,82

At point ● σ_c , due to split causes:

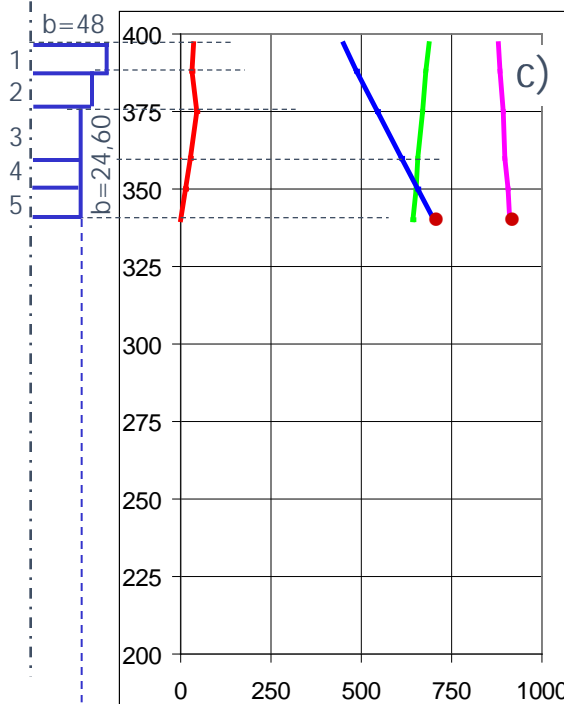
Thermal: 156 MPa

Disc own mass: 182 MPa

Blades & slots: 448 MPa

Total: 766 MPa

Half-disc centr. force: $5,49 \cdot 10^5$ N
 Half blades & slots force: $1,38 \cdot 10^6$ N
 Total diametral cross-section: 3831 mm²
 Total mean hoop stress σ_c : 503 MPa



max Tresca eq. stress ●: 702 MPa
 $R_{p0,2}$ at ● radius: 909 MPa
 eq. stress / $R_{p0,2}$ ratio: 0,77

At point ● σ_c , due to split causes:

Thermal: 78 MPa

Disc own mass: 190 MPa

Blades & slots: 435 MPa

Total: 702 MPa

Half-disc centr. force: $5,88 \cdot 10^5$ N
 Half blades & slots force: $1,38 \cdot 10^6$ N
 Total diametral cross-section: 3532 mm²
 Total mean hoop stress σ_c : 556 MPa

9. Burst design of a turbine disc - plasticity (1/4)

The reason why solution a) is to be preferred to b), and b) to c) is not evident from the elastic stress diagrams, where in fact the maximum hoop stress σ_c decreases slightly moving from solution a) to c). However, remark that this is due to the lower impact of thermal gradients when the disc has a lower radial extension.

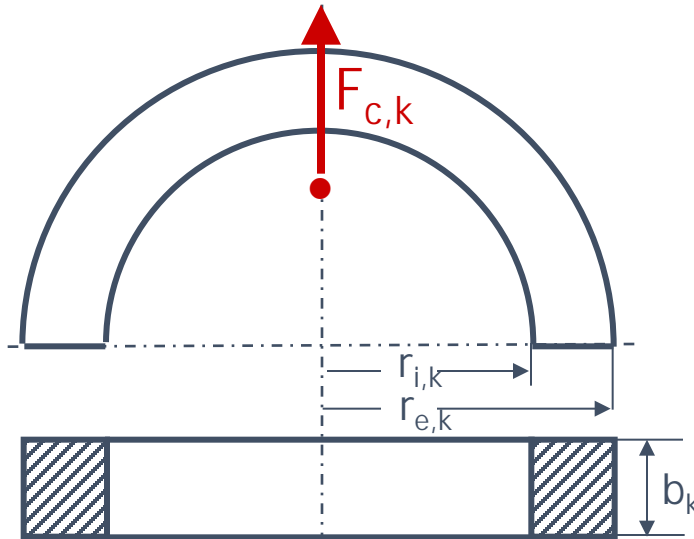
The semi-empirical criterion for design to burst was proposed by **Robinson** (1944)*, and is still used today as a rule-of-the-thumb for design to burst. It assumes that the disk will burst when the average hoop nominal stress $\sigma_{c,m}$ equals the tensile strength of the material R_m .

It is a very elementary example of plastic **limit-state** design.

The two halves of each k_{th} rotating ring which composes the disc are subjected to a separating centrifugal force F_c during rotation, due to its own mass, which is easily calculated as follows:

* Robinson E., Bursting Tests of Steam-Turbine Disk Wheels., A.S.M.E. Trans., vol. 66, no. 5, July 1944, pp. 373-380; discussion, pp. 380-38

9. Burst design of a turbine disc - plasticity (2/4)



$F_{c,k}$: half-disc centrifugal force

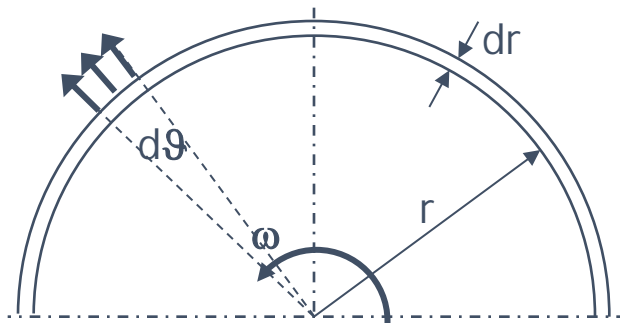
b_k : disc width

β_k : $r_{i,k}/r_{e,k}$, bore ratio

$$\begin{aligned} F_{c,k} &= \frac{2}{3} \rho \omega^2 b_k (r_{e,k}^3 - r_{i,k}^3) = \\ &= \frac{2}{3} \rho \omega^2 r_{e,k}^2 A_k (1 + \beta_k + \beta_k^2) = \\ &= M'_k \omega^2 r_{e,k} \frac{4}{3\pi} \frac{(1 + \beta_k + \beta_k^2)}{(1 + \beta_k)} \end{aligned}$$

A_k : $b_k(r_{e,k}-r_{i,k})$, ring cross section area

M'_k : half disc mass



centrifugal pressure : $\frac{\rho \omega^2 r (r d\theta b dr)}{r d\theta b} = \rho \omega^2 r dr$

radial resultant : $(\rho \omega^2 r dr) b 2r = 2\rho \omega^2 r^2 b dr$

integral on the disc : $2\rho \omega^2 b \int_{r_i}^{r_e} r^2 dr = \frac{2}{3} \rho \omega^2 b [r_e^3 - r_i^3]$

9. Burst design of a turbine disc - plasticity (3/4)

To this, add the resultant of the tension applied by the pull of blades and slots at the outer radius of the half rim; this tension was evaluated for the case examined in these slides (Sect. 6 sl. 2) at:

$$\sigma_{r,e} = 36,1 \text{ MPa}$$

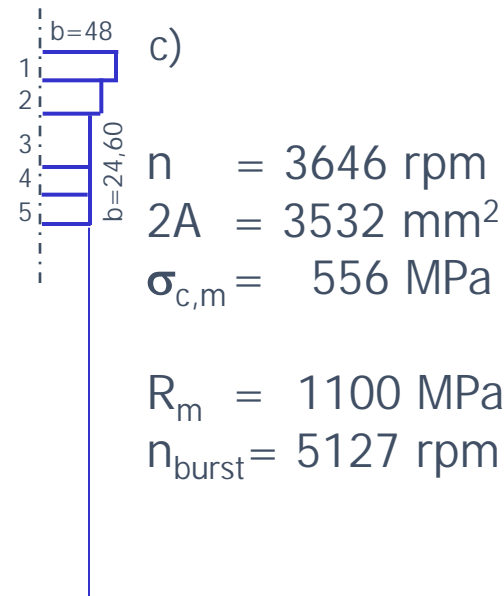
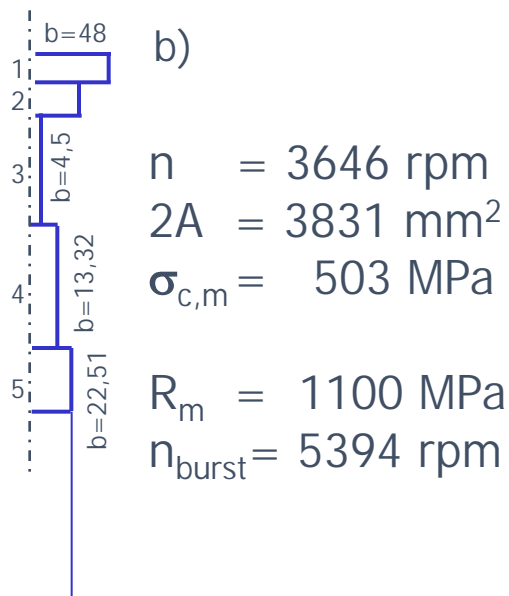
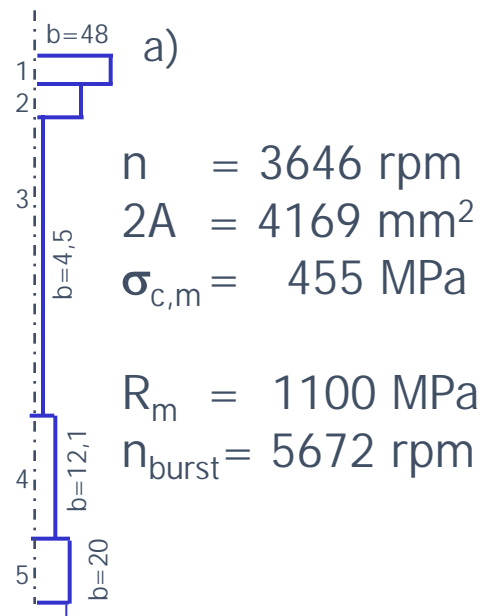
Then the average hoop stress σ_c on the two diametral cross sections is then, from simple radial equilibrium (with $A = \sum A_k$):

$$\sigma_{c,m} = \frac{\sum F_{c,k}}{2A} + \frac{\sigma_{r,e} b 2r_e}{2A} = \frac{\rho \omega^2}{3A} \sum r_{e,k}^2 A_k (1 + \beta_k + \beta_k^2) + \frac{\sigma_{r,e} b r_e}{A}$$

Note that thermal stresses are eliminated by the plastic flow of the – idealised – perfectly plastic material. Then only stresses proportional to ω^2 (or n^2 , rpm) are into play:

$$\frac{\sigma_{c,m}}{\omega^2} = \frac{R_m}{\omega_{burst}^2} \quad \text{or} \quad \frac{\sigma_{c,m}}{n^2} = \frac{R_m}{n_{burst}^2} \quad \text{i.e.} \quad n_{burst} = n \left(\frac{R_m}{\sigma_{c,m}} \right)^{0.5}$$

9. Burst design of a turbine disc - plasticity (4/4)



Here the burst criterion is [Robinson 1944], as said before.

The comparison above is based on a representative value or ultimate strength $R_m = 1100 \text{ MPa}$, reasonable as an average value for INCONEL 718 in the present range of temperatures. As a matter of fact, we should take slightly lower values for cases b) and c).

It is clear from this simple comparison why disc a) is preferred: it has a much larger safety margin to burst than discs b) and c).

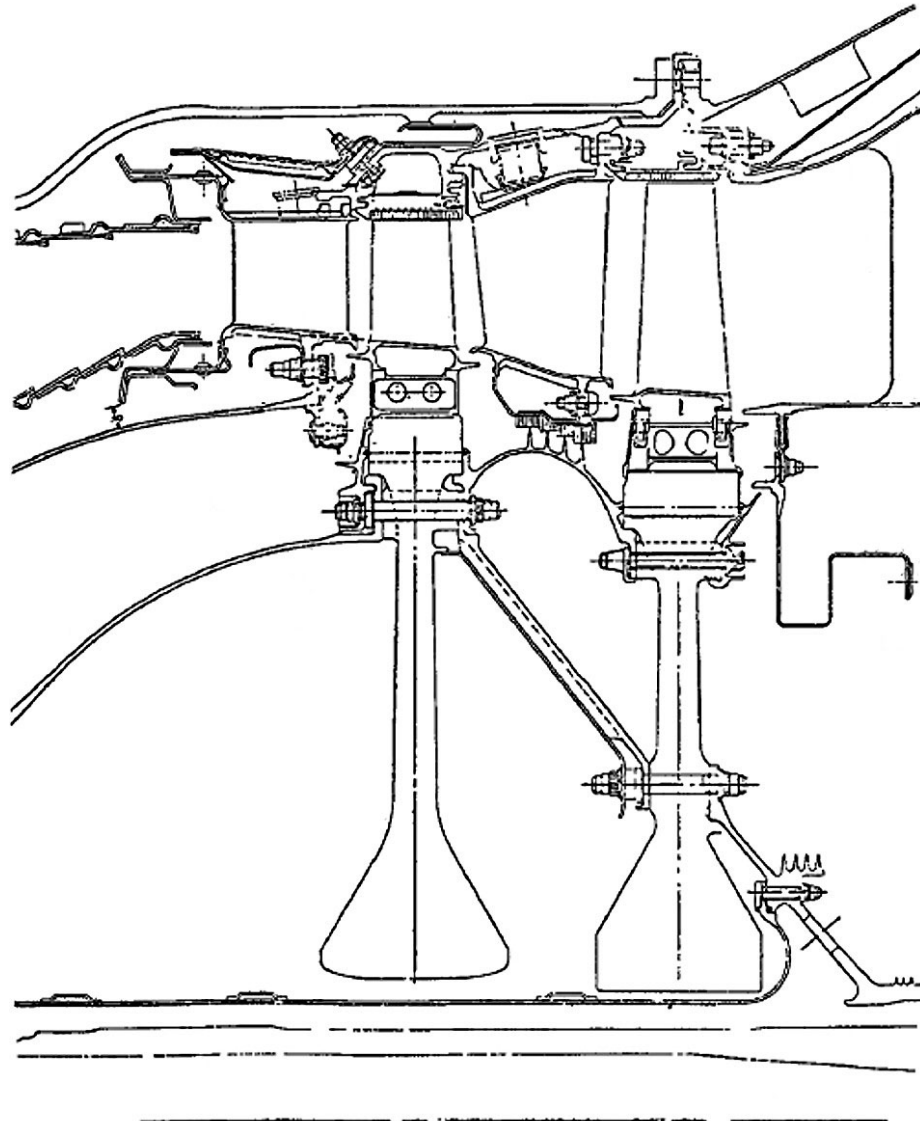
10. Summary of disc life and failure criteria (1/6)

Disc Life/Failure Analysis

First of all, a typical (design) flight profile must be defined, along with temperature response calculations to determine the metal temperatures as a function of time into the flight.

Transient and steady-state temperatures are then found.

Disc stress analysis includes the effects of blade loads, blade-to-disk attachments, thermal stresses, elasticity, creep, acceleration and deceleration transients, transfer of loads among joining elements.



GE CF6-50 High pressure turbine

10. Summary of disc life and failure criteria (2/6)

In detail, the following must be taken into consideration: for **burst stresses** :

- the average hoop stress, checked against R_m , if the semi-empirical criterion according to Robinson is adopted (however, refinements are welcome)

For **thermal stresses**:

- in high temperature applications the transient thermal gradients may be severe and affect the fatigue life of the component.

For composed **rotation and thermal stresses**:

- the radial stress in the web, checked against creep
- the total equivalent stress (composed by thermal plus rotation), checked against yield stress in order to avoid excessive deformation which could lead to contact between blade tips and casing elements
- the peak equivalent stresses - due to speed changes and associated thermal cycles - checked against fatigue ruptures at critical points such as fillets, disc dovetails, holes and grooves.

10. Summary of disc life and failure criteria (3/6)

The critical items of an aircraft engine disc failure analysis are connected to the particular failure mode being investigated, and to its consequence on safety grounds.

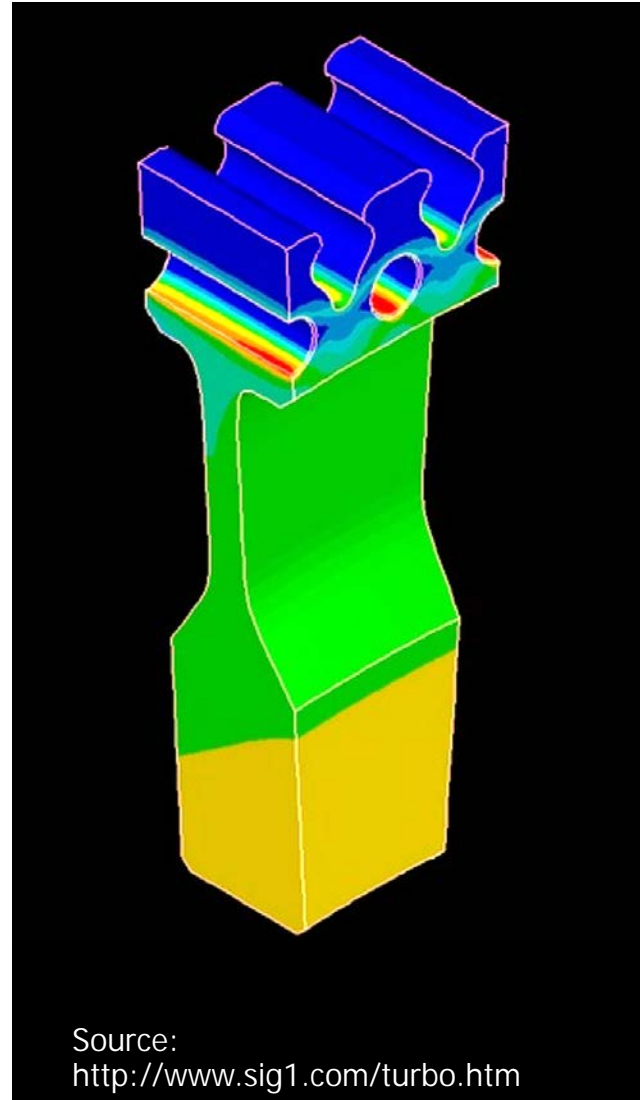
Typically, the following must be considered:

- Crack initiation analysis: low cycle fatigue, flight cycles to crack initiation
- Crack propagation analysis: fracture mechanics, initial defect size and flight cycles to failure
- Plastic creep analysis
- Burst: burst speed margin
- Fragmentation patterns: number and size of fragments
- Fragment energy: fragment kinetic energy available for penetration

10. Summary of disc life and failure criteria (4/6)

A caveat: while simplified (Grammel or Manson) analysis is sufficient to evaluate global stress / strain / displacement effects (like radial creep and radial elastic/plastic displacement) at a preliminary design stage, elastic peak stress analysis can be handled, due to its highly local features, only via a Finite Element analysis.

It emerges clearly the complex interaction of factors that play a role in the strength of a turbine or compressor disc; the reading proposed in the next two slides brings some fundamental aspects into the limelight.



Source:
<http://www.sig1.com/turbo.htm>

10. Summary of disc life and failure criteria (5/6)

Awareness of such a combination of problems has been growing during the last decades, as it can be gathered by the discussion contained in a quite obsolete however classic paper^{*}:

Mr. B. R. Dudley, B.Sc. (Eng.) (Associate Member), and Mr. M. J. Owen further wrote that while supporting the plastic design method for rotating discs there was another mode of failure which was becoming of importance, namely, failure by fatigue due to cycles of stress associated with speed changes. The possibility of fatigue failure was obviously greater in applications where frequent stopping and starting and variations of speed occurred. Each sequence start-runstop provided one cycle of stress with, possibly, cycles of smaller amplitude superimposed due, for example, to speed changes from "cruise" or "idle" to maximum power.

In aircraft gas-turbines, particularly, high working stresses were used with high-strength alloy steels which did not have a proportionally high fatigue limit. Consequently, a design which was safe for operation at steady speed (whether the design be based on elastic or plastic considerations) might have a fatigue life less than the probable number of cycles in its operating life.

^{*} Heyman J., Plastic design of rotating discs, Proceedings Institution Mechanical Engineers 1847-1996, Vol. 172 , 1958

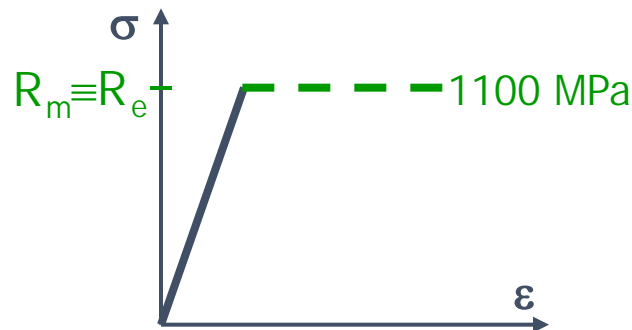
10. Summary of disc life and failure criteria (6/6)

Too little was known about fatigue, particularly under conditions of combined stress, for it to be possible to predict the life of a complicated component even if its elastic stress distribution were known, but designs could frequently be greatly improved by attention to detail and avoidance of unnecessary stress raisers. It was worth noting that those might be fully operative since at running speed the stresses would normally be less than the elastic limit.

It was suggested that when fatigue was worthy of consideration a wise procedure would be to use the plastic analysis method to design the profile of the disc and then to calculate the elastic stress distribution. The elastic stress distribution should be examined in the light of fatigue data and operating experience. Finally, the detail design should be critically examined for stress raisers, particular attention being paid to changes of section at spacing flanges, balancing rings, and similar features.

Appendices - Increasing disc speed up to burst

Sections 11 and 12 show the frames of movies where we can see von Mises equivalent stresses and radius increase while the disc is subjected to an increasing rotation speed up to burst, which is here defined as the condition when the von Mises stress reaches R_e .



Material behaviour is here oversimplified to elastic-ideally plastic.

Section 11 deals with the case of disc-only, i.e., no blades and slots are present.

Burst speed is predicted at 11400 rpm.

Plastic front starts at inner radius and propagates outwards.

Remark that in these numerical simulations yield is governed by von Mises criterion.

11. App. 1 - Disc only, without slots and blades (1/21)

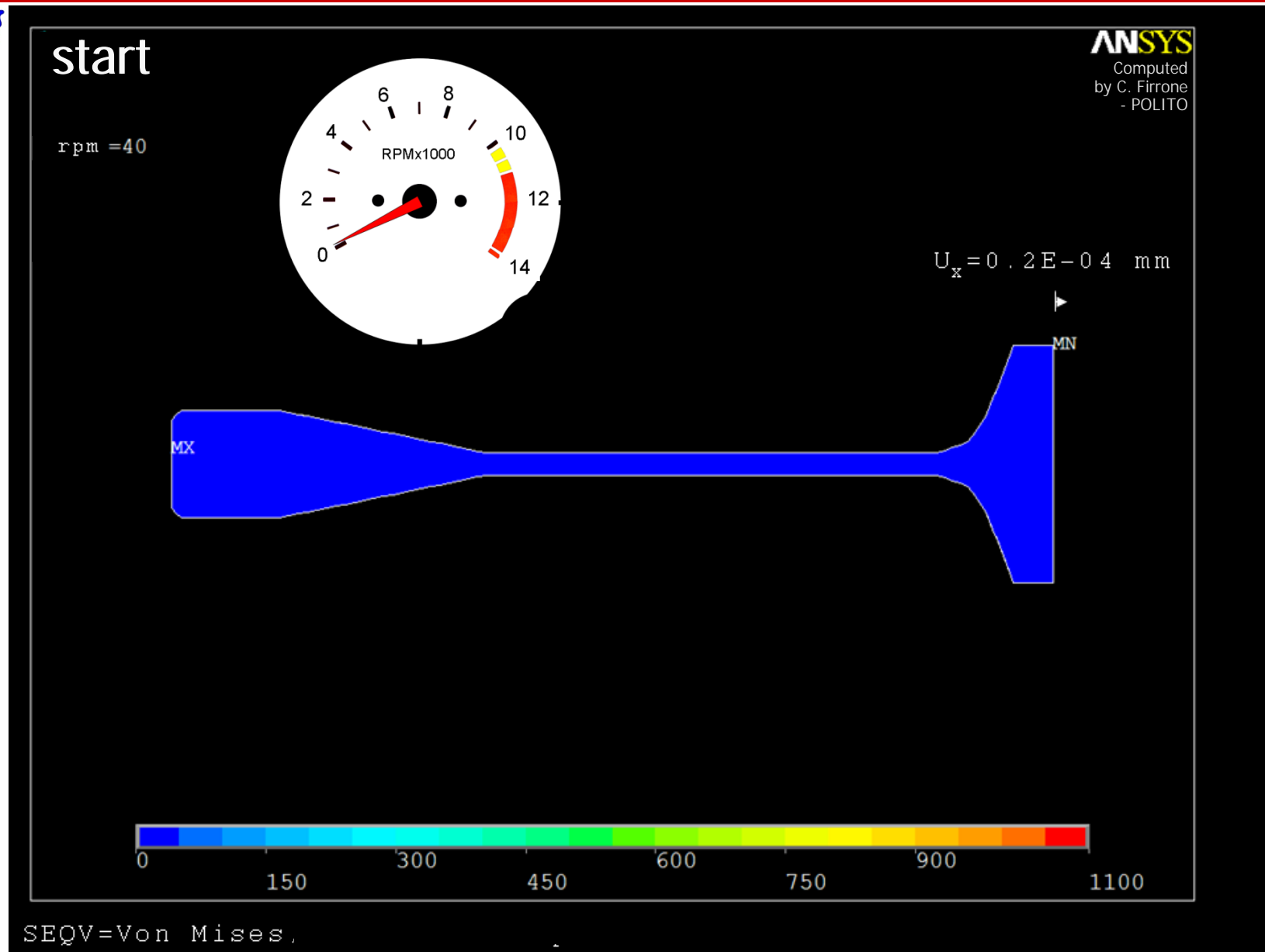


click

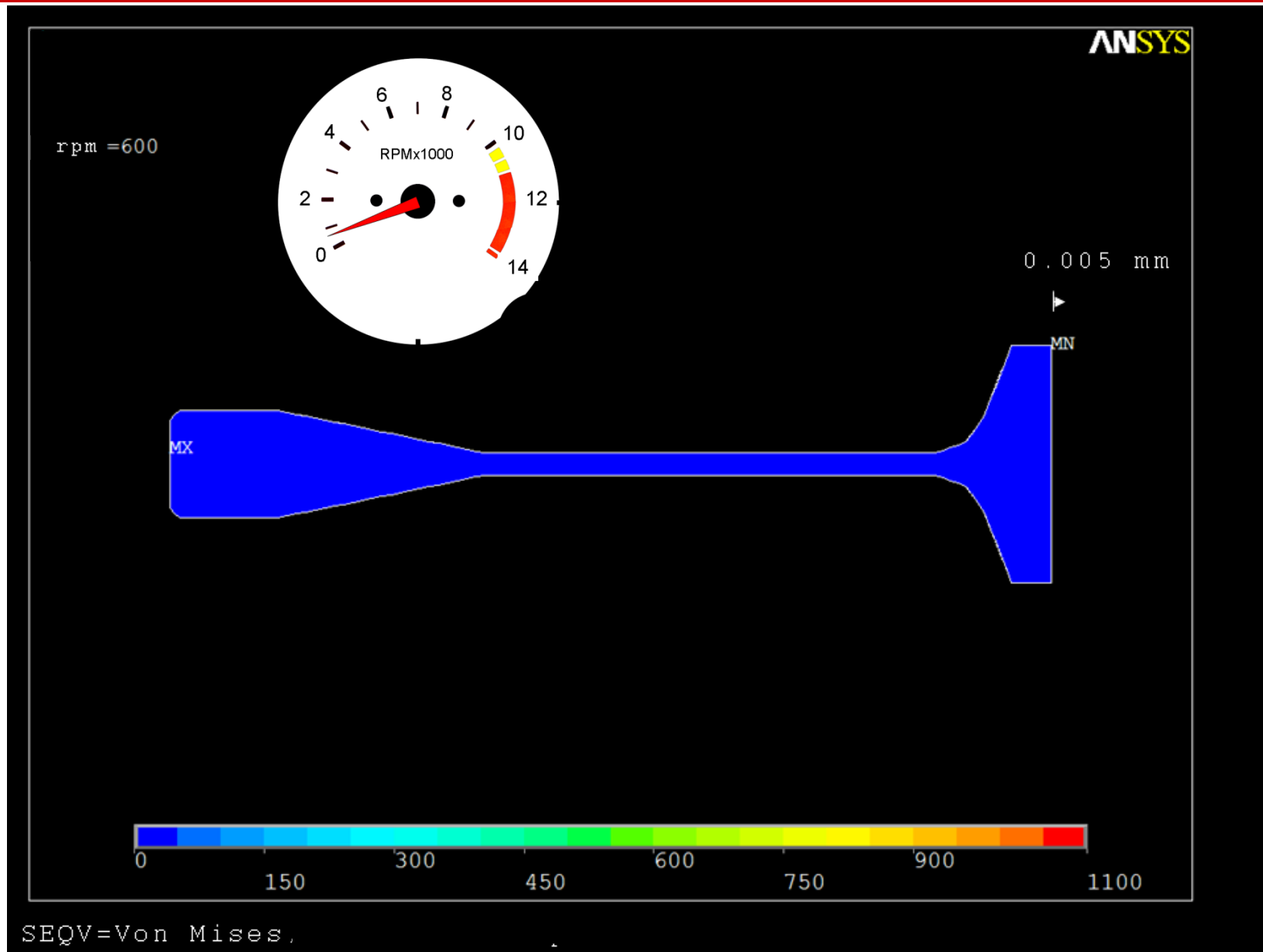
click

click

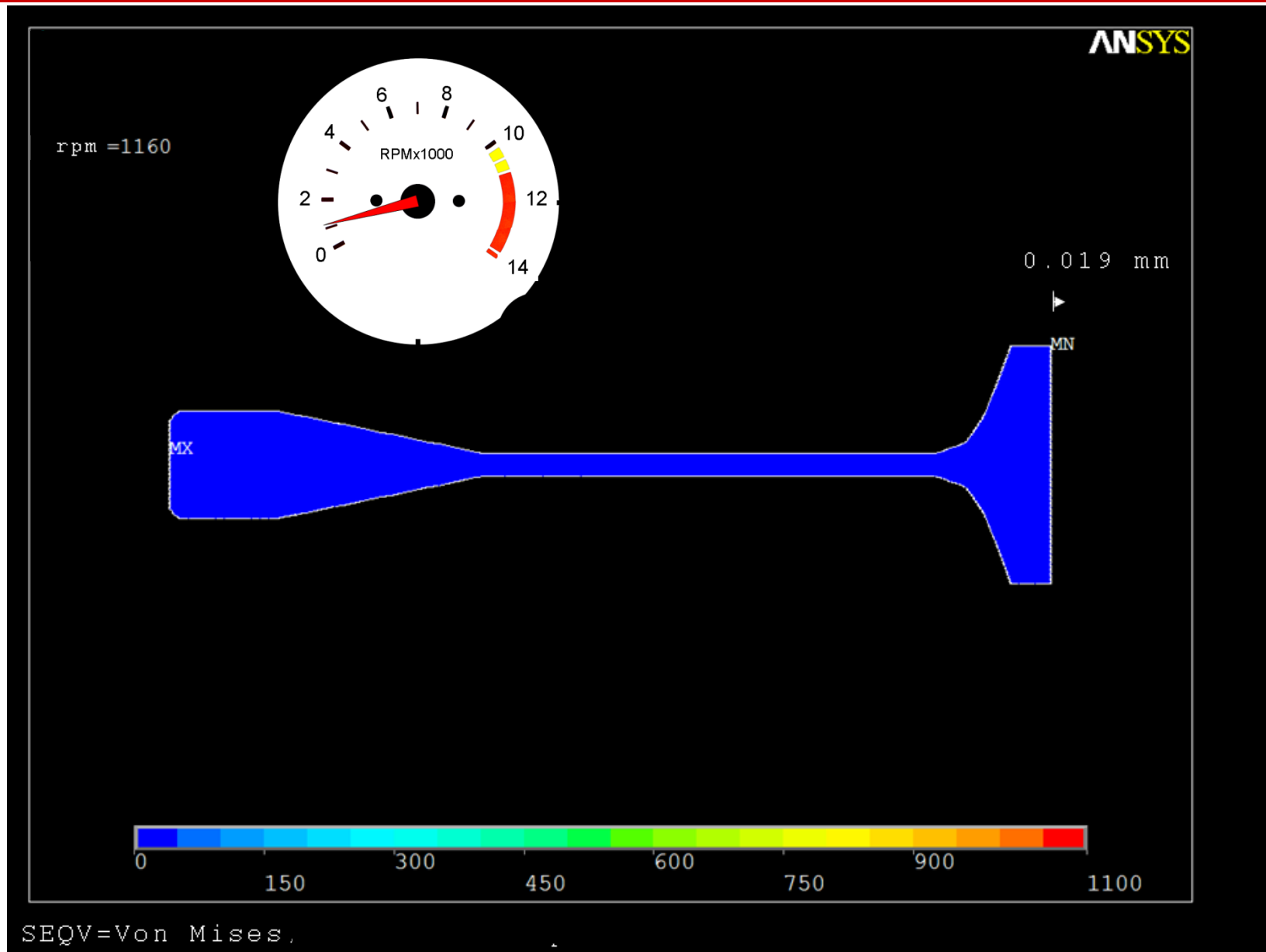
... ...



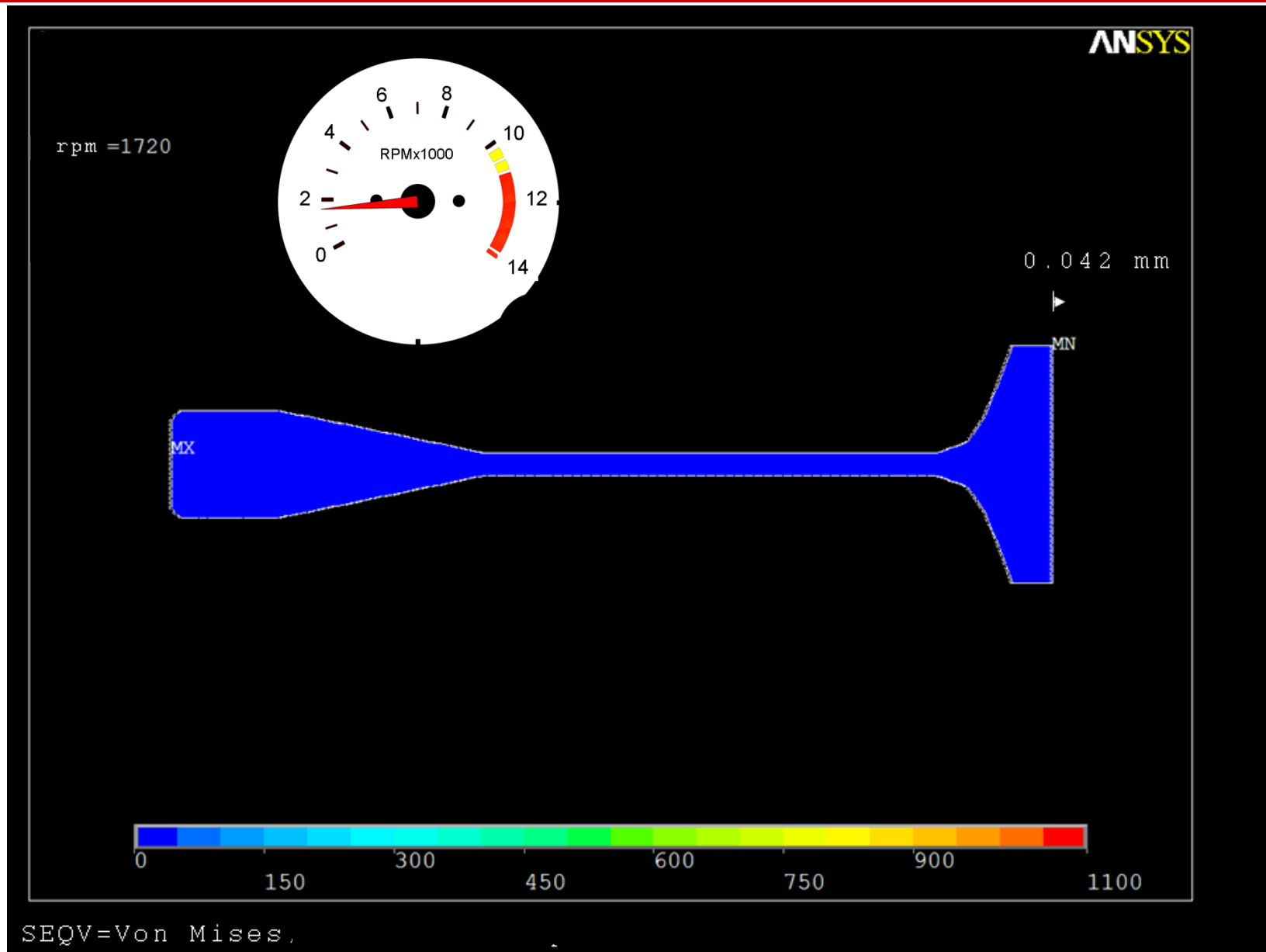
11. App. 1 - Disc only, without slots and blades (2/21)



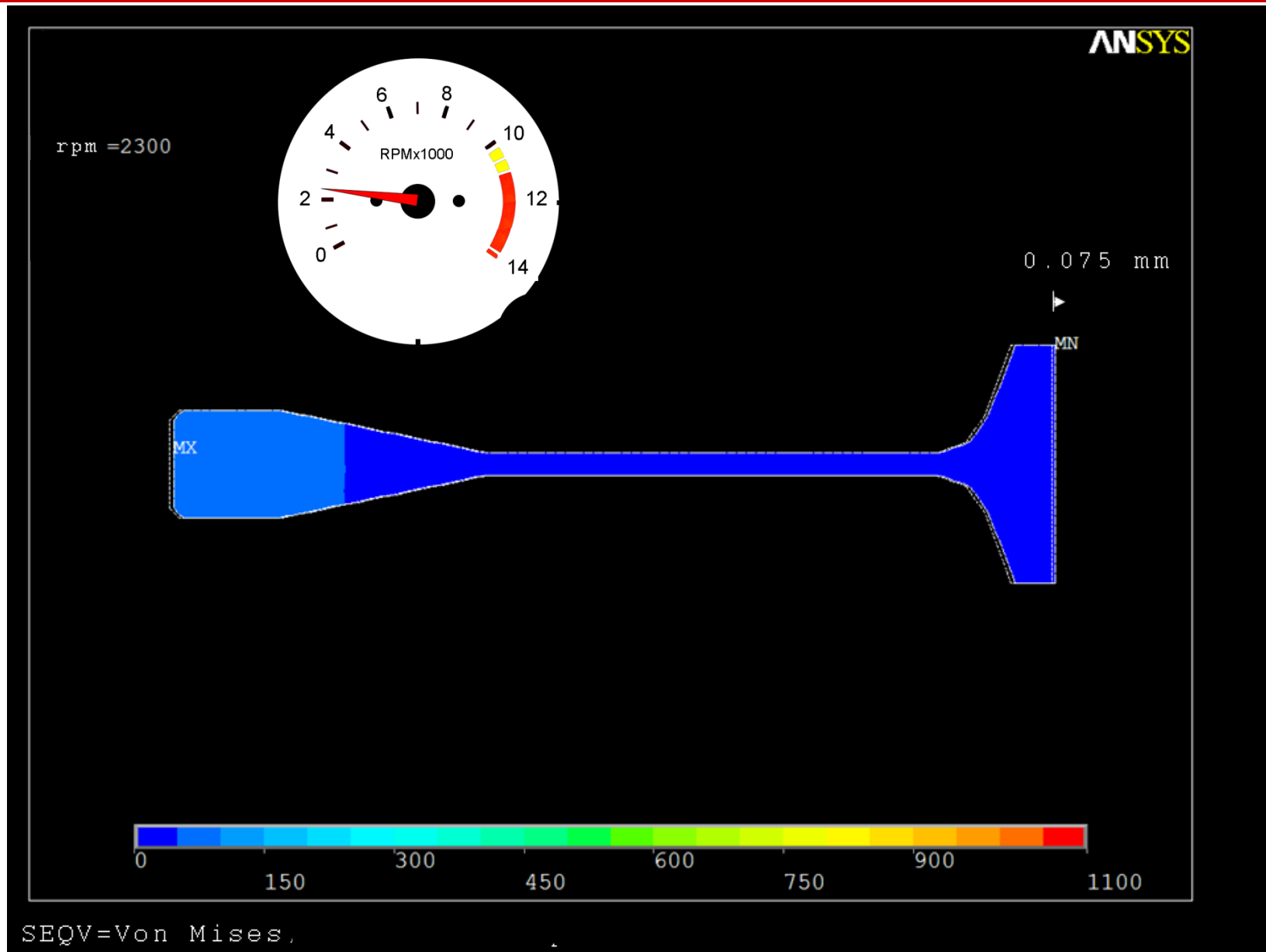
11. App. 1 - Disc only, without slots and blades (3/21)



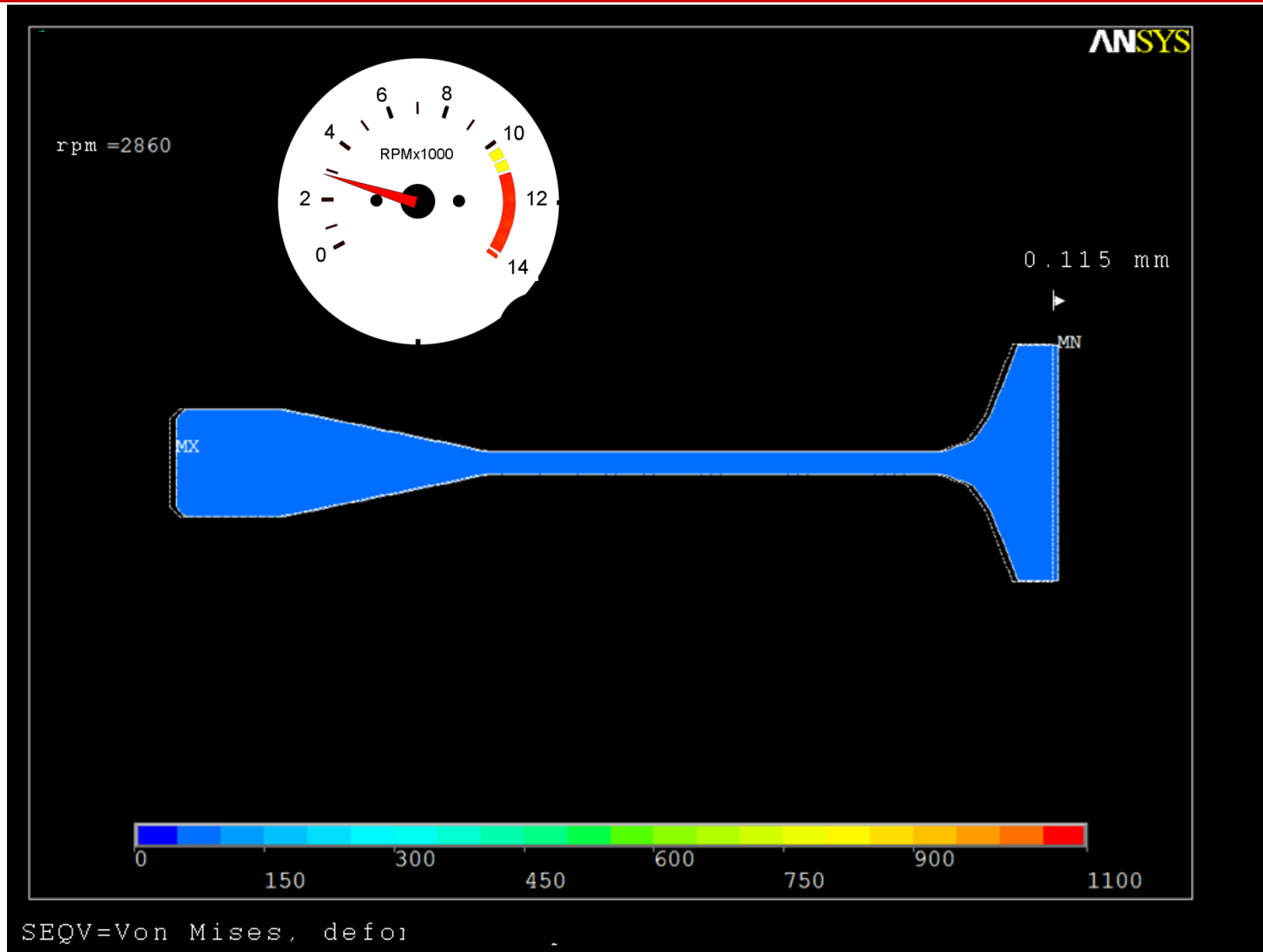
11. App. 1 - Disc only, without slots and blades (4/21)



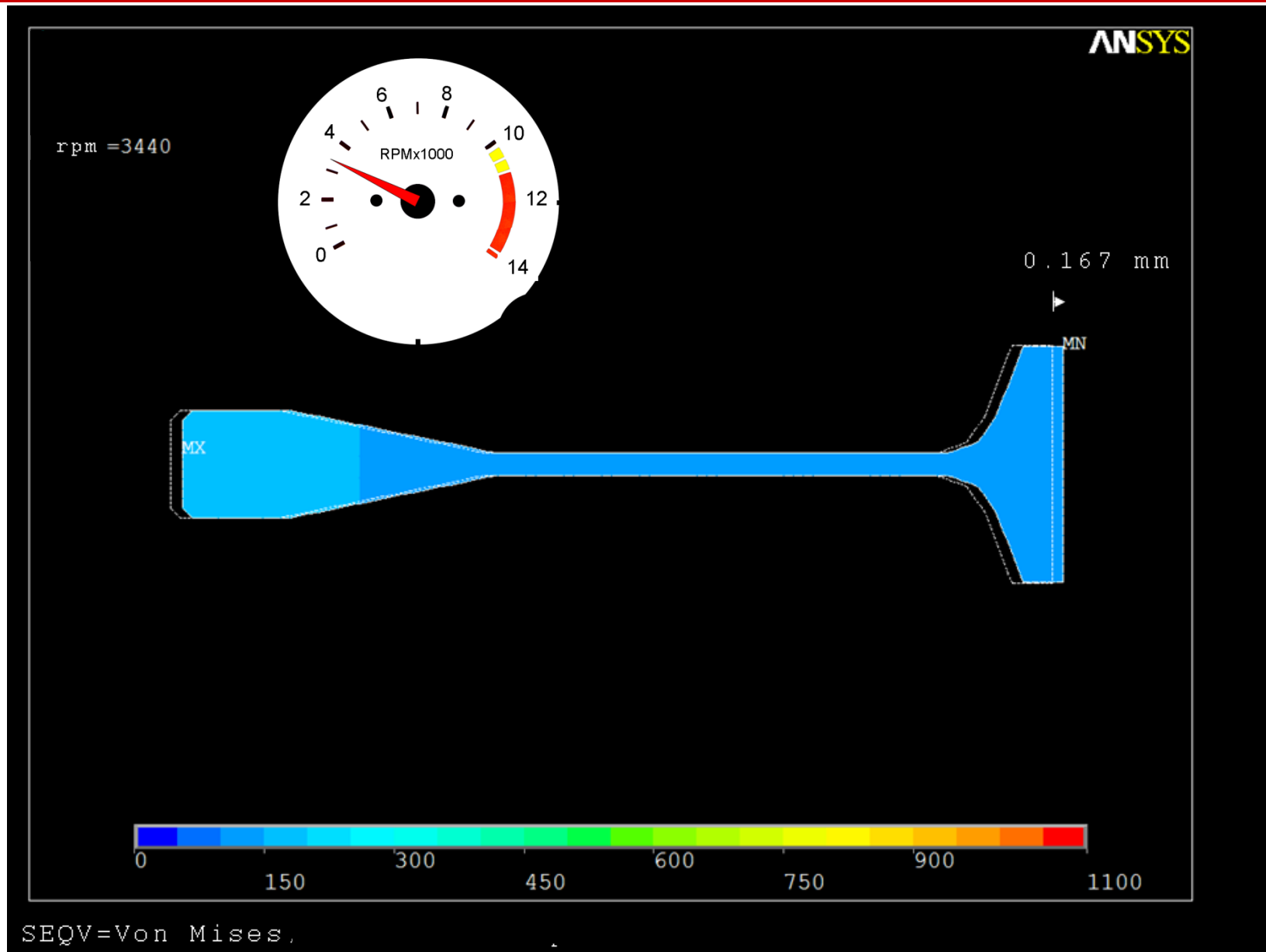
11. App. 1 - Disc only, without slots and blades (5/21)



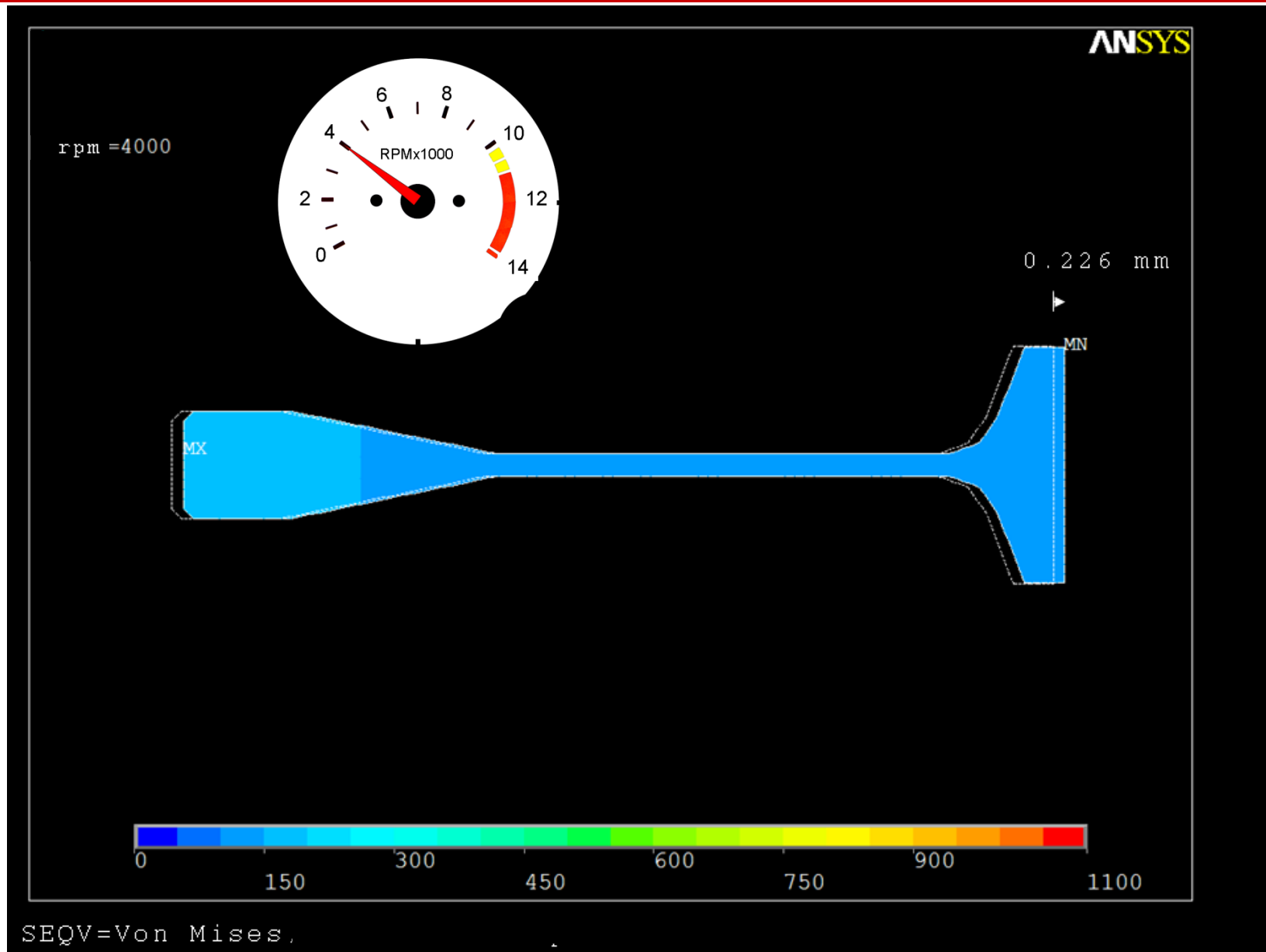
11. App. 1 - Disc only, without slots and blades (6/21)



11. App. 1 - Disc only, without slots and blades (7/21)

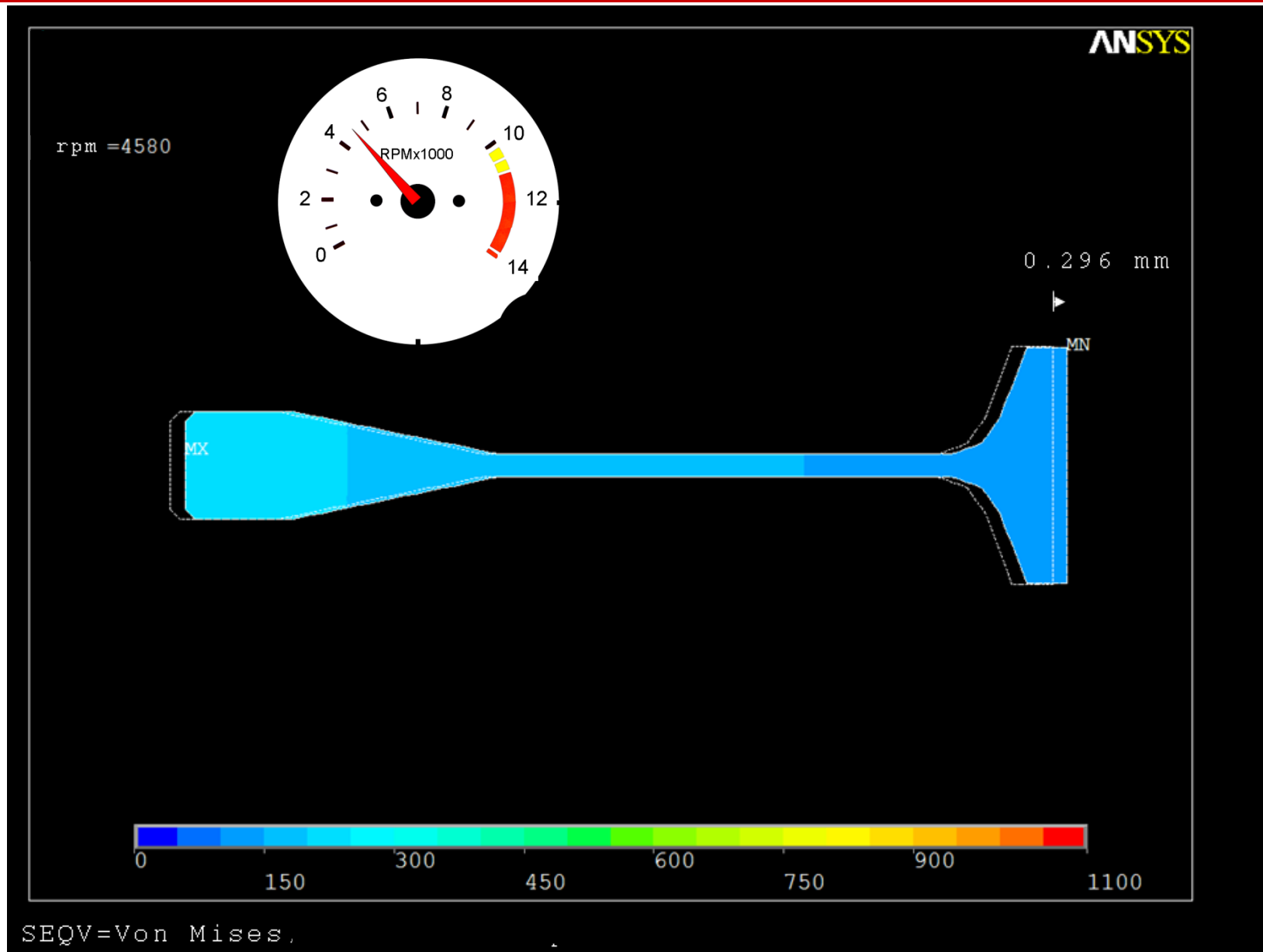


11. App. 1 - Disc only, without slots and blades (8/21)

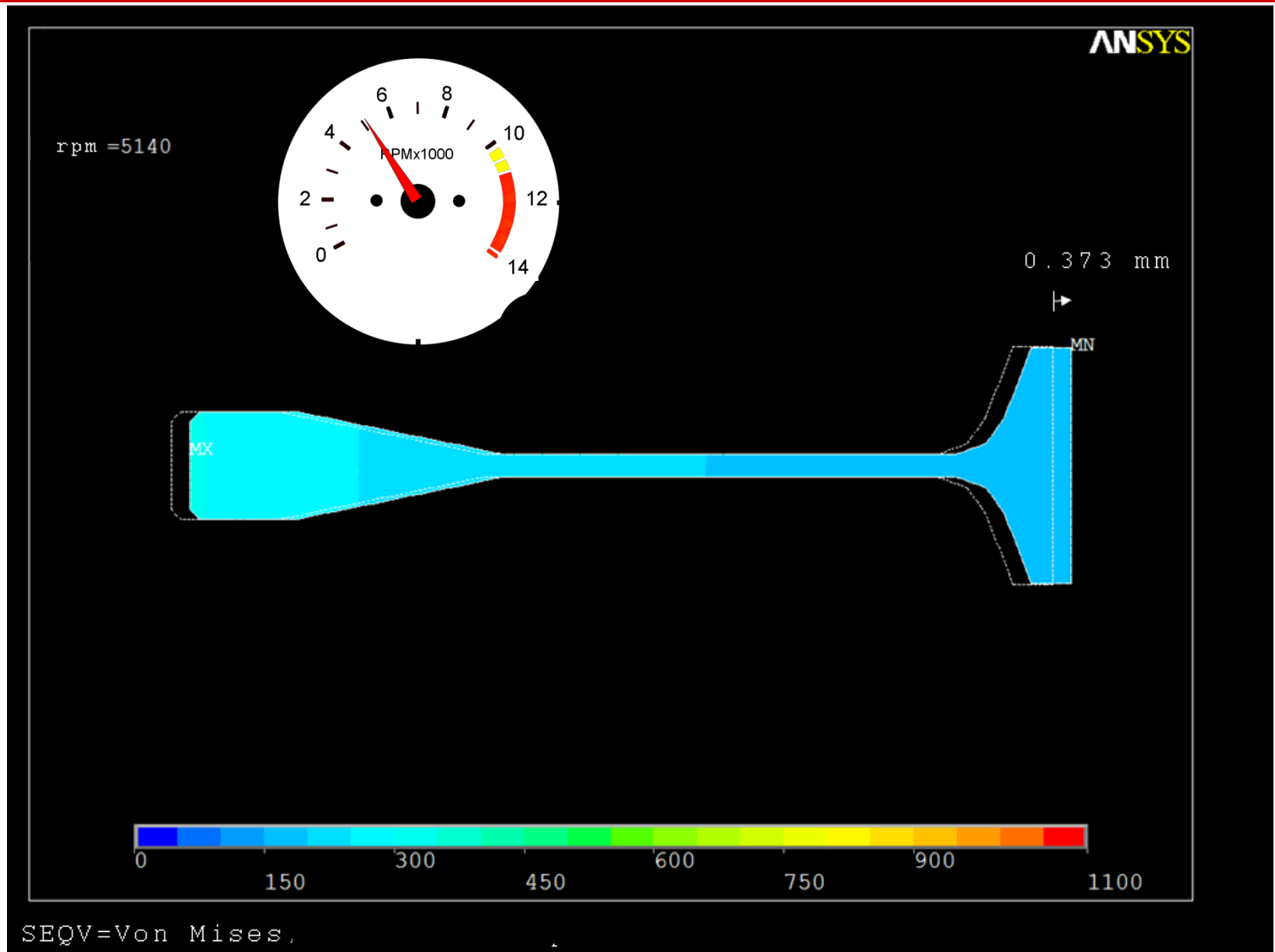


SEQV=Von Mises,

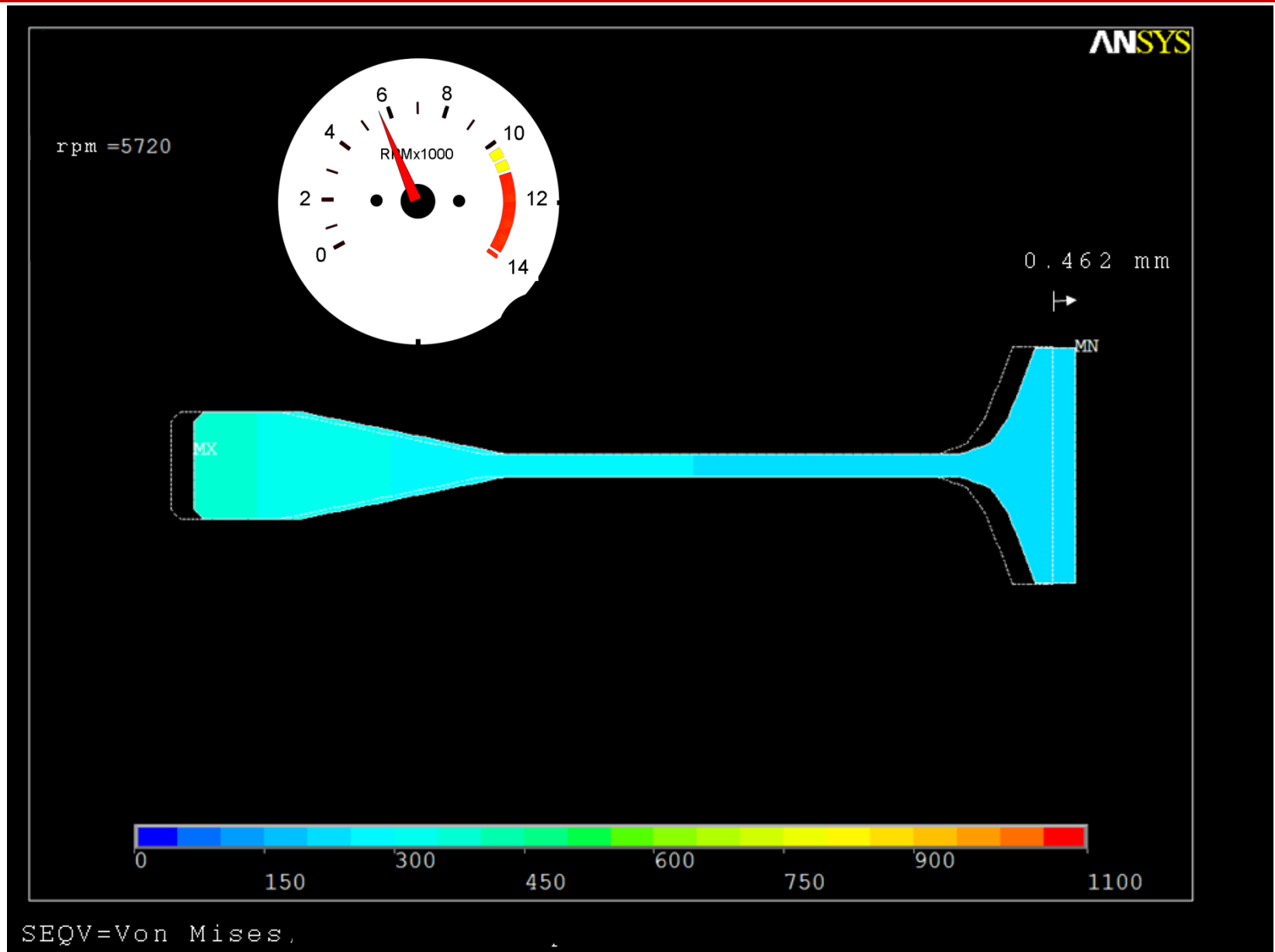
11. App. 1 - Disc only, without slots and blades (9/21)



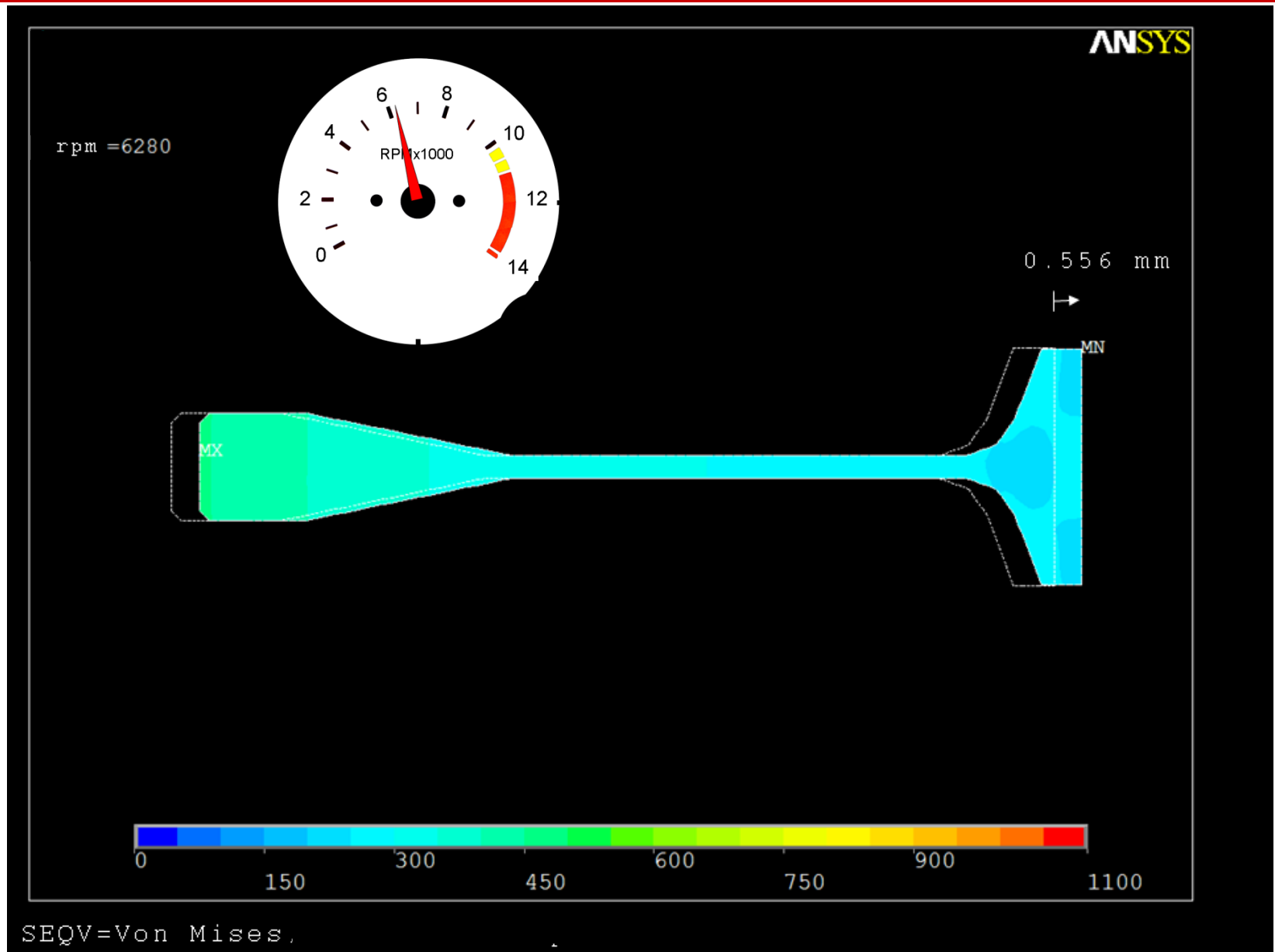
11. App. 1 - Disc only, without slots and blades (10/21)



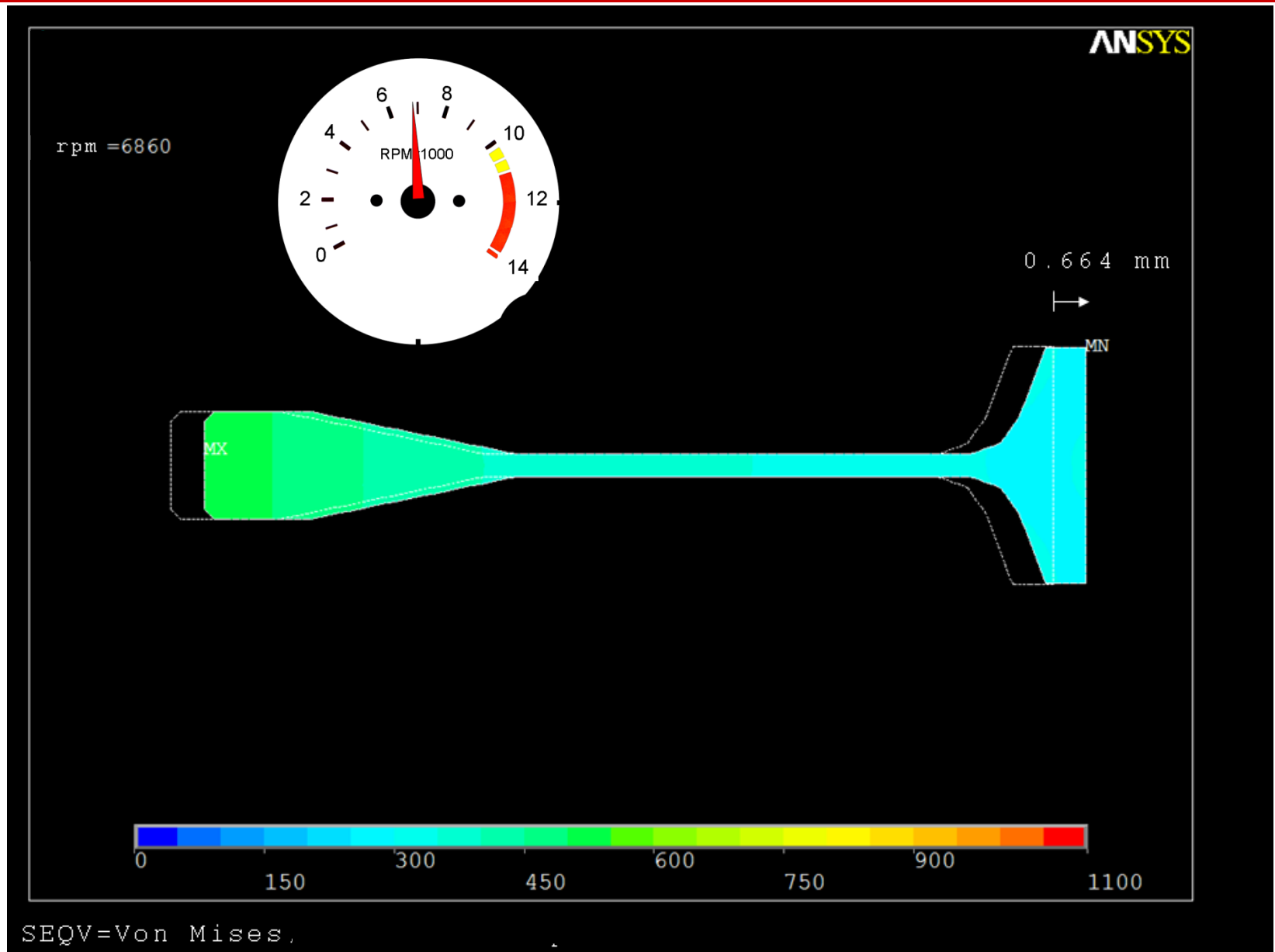
11. App. 1 - Disc only, without slots and blades (11/21)



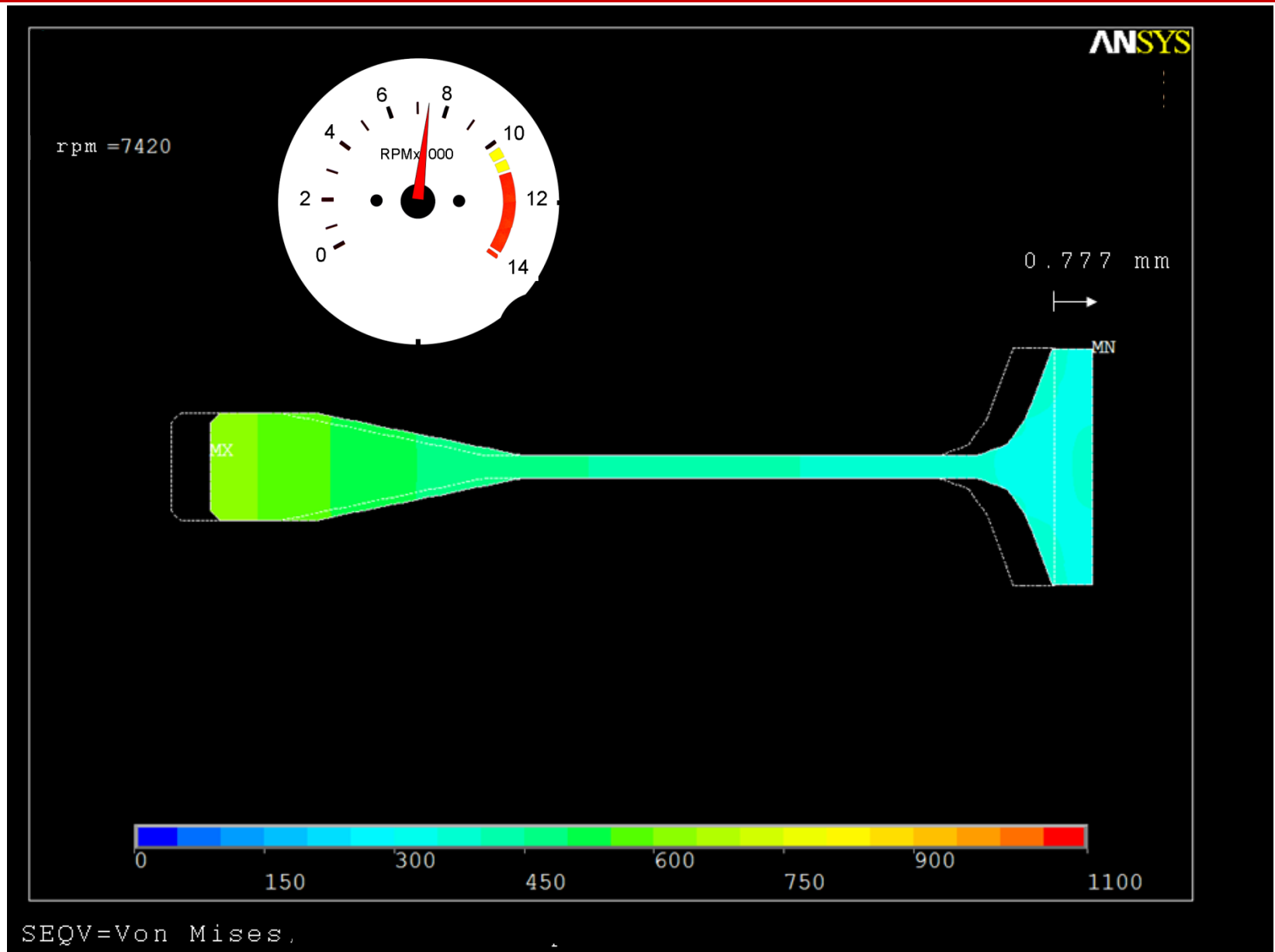
11. App. 1 - Disc only, without slots and blades (12/21)



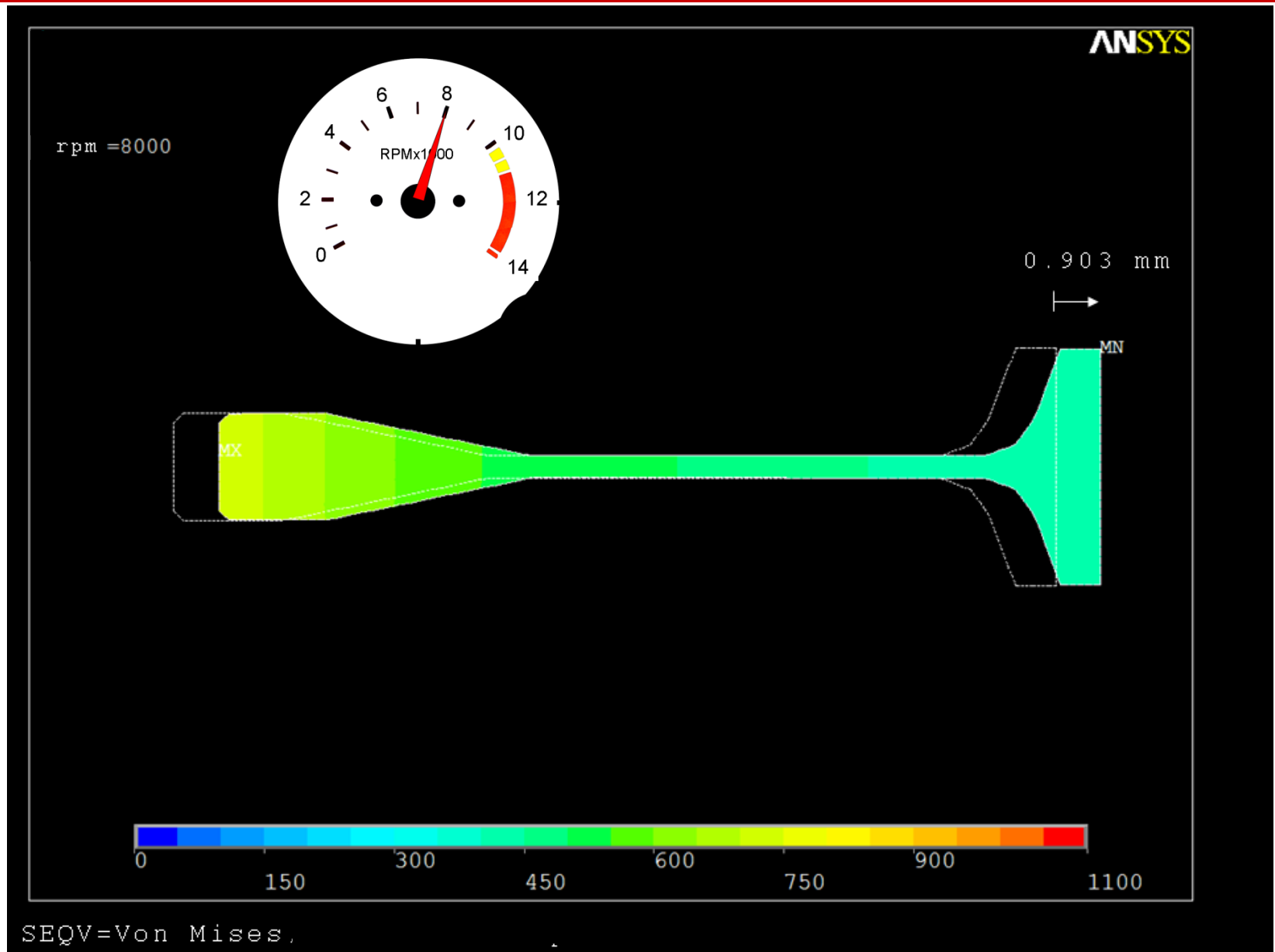
11. App. 1 - Disc only, without slots and blades (13/21)



11. App. 1 - Disc only, without slots and blades (14/21)

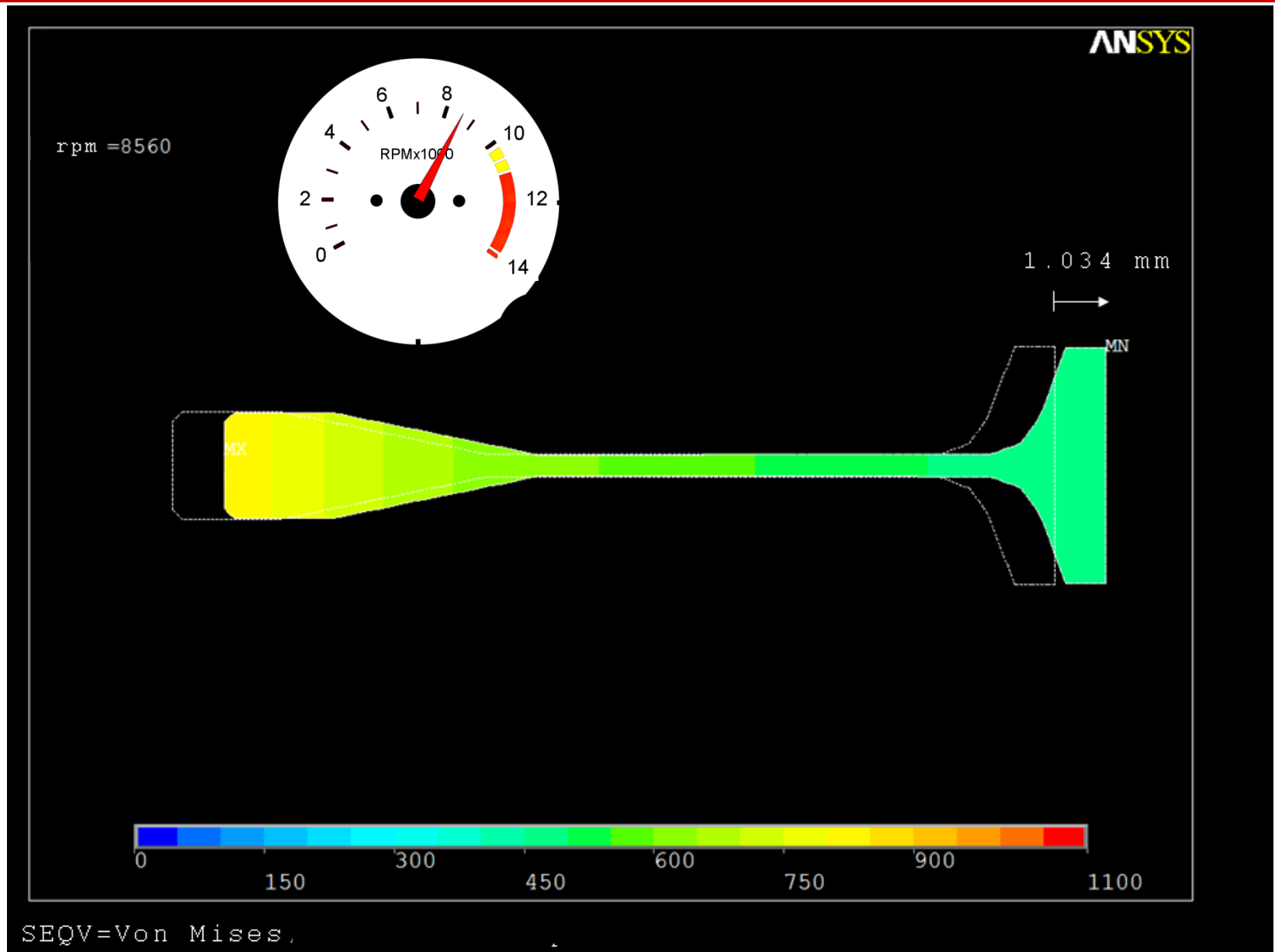


11. App. 1 - Disc only, without slots and blades (15/21)

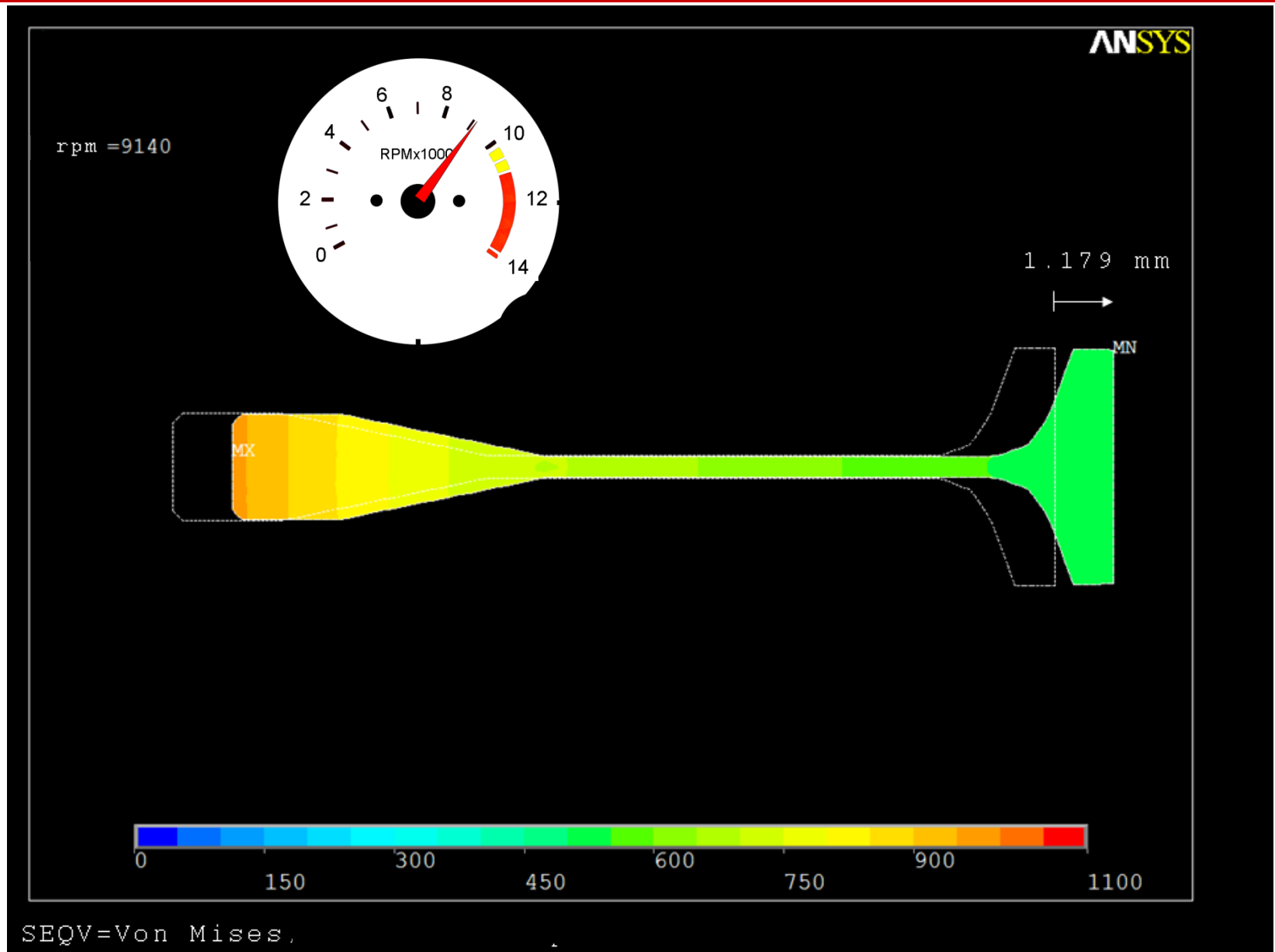


SEQV=Von Mises

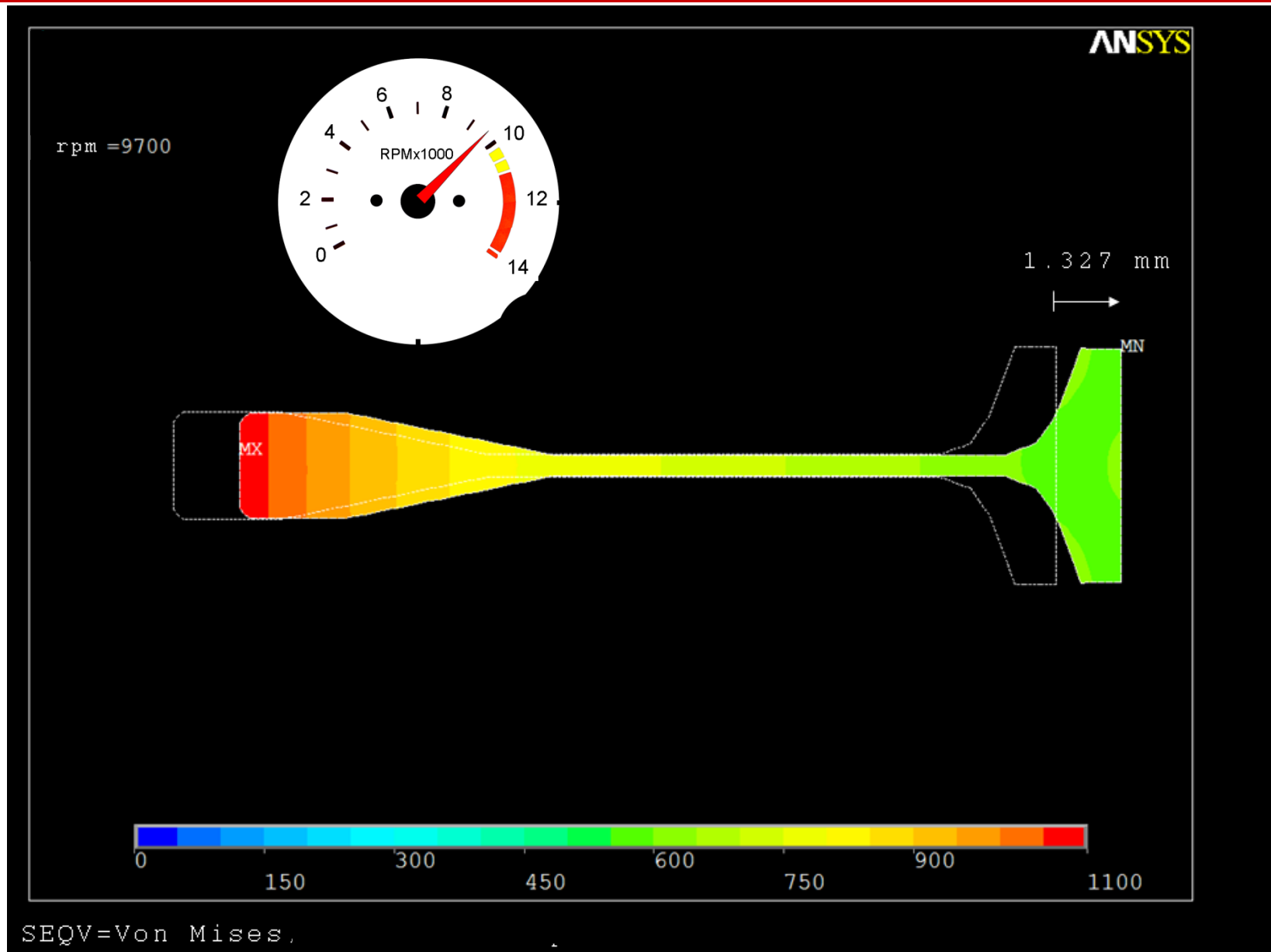
11. App. 1 - Disc only, without slots and blades (16/21)



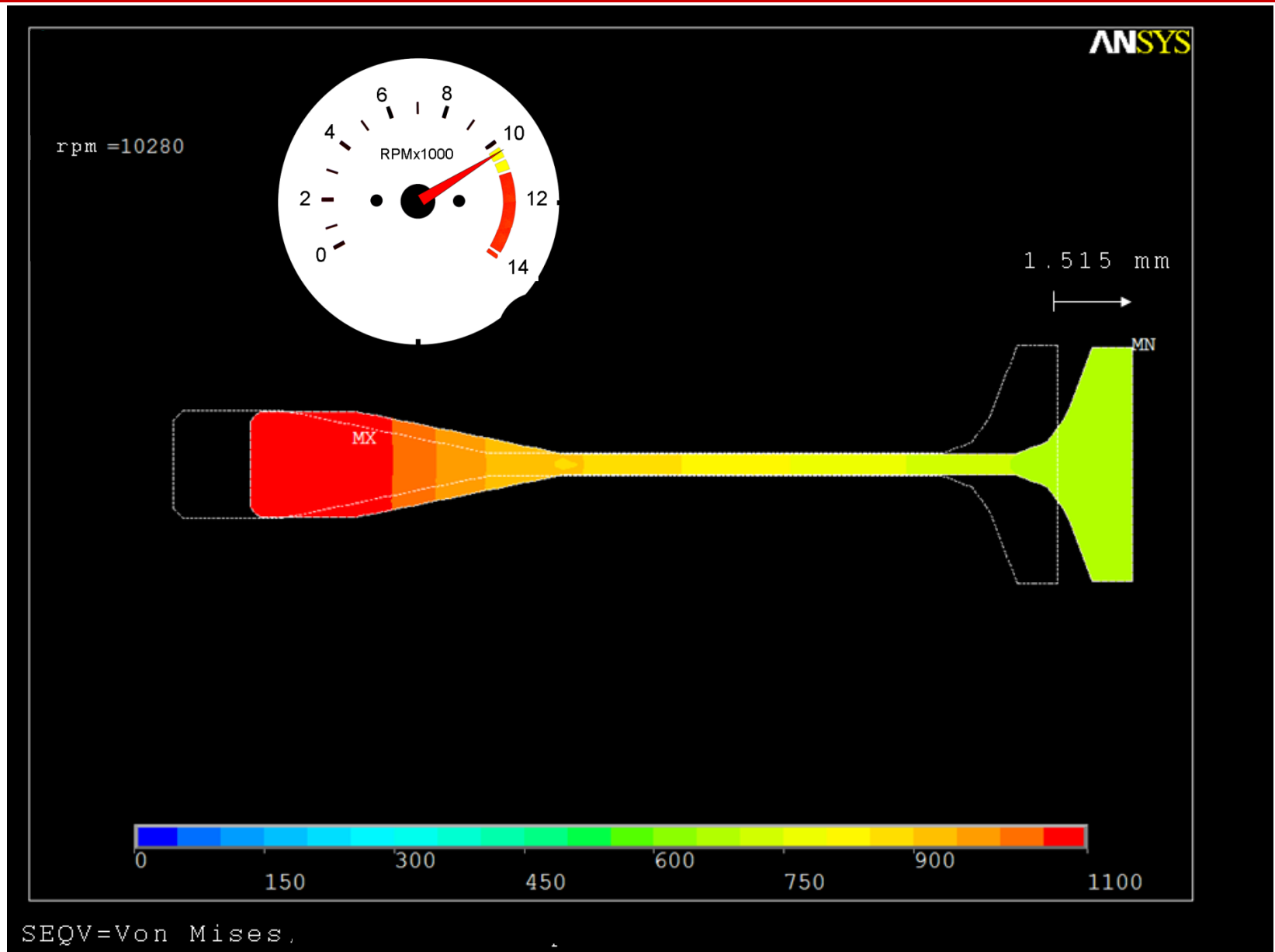
11. App. 1 - Disc only, without slots and blades (17/21)



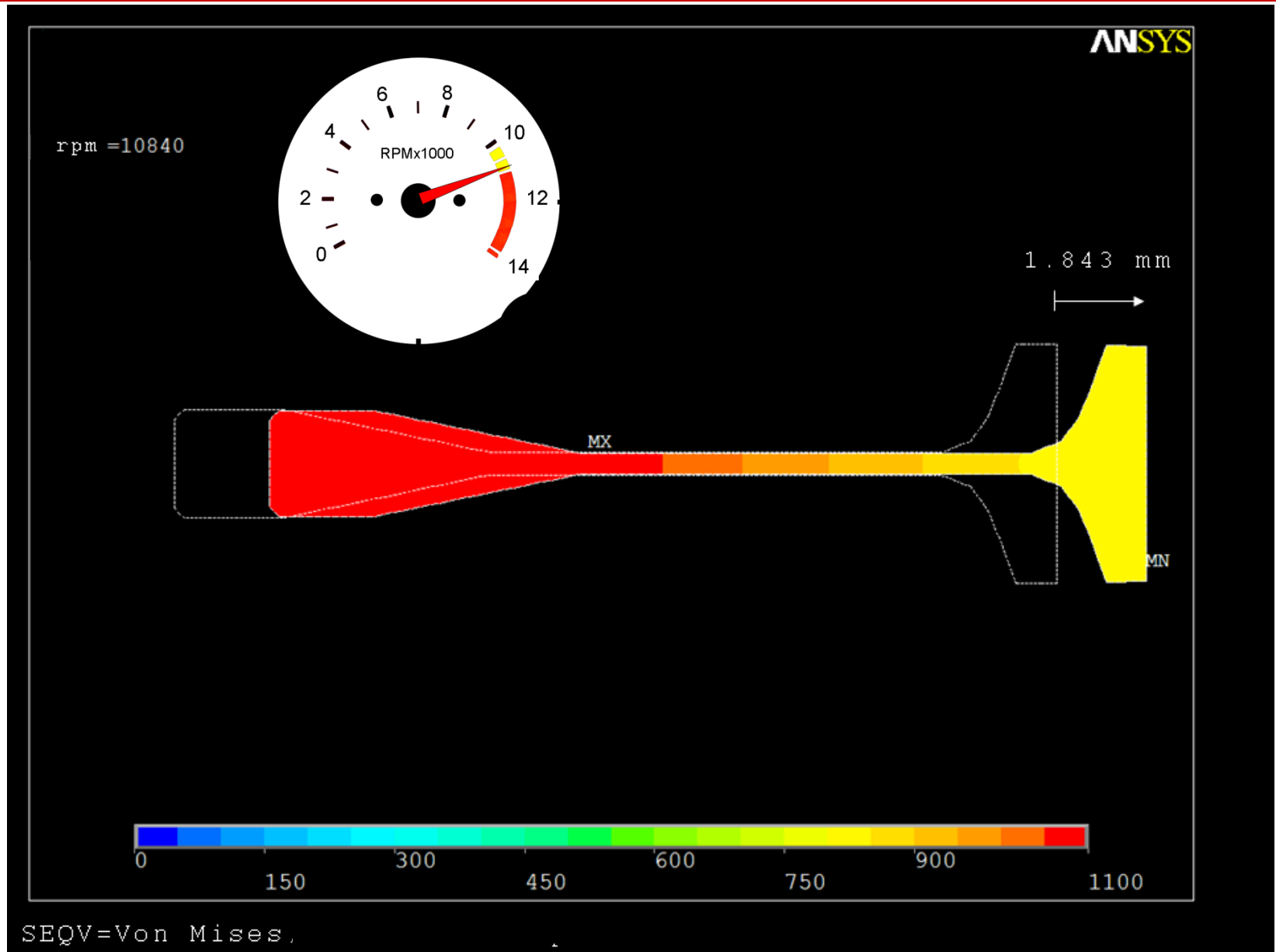
11. App. 1 - Disc only, without slots and blades (18/21)



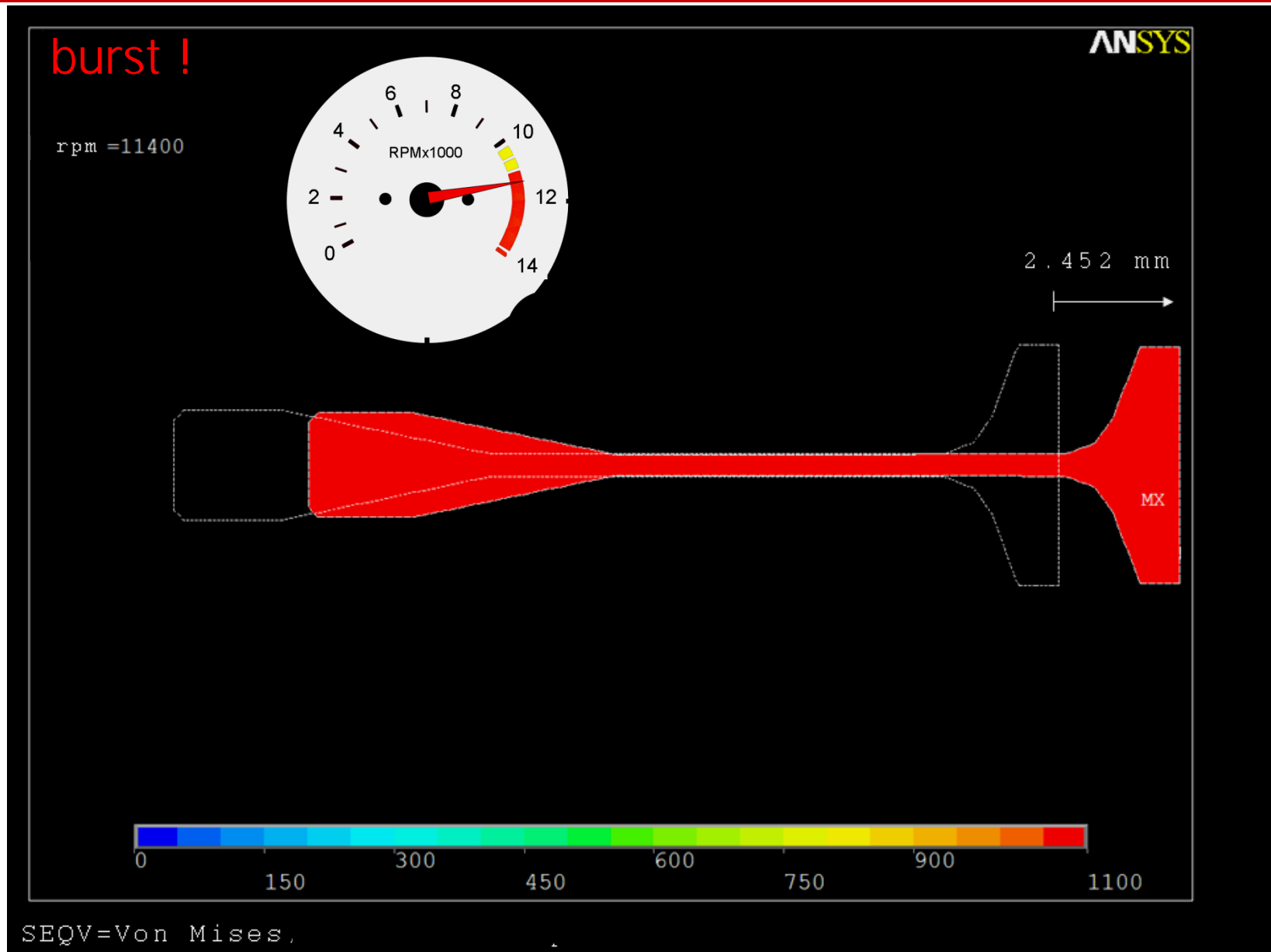
11. App. 1 - Disc only, without slots and blades (19/21)



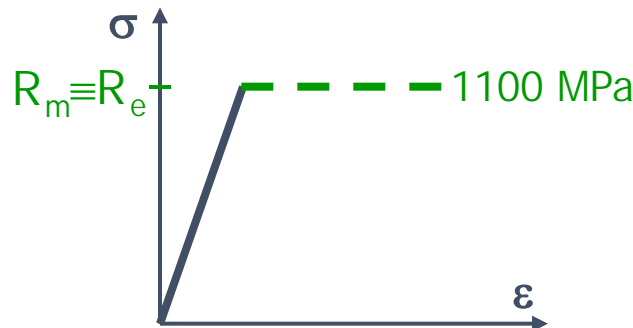
11. App. 1 - Disc only, without slots and blades (20/21)



11. App. 1 - Disc only, without slots and blades (21/21)



Appendices - Increasing disc speed up to burst



Section 12 deals with the case of a disc with blades and slots, to show that this additional mass produces, in this particular case and due to the small thickness of the web, two plastic fronts starting both at the inner radius and at the hub-web junction.

Burst is predicted at 6020 rpm. Remark that in these numerical simulations yield is governed by von Mises criterion.

Compare with Sect. 9 sl. 4, where Robinson criterion together with Tresca was applied: burst was predicted there at 5672 rpm.

12. App. 2 - Rotating disk with slots and blades (1/22)



click

click

click

... ...

ANSYS

Computed
by C. Firrone
- POLITO

start

rpm = 20

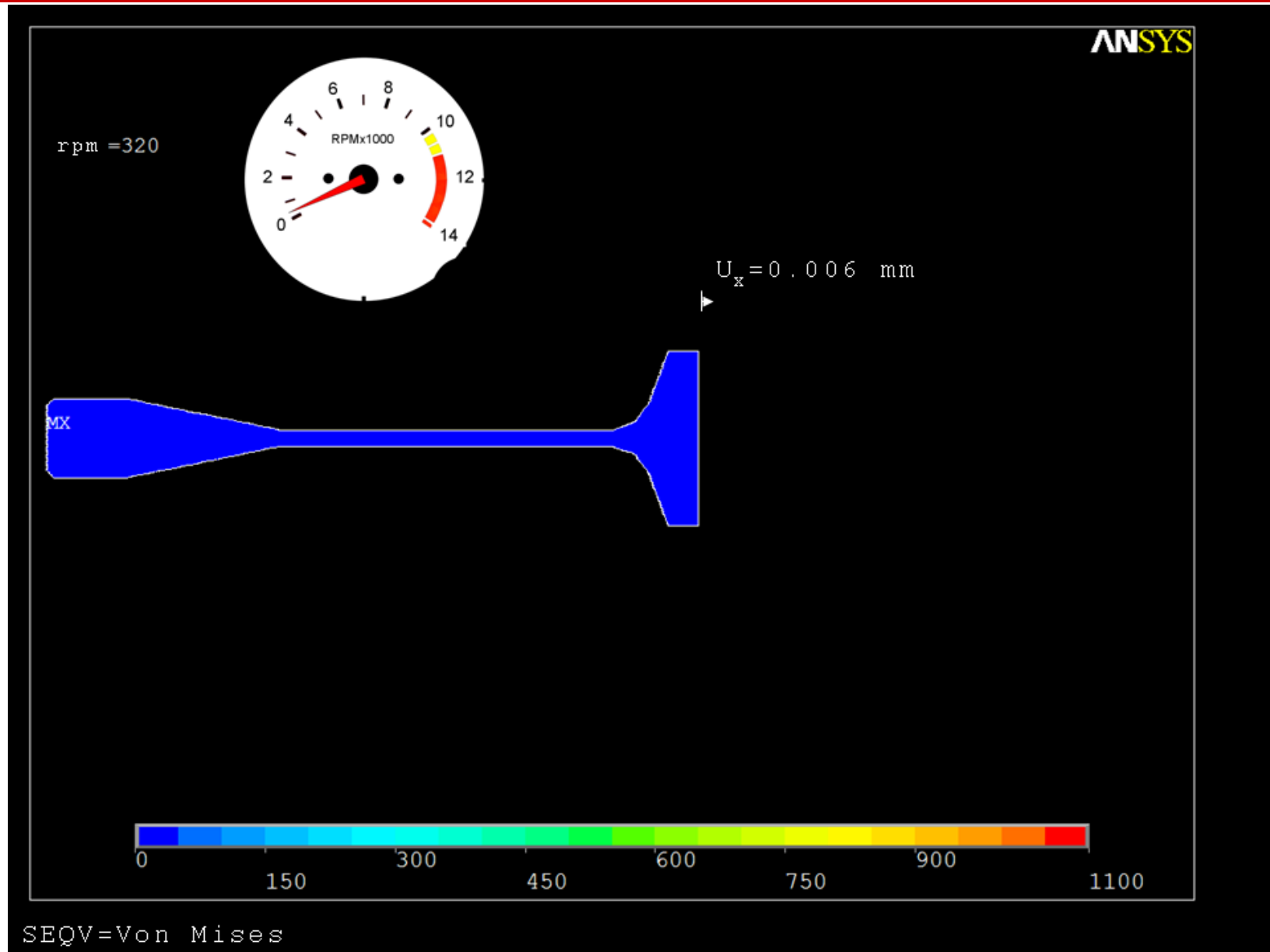


$$U_x = 0.2 \times 10^{-4} \text{ mm}$$

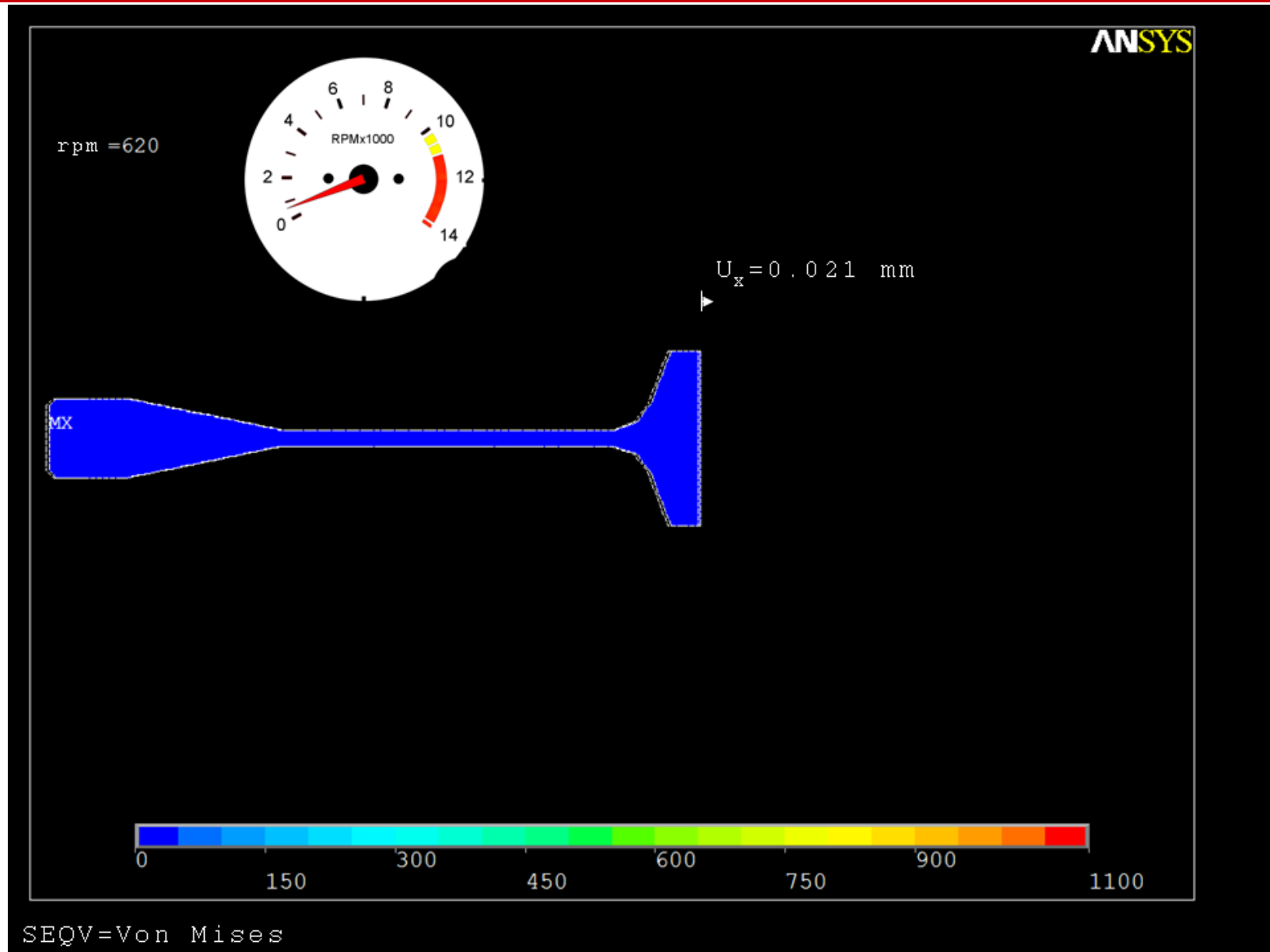


SEQV=Von Mises

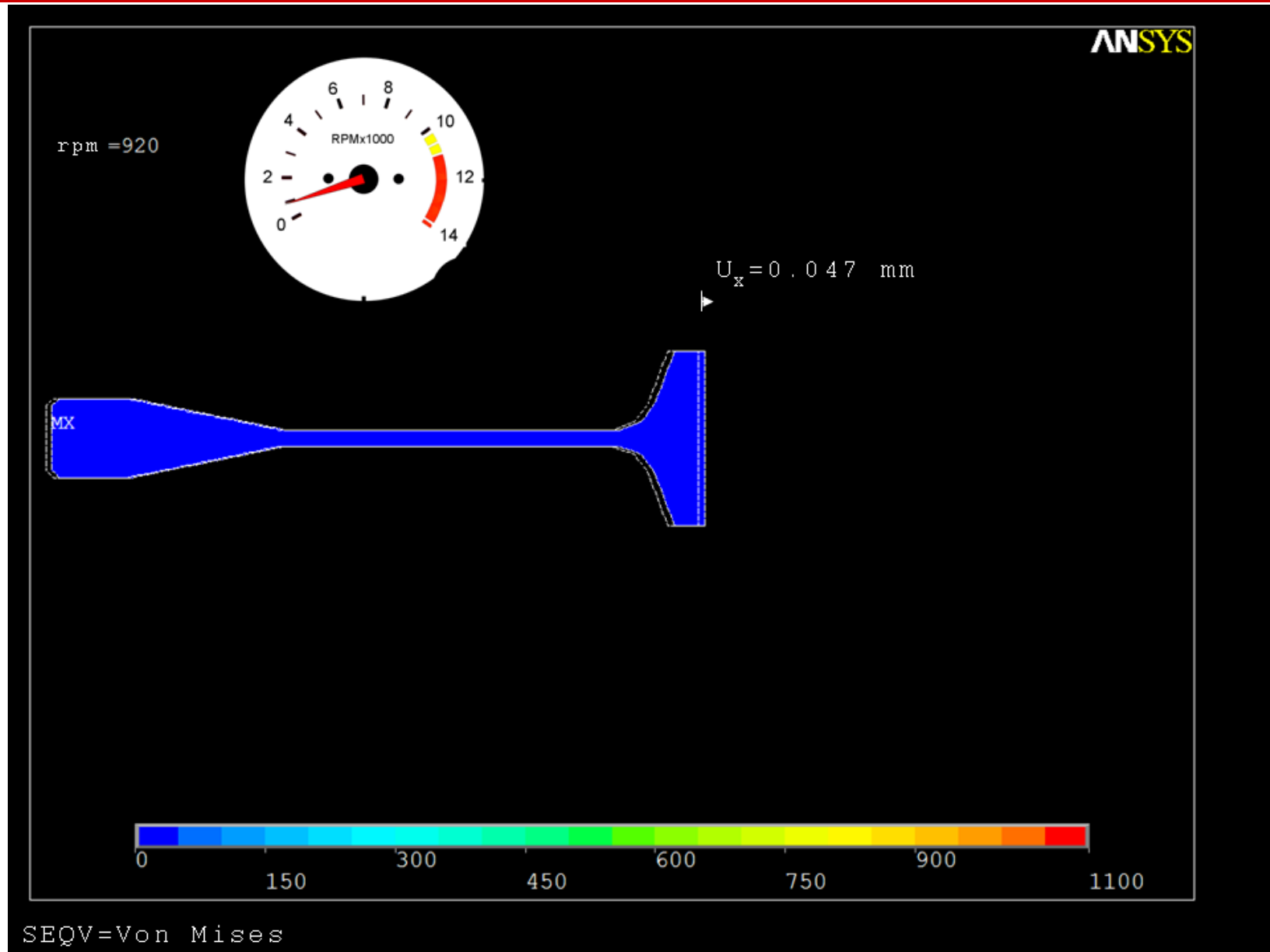
12. App. 2 - Rotating disk with slots and blades (2/22)



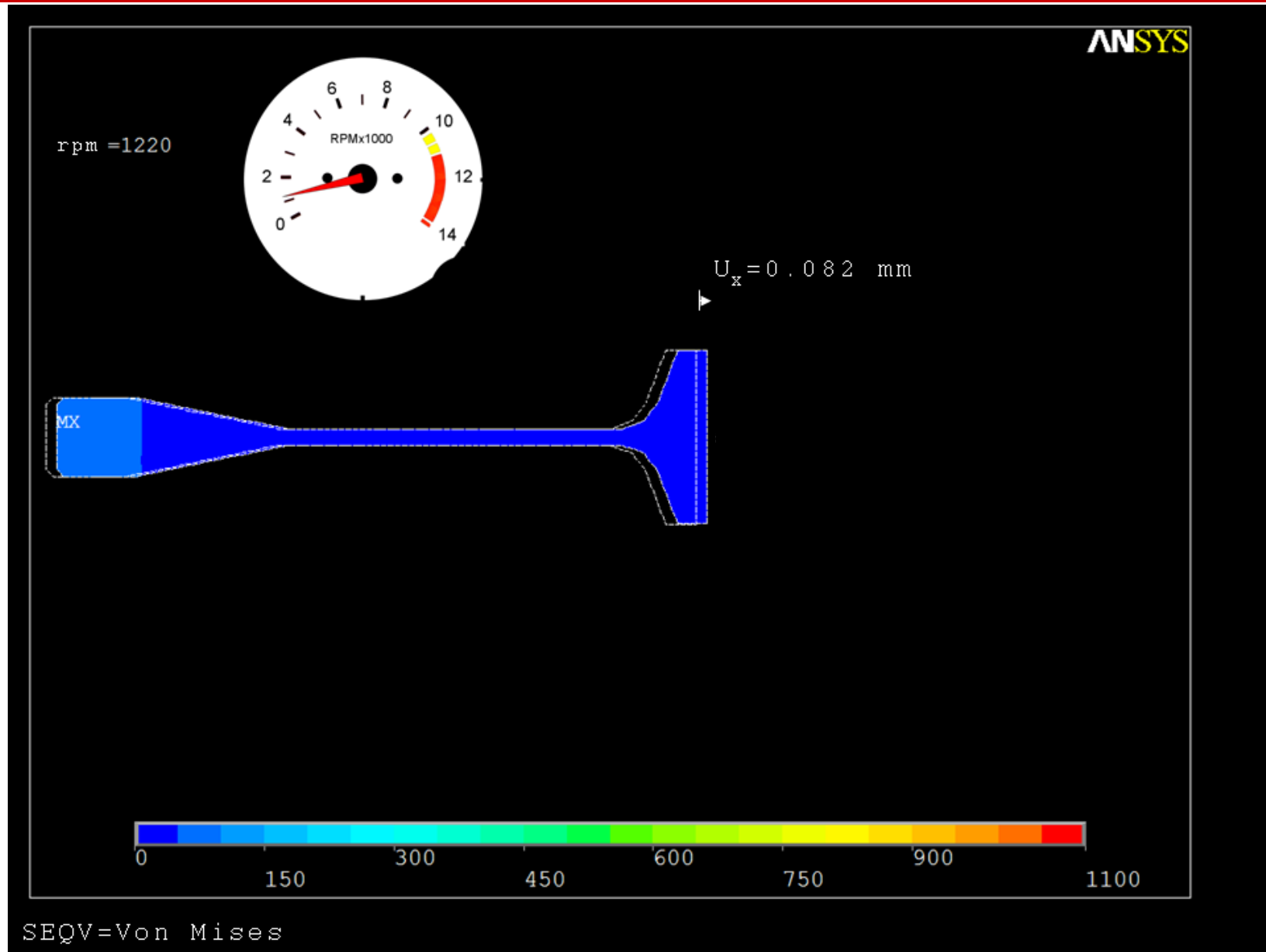
12. App. 2 - Rotating disk with slots and blades (3/22)



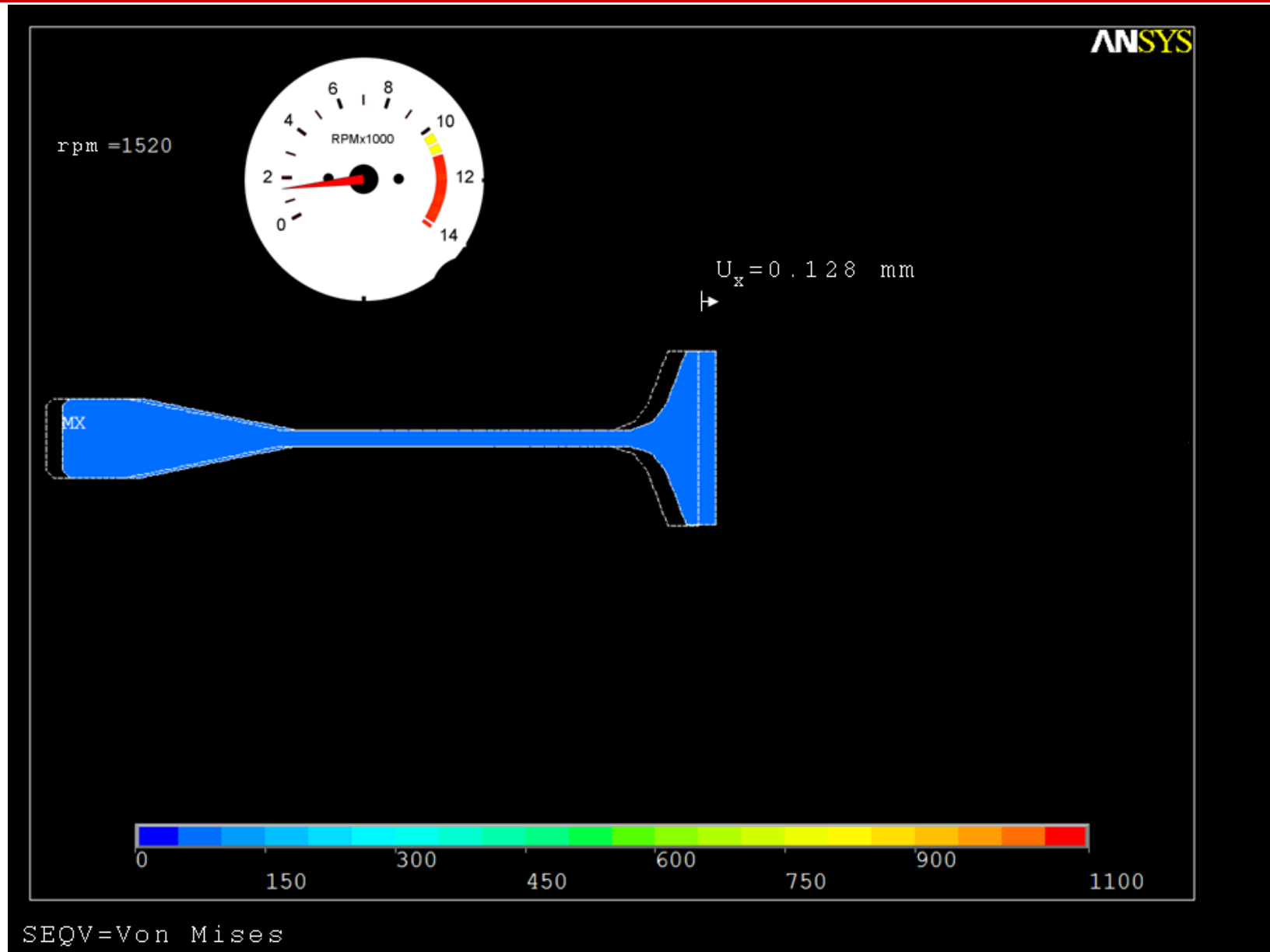
12. App. 2 - Rotating disk with slots and blades (4/22)



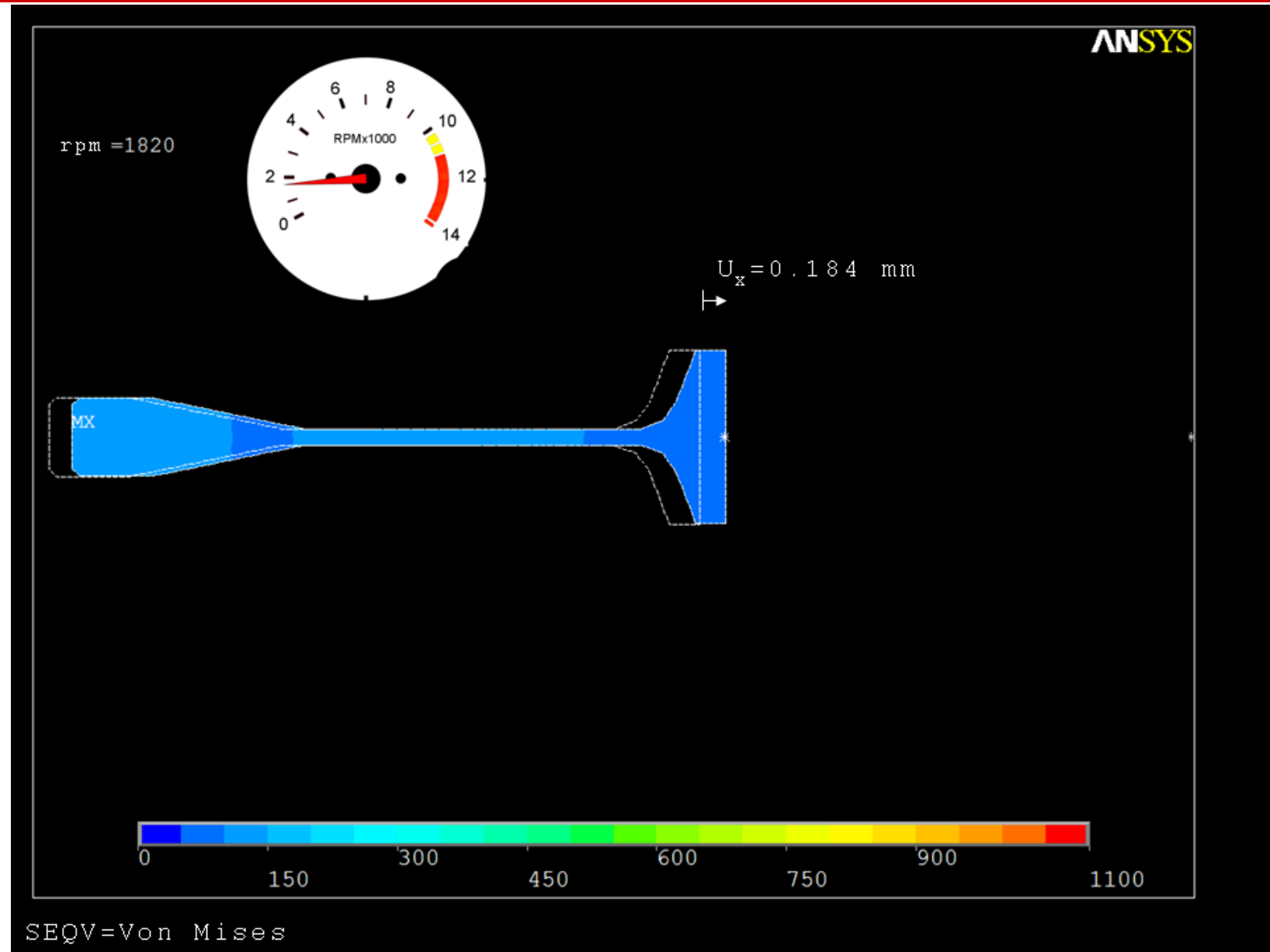
12. App. 2 - Rotating disk with slots and blades (5/22)



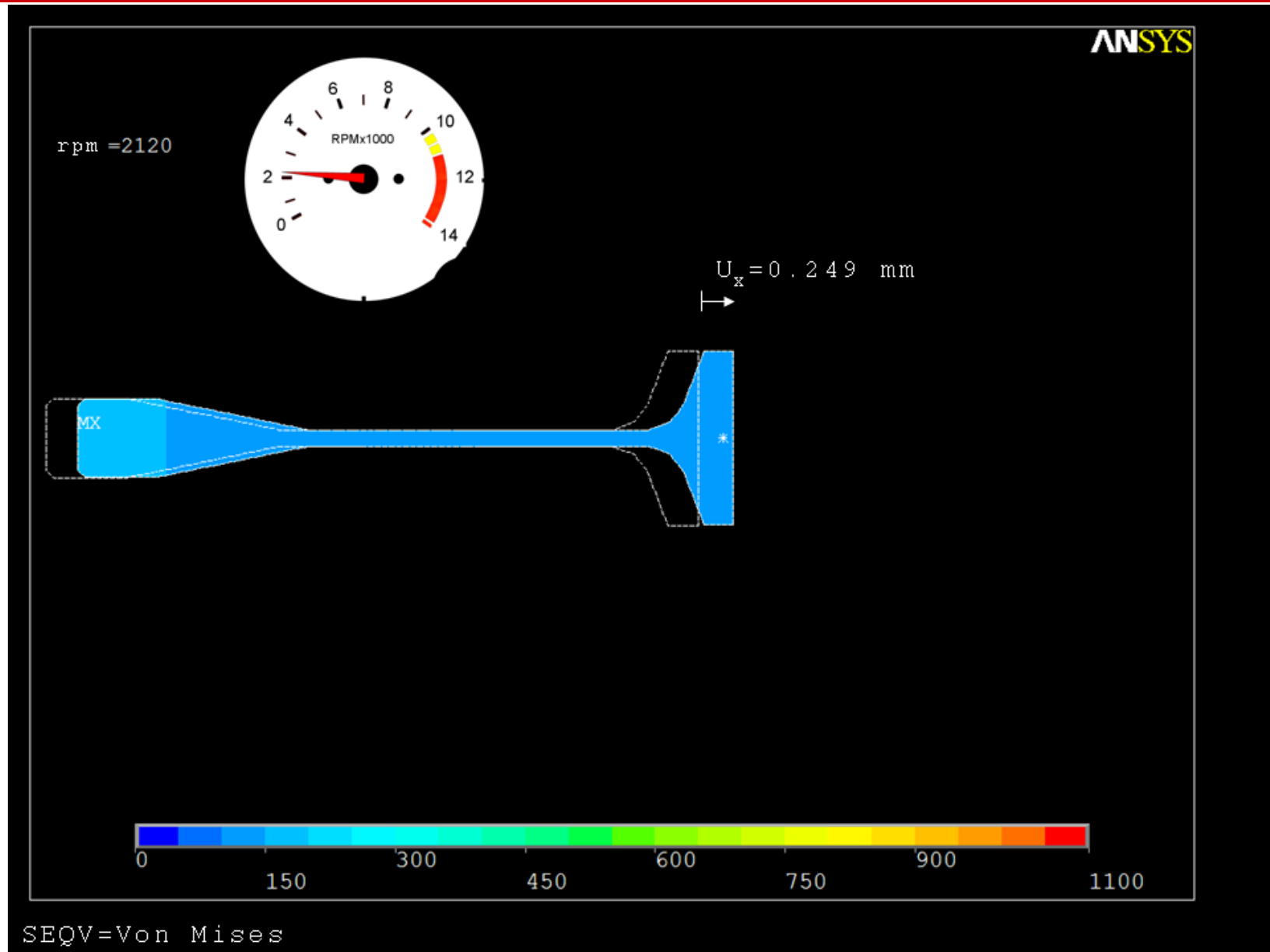
12. App. 2 - Rotating disk with slots and blades (6/22)



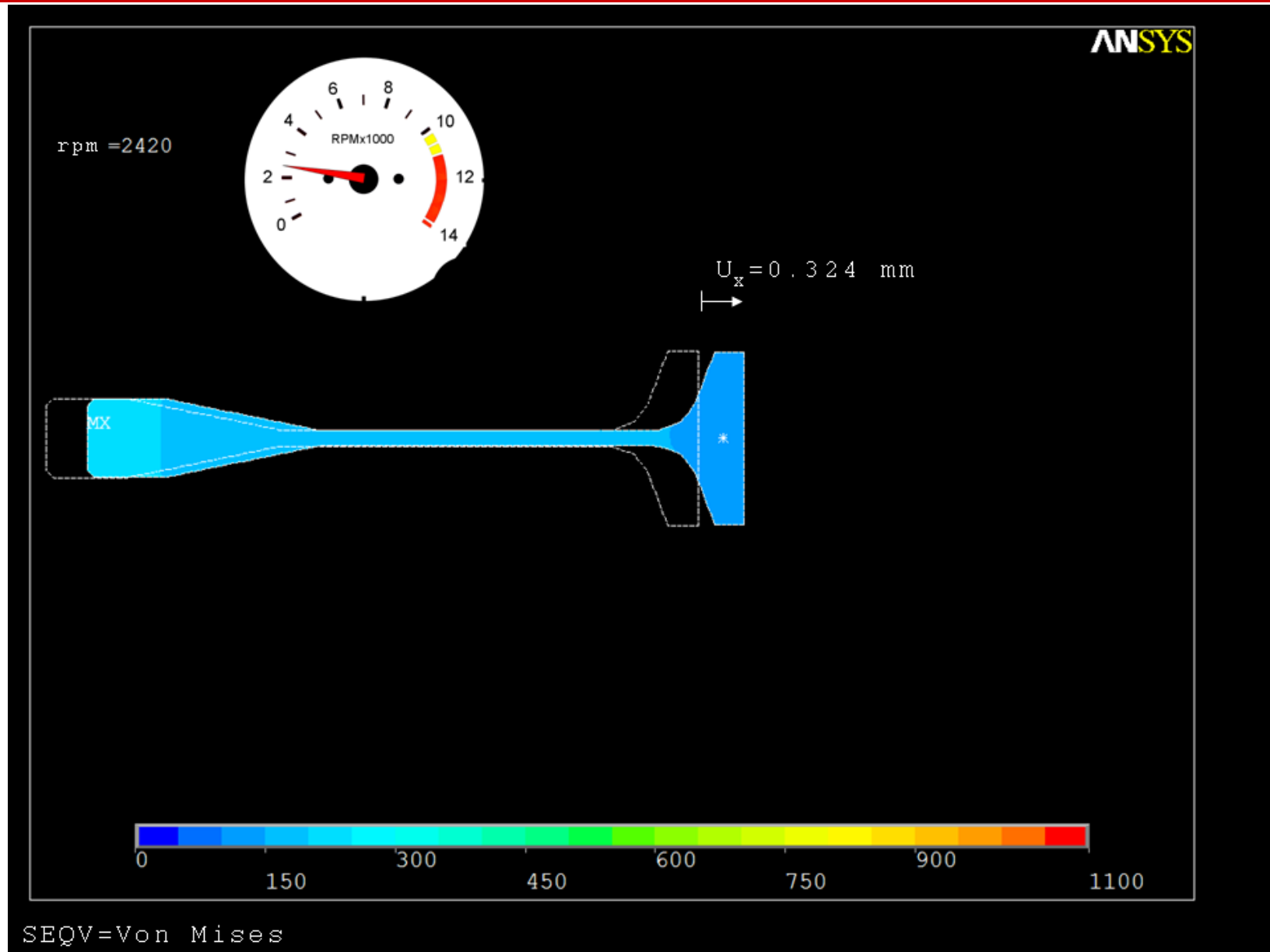
12. App. 2 - Rotating disk with slots and blades (7/22)



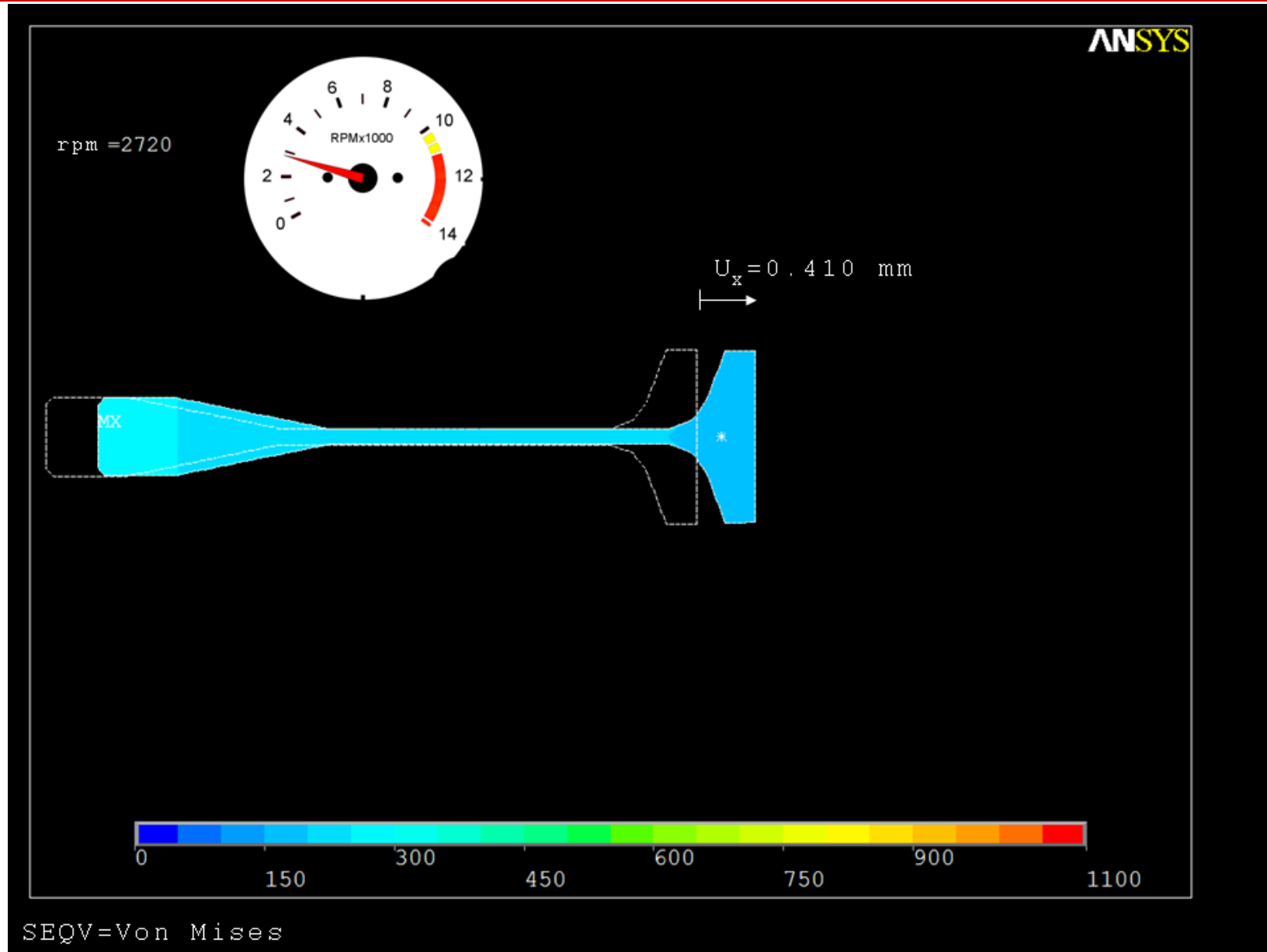
12. App. 2 - Rotating disk with slots and blades (8/22)



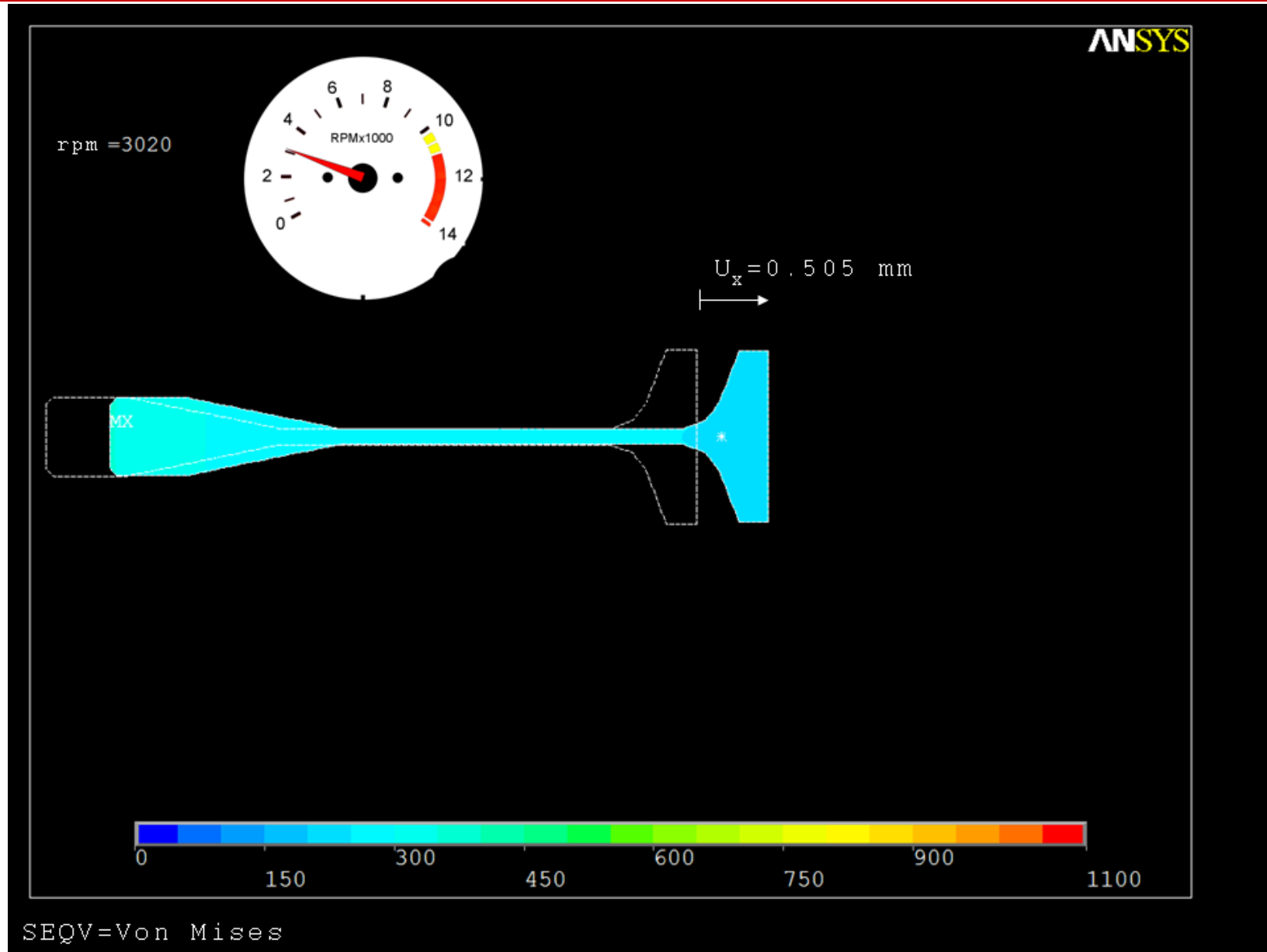
12. App. 2 - Rotating disk with slots and blades (9/22)



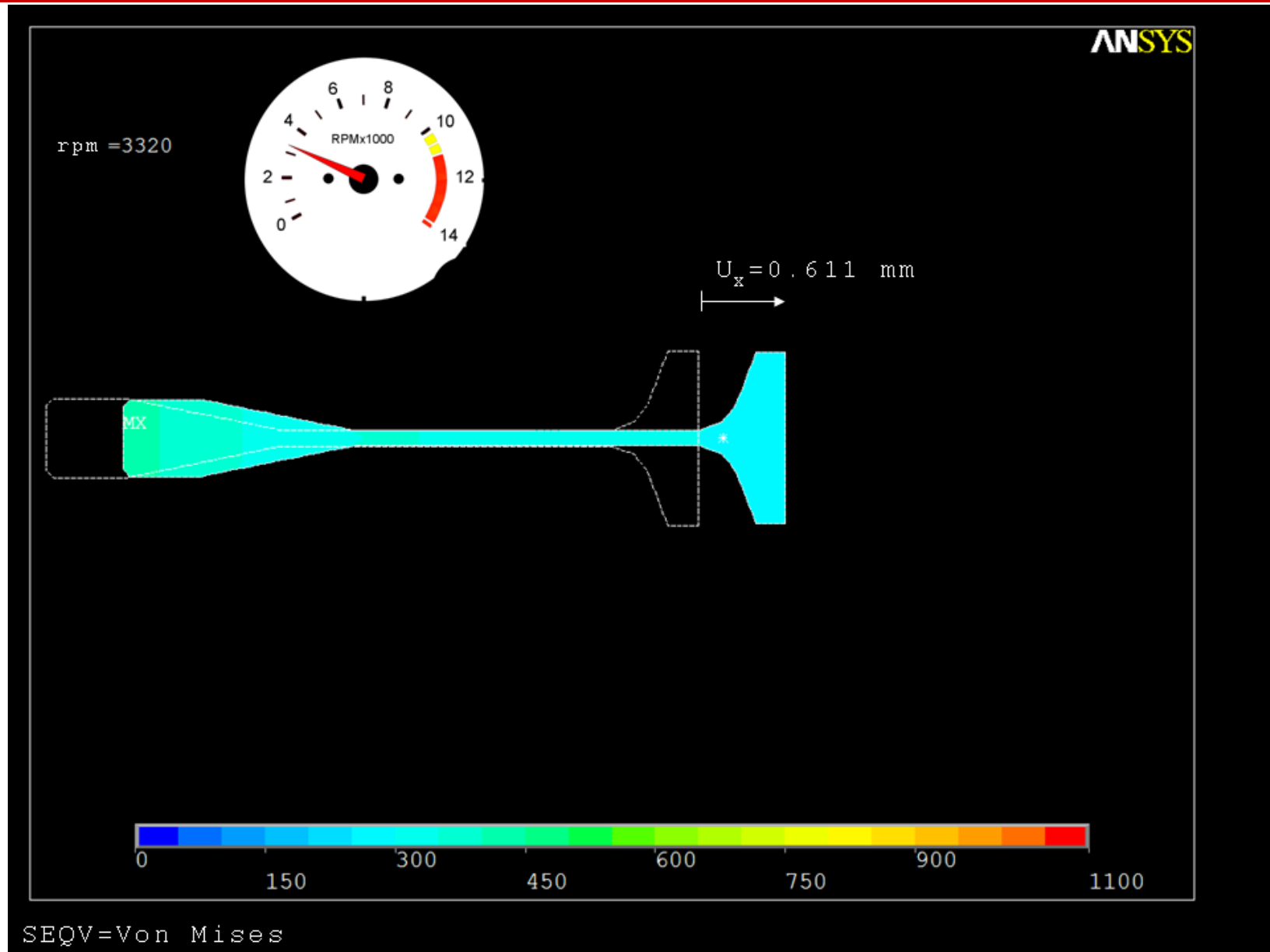
12. App. 2 - Rotating disk with slots and blades (10/22)



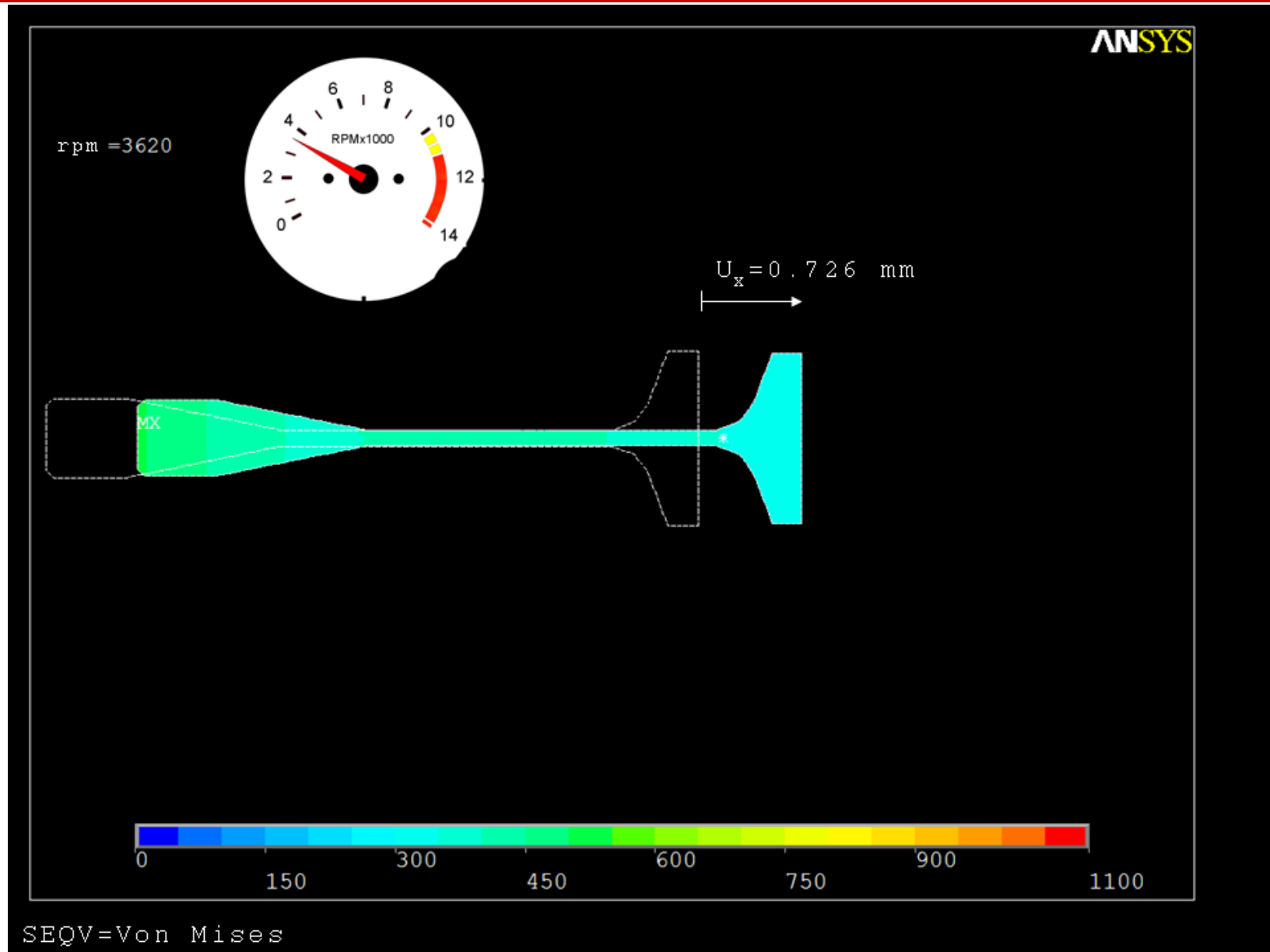
12. App. 2 - Rotating disk with slots and blades (11/22)



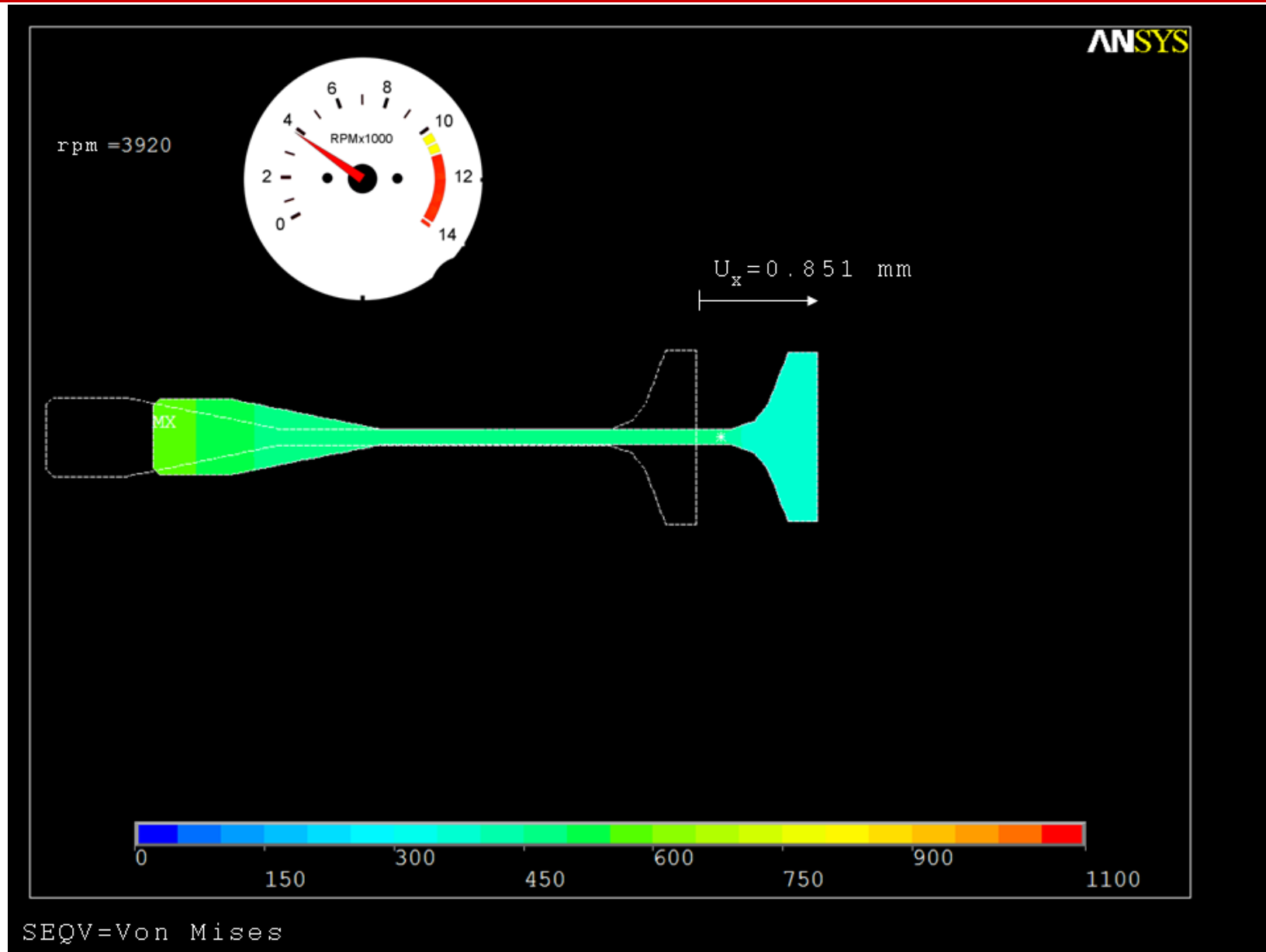
12. App. 2 - Rotating disk with slots and blades (12/22)



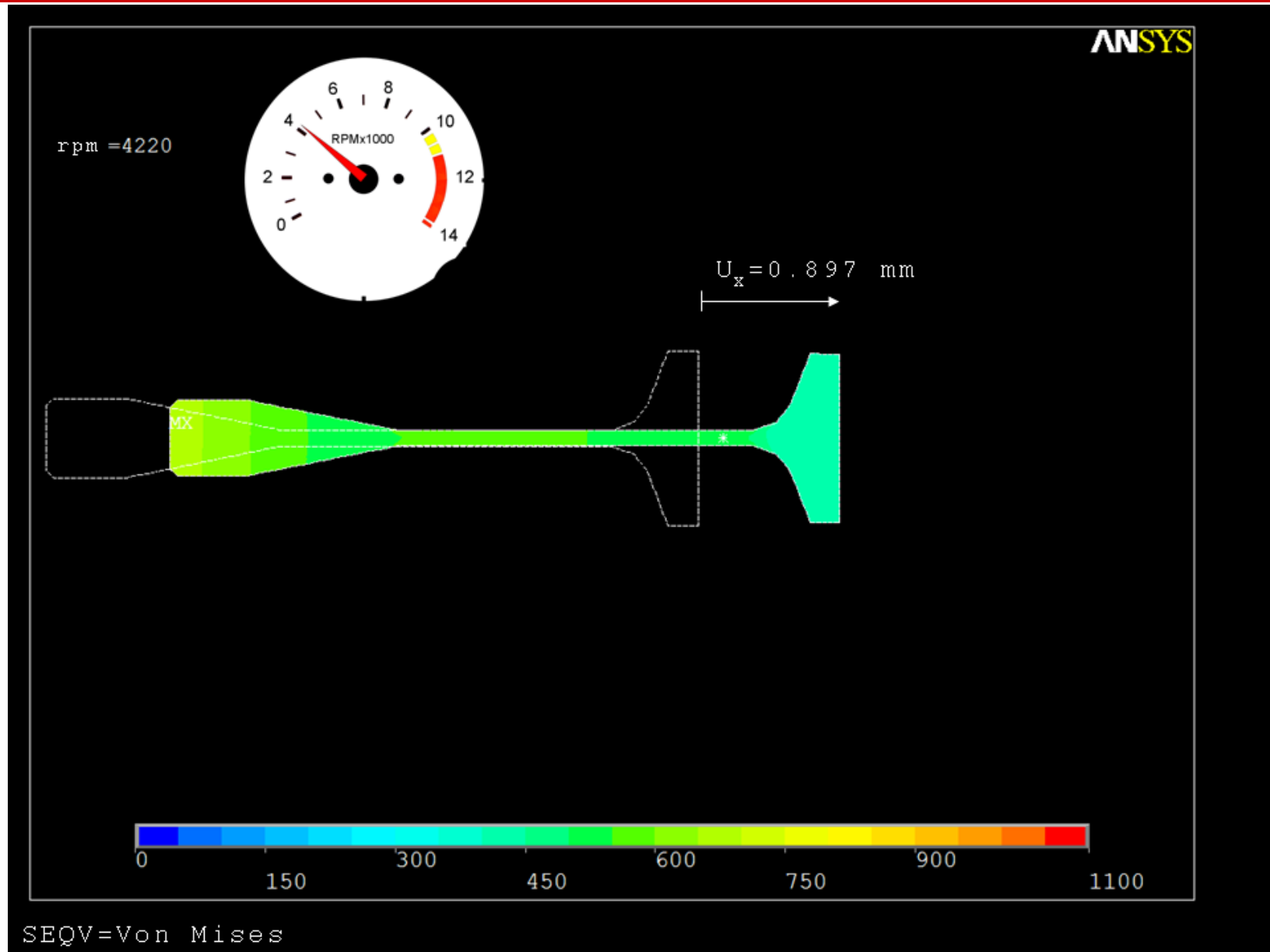
12. App. 2 - Rotating disk with slots and blades (13/22)



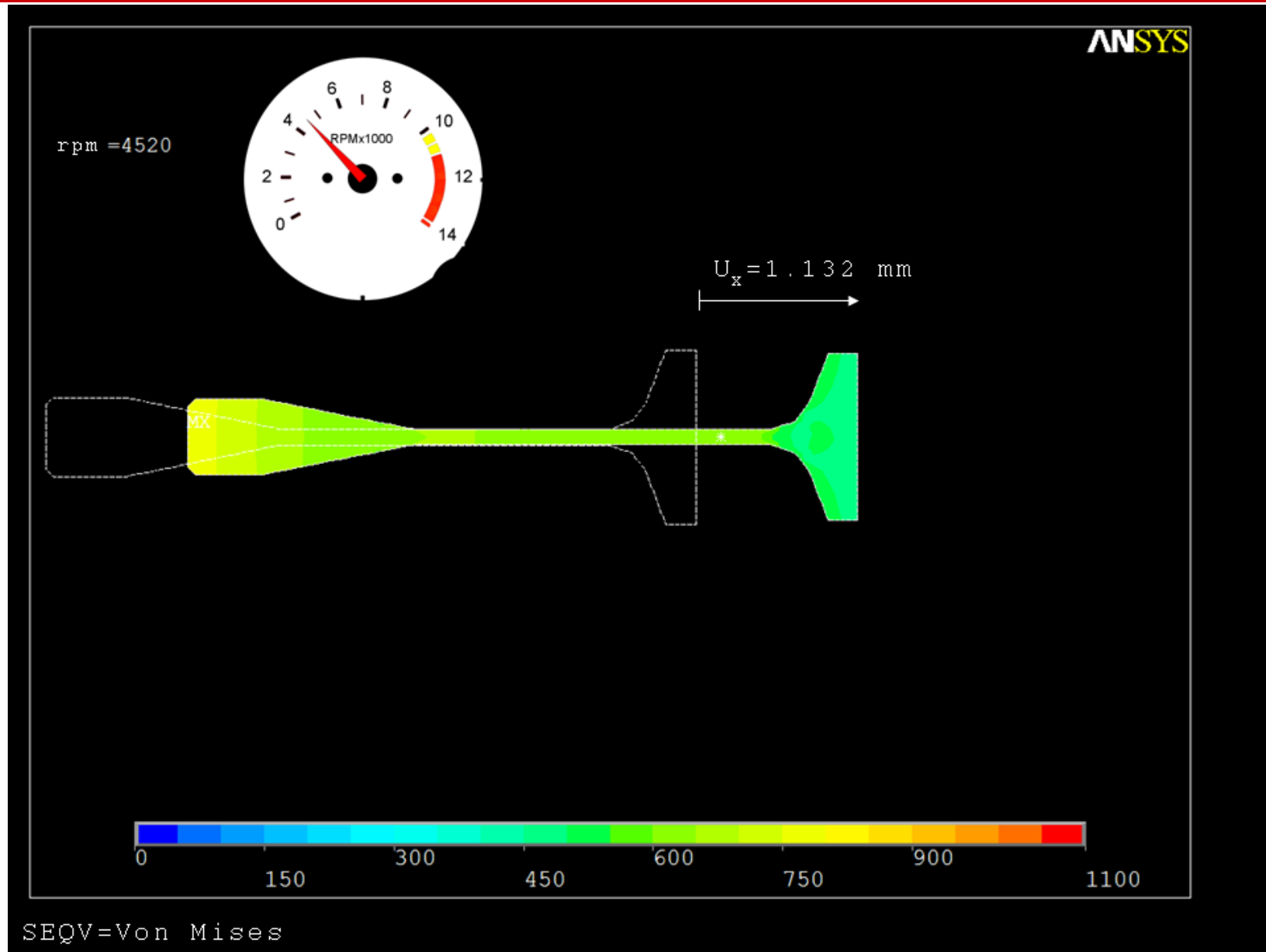
12. App. 2 - Rotating disk with slots and blades (14/22)



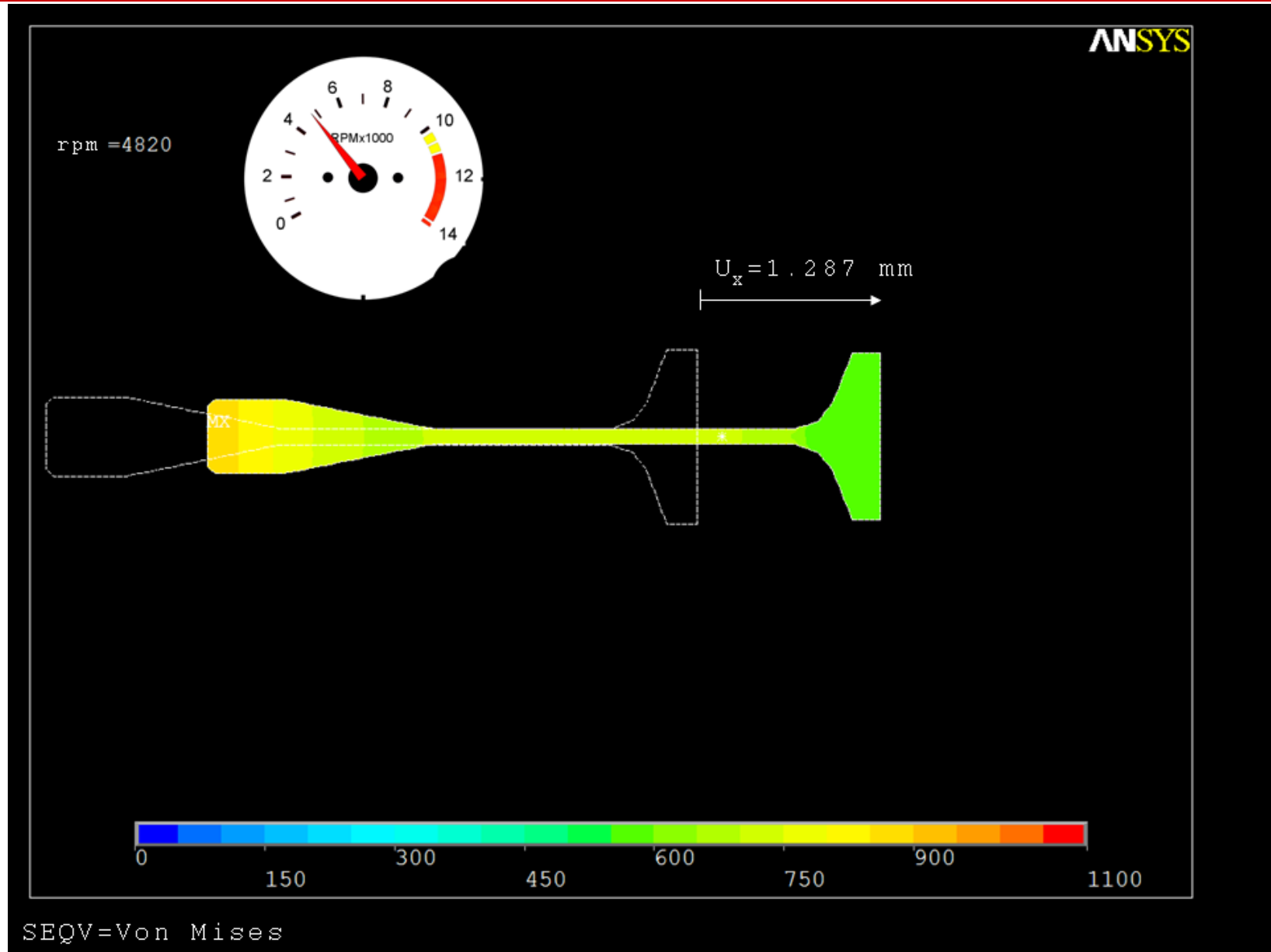
12. App. 2 - Rotating disk with slots and blades (15/22)



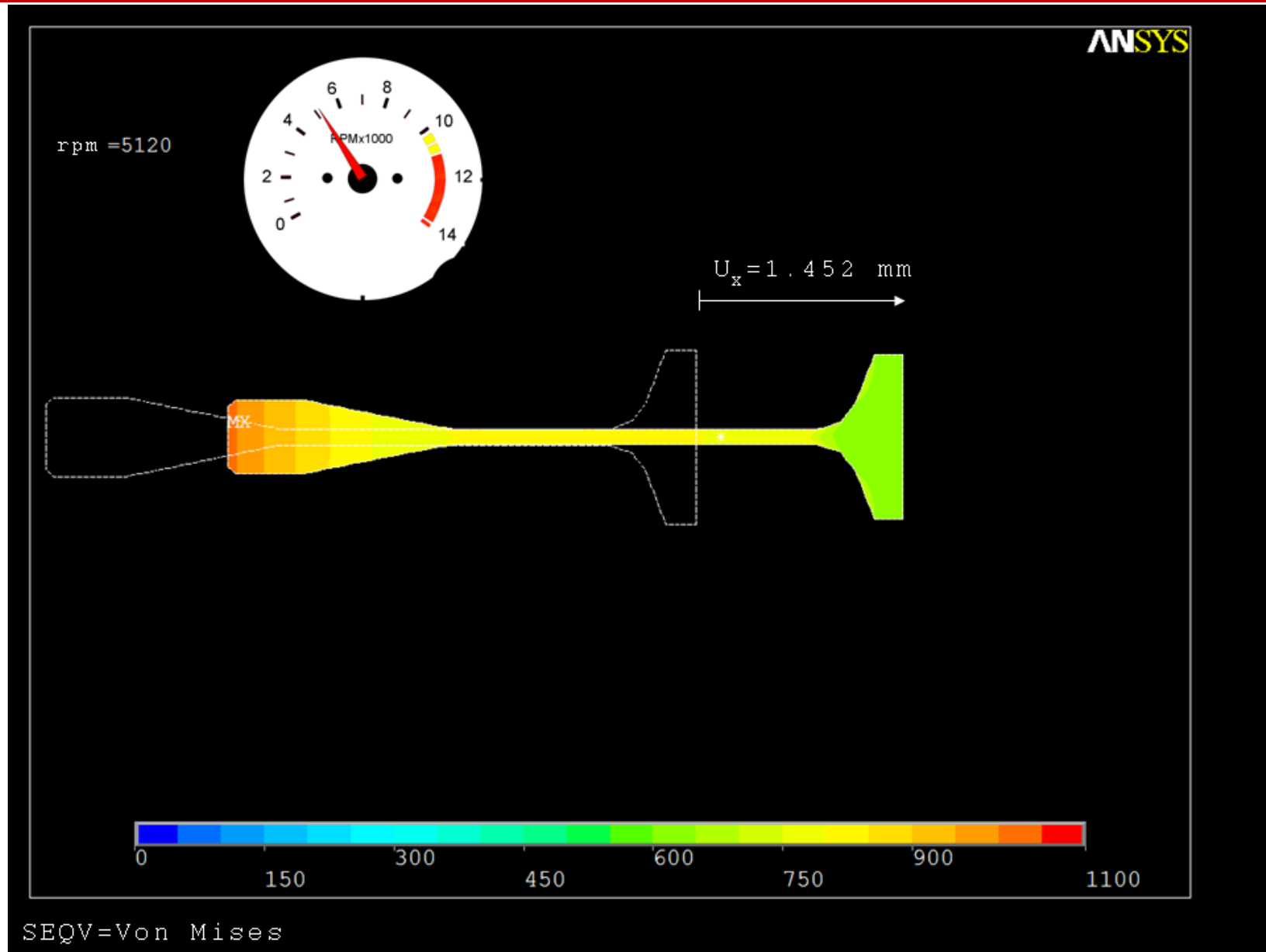
12. App. 2 - Rotating disk with slots and blades (16/22)



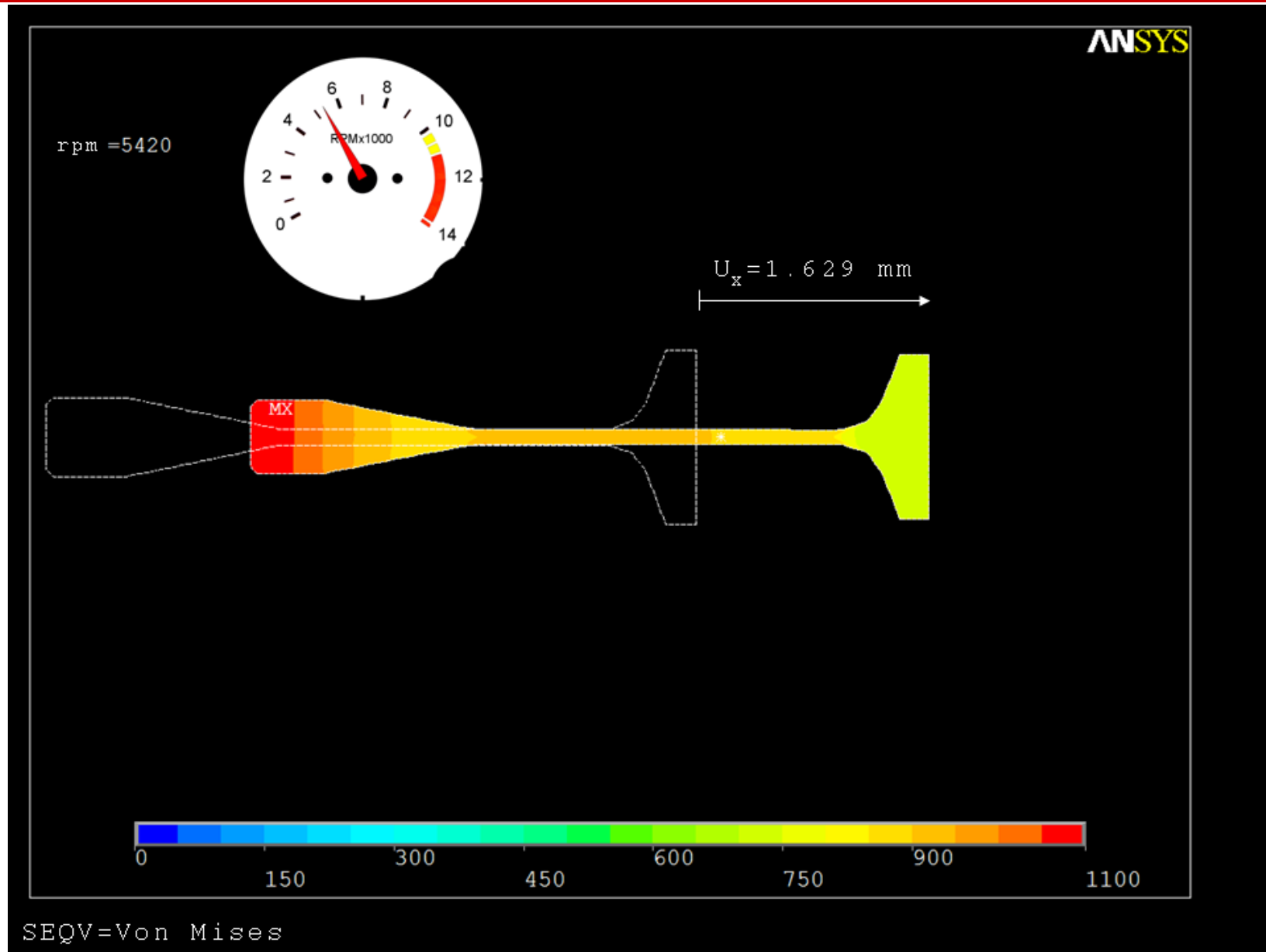
12. App. 2 - Rotating disk with slots and blades (17/22)



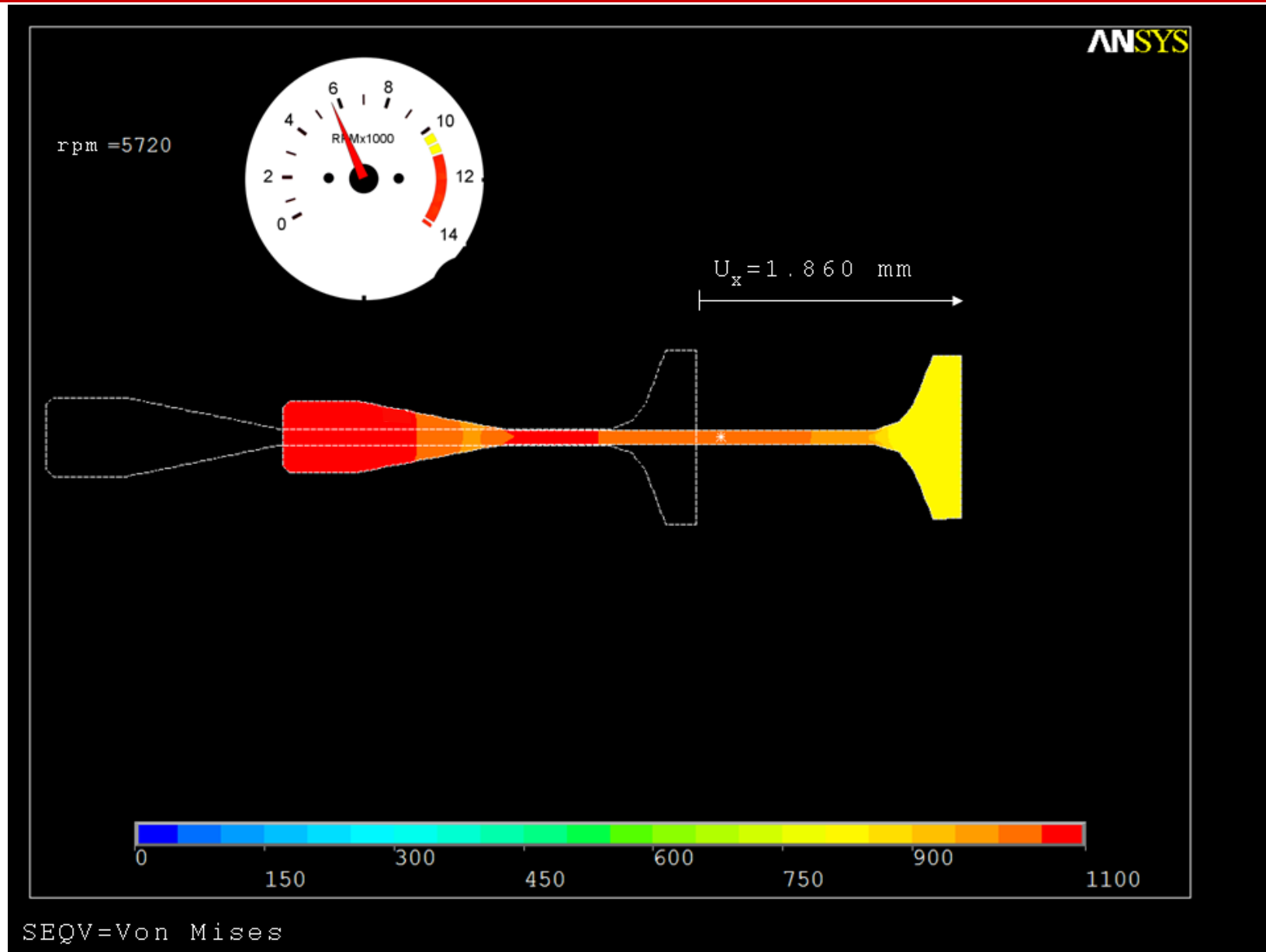
12. App. 2 - Rotating disk with slots and blades (18/22)



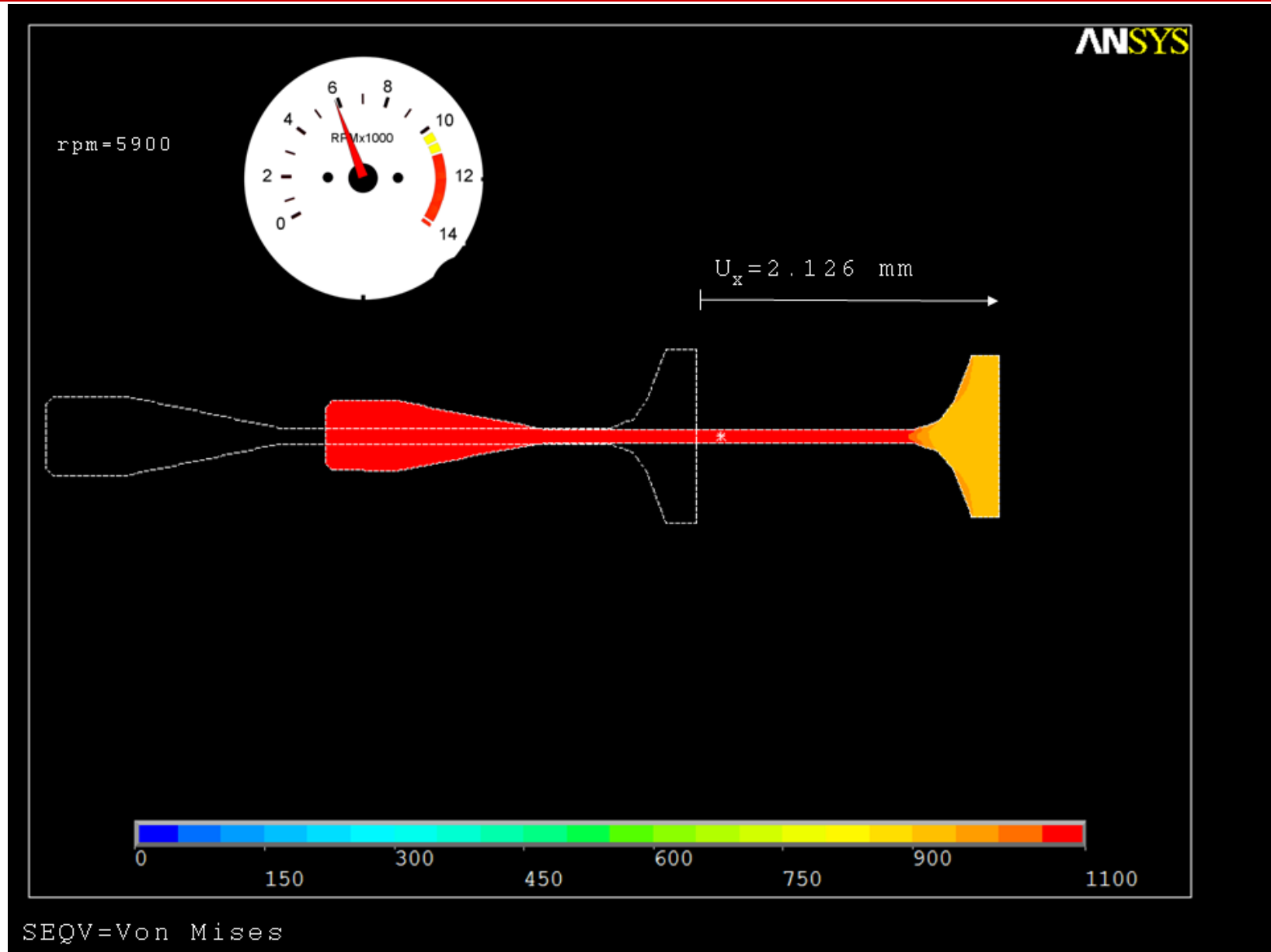
12. App. 2 - Rotating disk with slots and blades (19/22)



12. App. 2 - Rotating disk with slots and blades (20/22)

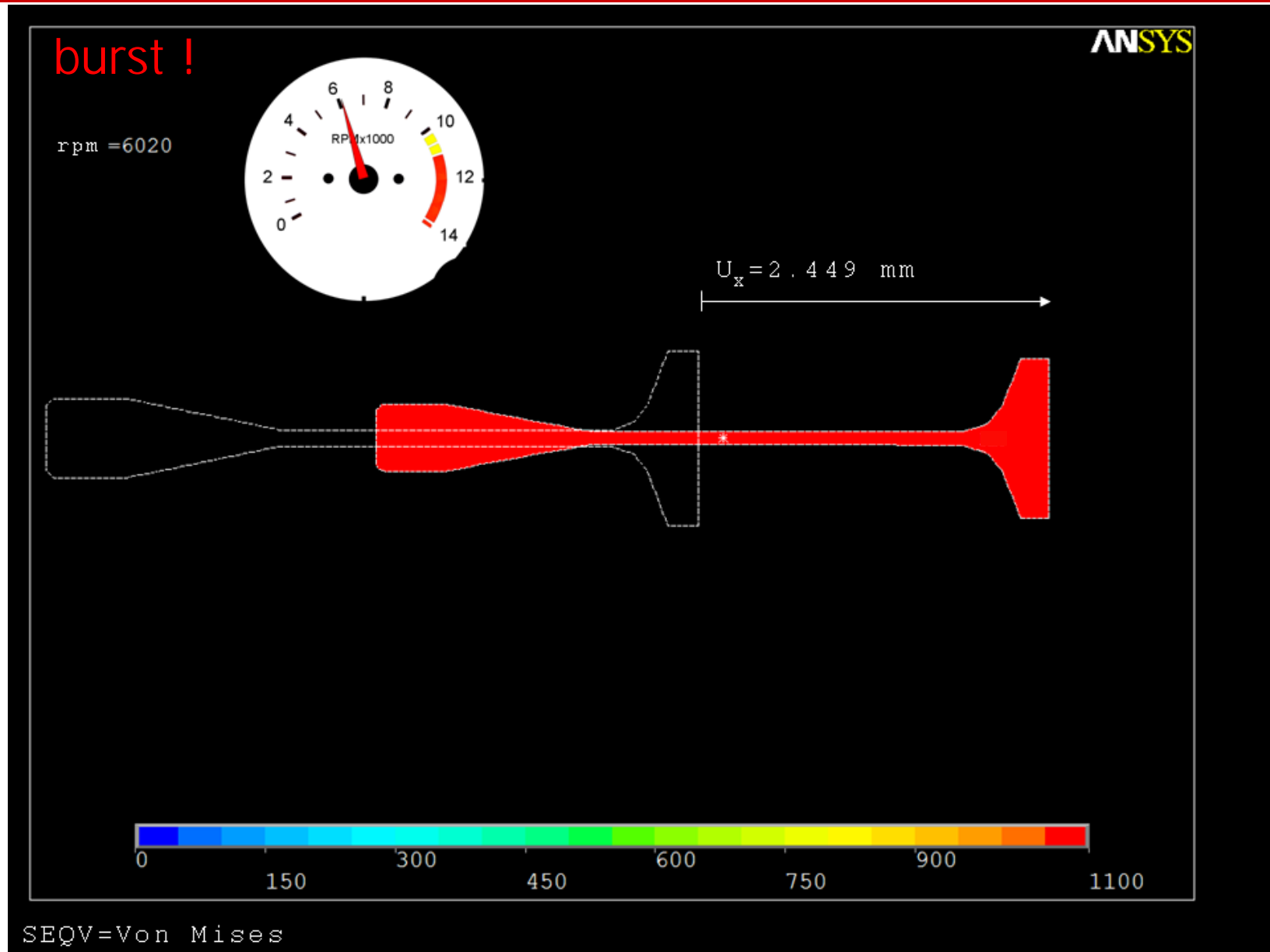


12. App. 2 - Rotating disk with slots and blades (21/22)



SEQV=Von Mises

12. App. 2 - Rotating disk with slots and blades (22/22)



13. Appendix 3: the Hallinan burst criterion

An alternative approach to the Robinson criterion for burst, see. Sect.9 sl.1, is the “Hallinan criterion”, expressed by the formula^{*}:

$$N_b = 0,95 N \left[S \left(\sqrt{\frac{R_m}{\sigma_{c,avg}}} - \sqrt{\frac{R_m}{\sigma_{c,max}}} \right) + \sqrt{\frac{R_m}{\sigma_{c,max}}} \right]$$

N_b = burst speed (rpm)

N = speed at which stresses are determined

R_m = ultimate (circumferential) strength of disk material at room temperature

$\sigma_{c,avg}$ = average hoop (circumferential) disk stress at N rpm

$\sigma_{c,max}$ = maximum hoop (circumferential) disk stress at N rpm

S = empirical constant determined for the ratio of nominal ultimate tensile strength to the notched bar ultimate tensile strength

* W.N. Barack and P.A. Domas, An Improved Turbine Disk Design To Increase Reliability Of Aircraft Jet Engines, (General Electric Co.), NASA CR-135033, 1976